Universitatea Transilvania din Brașov

HABILITATION THESIS

Title: Biofuels and Road Safety: Challenges and Solutions in the Context of Sustainable Mobility

Domain: Automotive Engineering

Author: Assoc. Prof. Dr. DUMITRAȘCU Dorin-Ion

Transilvania University of Brașov

BRAŞOV, 2024

CONTENTS

(A) Rezumat

Prezenta teză de abilitare conține o sinteză a realizărilor științifice și profesionale ale autorului efectuate de la conferirea titlului de doctor în 2011 în domeniul Științe inginerești, domeniul de profil Inginerie mecanică.

Teza de abilitare cu titlul Biocombustibili și siguranță rutieră: provocări și soluții în contextul mobilității sustenabile este structurată în două secțiuni: (A) Rezumat, (B) Realizări științifice și profesionale și planuri de evoluție și dezvoltare a carierei, ce cuprinde trei părți (B-i) Realizări științifice și profesionale, (B-ii) Planuri de evoluție și dezvoltare a carierei și (B-iii) Bibliografie.

În secțiunea (B-i) a tezei de abilitare sunt redate contribuțiile științifice ale autorului în două domenii prioritare ale ingineriei autovehiculelor: combustibilii alternativi în varianta "bio" a acestora și siguranța rutieră. Sunt detaliate aspecte privind parametrii fizico-chimici, respectiv funcționali privind biocarburanții sau combustibilii verzi pornind de la biomasă, ca surse energetice alternative utilizate în motoarele cu ardere internă. Sunt analizate performanțele energetice și ecologice ale anumitor categorii ale acestora.

În continuare este analizată influența proiectării infrastructurii rutiere asupra severității accidentelor rutiere, respectiv aspecte privind influenta fabricației sistemului airbag bord asupra siguranței ocupanților.

În capitolul 1 se prezintă contribuțiile principale ale autorului în zona cercetării combustiilor alternativi, în speță a biocarburanților, având în vedere perspectivele cele mai sigure de utilizare ale acestora și date fiind posibilitățile de producție, stocare, distribuție și corelare a proprietăților lor la cerințele actuale ale motoarelor cu ardere internă. În acest context au fost analizate trei categorii principale de produși: alcoolii, derivații lor eterii și esterii uleiurilor vegetale din perspectiva utilizării acestora în calitate de componenți carburanți, în diferite proporții în benzină și motorină. În funcție de tipologia testelor efectuate și disponibilitatea echipamentelor de cercetare au fost analizate performanțele energetice și ecologice ale unor motoare cu ardere internă alimentate cu diferite rețete de combustibili (clasici și biocarburanții). Rezultatele testelor relevă utilitatea folosirii biocarburanților în m.a.i., fiind o alternativă viabilă pentru reducerea dependenței față de combustibilii fosili cu proprietăți energetice apropiate și ecologice superioare.

În capitolul 2 este abordată tematica influenței proiectării infrastructurii rutiere asupra severității accidentelor rutiere, cum implementarea anumitor soluții tehnice acționează ca factor agravant al nivelului de avariere și al gradului de vătămare a ocupanților autovehiculelor. Se face o analiză detaliată a conceptului *forgiving roadsides*, ca parte integrantă a sistemului de management al securității rutiere. Conceptul se referă proiectarea, realizarea și modificarea elementelor marginilor părții carosabile astfel încât să se evite sau minimizeze efectele accidentelor în care autovehiculele părăsesc drumul și se lovesc de obstacole aflate în

vecinătatea drumului. La nivelul Uniunii Europene un procent important este reprezentat de accidentele de tipul autovehicul – obstacol. Așa cum s-a specificat anterior, conceptul vine să elimine sau să reducă incidența acestui tip de eveniment rutier. S-a realizat clasificarea și detalierea acelor categorii de obstacole aflate în proximitatea părții carosabile, care in cazul unui impact cresc severitatea acestuia; au fost propuse și măsuri de îmbunătățire.

Pornind de la elementele specificate anterior, în cadrul capitolului a fost prezentat și un studiu de caz privind impactul autovehicul – șanț inspirat de frecventele accidente de acest tip produse pe tronsonul de drum analizat de pe DN1. Au fost analizate dinamica și efectele accidentului atât asupra autoturismului cât și asupra ocupanților acestuia și au fost propuse o serie de măsuri de îmbunătățire pe baza conceptului *forgiving roadsides.*

Studiul relevă, de asemenea, utilitatea practică a dezvoltării unui sistem de siguranță rutieră, incluzând soluții tehnice adecvate pentru a face un drum sigur cu efect direct asupra securității rutiere. Din acest punct de vedere, soluțiile tehnice relevante și experiența de bune practici pot fi punctul de plecare pentru o standardizare în domeniul siguranței rutiere.

În capitolul 3 este analizată influența parametrilor procesului de micro-perforare cu laser a ansamblului bord – airbag asupra eficienței și siguranței pasagerilor în timpul unui impact. Următoarele aspecte au fost considerate: importanța declanșării corecte, regimul de micro-perforare cu laser, rolul micro-perforării bordului în zona airbag-ului pasagerului; parametrii tehnici ai regimului de micro-perforare cu laser, influența parametrilor de micro-perforare asupra performanței airbag-ului, timpul optim de declanșare a airbag-ului, analiza procesului de micro-perforare cu laser pentru piese din piele sintetică auto, influența nivelului de zgomot electromagnetic în timpul procesului de micro-perforare cu laser.

În industria auto, siguranța pasagerilor este o prioritate de top. Influența regimului de micro-perforare cu laser este foarte importantă pentru sistemul de siguranță. Airbag-ul este una dintre cele mai critice componente ale sistemelor de siguranță pasivă, concepută pentru a proteja pasagerii în timpul unei coliziuni. În zona în care este montat airbag-ul pasagerului, este necesară o reducere discretă a rezistenței materialului pentru a se asigura că airbag-ul poate străpunge suprafața fără întârzieri, blocaje sau dislocări de material. În acest context, regimul de perforare cu laser implică stabilirea unor parametri tehnici critici, cum ar fi dimensiunea microperforațiilor și densitatea acestora, adâncimea de tăiere și distanța dintre microperforații. Acești parametri trebuie ajustați cu atenție pentru a echilibra estetica, rezistența materialului și declanșarea eficientă a airbag-ului.

Pentru a evita o întârziere critică în declanșarea completă, airbag-ul poate întâmpina o rezistență mecanică mai mare dacă zona omoloagă a panoului bordului este fabricat fără această reducere predefinită a rezistenței mecanice a materialului. Un regim de micro-perforare bine optimizat permite airbag-ului să spargă materialul bordului aproape instantaneu, asigurând o protecție eficientă a pasagerilor. Micro-perforarea cu laser a zonei airbag-ului pasagerului are un impact semnificativ asupra modului în care airbag-ul se deschide în timpul unui impact. Fără o micro-perforare adecvată, materialul de acoperire al

planșei de bord, cum ar fi pielea sintetică, poate întârzia sau împiedica declanșarea airbag-ului, ceea ce ar putea compromite siguranța pasagerilor. Micro-perforarea cu laser creează o amorsă de rupere controlată, făcând materialul să cedeze corespunzător și eliberează airbag-ul fără rezistență semnificativă. Acest lucru este esențial deoarece o deschidere întârziată sau incompletă poate afecta grav siguranța în timpul unui accident. Parametrii de micro-perforare influențează direct performanța airbag-ului și, în consecință, nivelul de siguranță oferit pasagerilor.

(B) Scientific and professional achievements and the evolution and development plans for career development

(B-i) Scientific and professional achievements

Introduction

The scientific, professional activities and achievements had as a starting point the year 2001 when I graduated the Faculty of Mechanics, Automotive engineering specialization, as head of promotion. In the same year, I became a member of the Department of Automotive and engines at Faculty of Mechanics, Transilvania University of Brasov, as a full-time doctoral student. Since 2002, I have been employed as a university assistant in the same department, then following all the stages of my university career until now when I hold the position of associate professor.

My professional and scientific activity took place within the High-tech products for automotive Research Center as part of Research and Development Institute of Transilvania University of Brasov, in the following main research fields: advanced propulsion system solutions, alternative fuels usage in internal combustion engines, unconventional propulsion systems, road safety, accident analysis and reconstruction, project and quality management in automotive industry.

In the developed scientific papers and research contracts, I have constantly considered the following research topics with practical applicability:

- ✓ energetical and ecological performances of internal combustion engines fueled with classical and alternative fuels;
- ✓ compressed air propulsion systems;
- ✓ traffic safety and accidents analysis and reconstruction;
- ✓ project management in automotive industry;
- ✓ estimation of the automotive products reliability;
- ✓ influence of hazard exposures and health effects of forestry vehicle operators;
- ✓ failure mode and effects analyses specific to manufacturing of automotive parts;
- ✓ evaluation, analysis and improvement of automotive product quality.

During my didactic activity, I have performed teaching activities at the following subjects:

- ✓ Internal combustion engines;
- ✓ Fuels, lubricants and special materials for motor vehicles;
- ✓ Project management;
- ✓ Quality assurance methods;
- ✓ Multimodal transport systems;

- ✓ Vehicle dynamics;
- ✓ Plastics, ceramics and composites;
- ✓ Computer aided design;
- ✓ Computer basics.

Since 2015 I have been the coordinator of the master's degree program entitled "Motor vehicles and Future Technologies" where with my colleagues, I'm involved in continuous adaptation of curricula in line with the evolution of the automotive industry.

In High-tech products for automotive Research Center from Research and Development Institute of Transilvania University of Brasov, I am the manager of the Laboratory for fuels and lubricants for motor vehicles. Within this laboratory, scientific research and teaching activities were carried out regarding the determination of certain physico-chemical parameters such as: octane number, fractional distillation, water content in fuels, density, flash point, viscosity, etc.

Visibility and international recognition are highlighted by publishing articles in prestigious international journals indexed by WOS with impact factor, classified in the Q1, Q2, ISI Thomson proceeding area, indexed in international databases, and at various national or international conferences, articles that highlight both the practical component accumulated in time as a specialist, as well as the specialized professional training in the automotive field.

In addition to didactic activity, the professional qualities in the field of scientific research are proven by being the project manager of two research projects won in national competitions and through participation in research teams of grants/contracts having as research themes the following:

- ✓ construction and rehabilitation of forest roads;
- ✓ crash tests and accidents reconstruction;
- ✓ optimizing the energetical and ecological solution for a single-cylinder diesel engine with direct injection;
- ✓ random oscillatory processes in liquids, used in hydrostatic energy recovery systems dissipated in vehicle shock absorbers;
- ✓ influence of the frontal profile of the car body on pedestrian injury;
- ✓ the head impact of vehicle occupants in various types of collisions.

In addition to research projects, I was also involved in the research infrastructure project team, for example the "Advanced Systems for Motor Vehicles and Road Transport - SAVAT" training and research platform.

In the period 2019 -2021 I was the team leader of a group of students, together participating to Emerson's AVENTICS Pneumobile International competition in Hungary, intended for pneumatically propelled vehicles. In order to participate, we designed and built a single-seat car going through all the preliminary elimination stages, until we could actually participate in the main events of the competition.

During the years I've coordinated many project diploma and dissertations, some of them

having practical applications such as building a competition engine, engine performances testing, engine software optimization, a buggy, etc.

The scientific research activity is also based on initiatives to attract funds through project proposals in the field of biofuels and the use of alternative propulsion sources, which, however, did not materialize for reasons beyond my control.

Also, the scientific activity in the field of fuels is also complemented by collaborations with the National Institute for Research & Development in Chemistry and Petrochemistry ICECHIM, research area Alternative bioresources and biofuels. Together we tested different biodiesel recipes, evaluating the energetic performances and emissions.

My professional activity also includes membership in scientific and organizational committees of international congresses and conferences such as CONAT, EEM-ESSS, ACMOS.

Between 2012 and 2016 I was a member of the council of the Faculty of Mechanical Engineering. My activity also includes another diverse administrative activity.

In parallel with my academic involvement, the professional activity was completed by the following:

- ✓ From 2011 to present I am a judicial technical expert in the domain Motor vehicles, road traffic being authorized by the Ministry of Justice. In order to continuously improve my professional activity in the field of traffic accident analysis and reconstruction, periodically I participated at accidentology seminars organized at national level in Brașov and in Linz, Austria at an international technical and scientific seminar organized by DSD Linz. The main approached subjects refer to crash tests, case study simulation using PC-Crash specialized software for the reconstruction and analysis of vehicle accidents and other incidents. (e.g. calculation of multiple collisions between several cars, mesh model, rollover model, advanced collision optimizer, trailer simulation, multi-body simulation, calculation of occupant movements and loads with multibody occupant and seat model (belted and unbelted), interaction with the car interior, pedestrian model, scalable pedestrians by anthropometrical data, bicycle and motorcycle models, etc.).
- ✓ In the private sector, I worked as a design engineer and project manager at companies in the automotive industry field, having european vehicle manufacturers as beneficiaries. The main activities consisted of: project planning, project management documentation, quality documentation, development of technical working procedures, CAD for automotive mechanical and electrical parts, the design of welding devices for the car body, etc.

The doctoral thesis entitled Project management of an efficient single cylinder engine, through its interdisciplinary addressed theme, constituted a premise for my further professional development, which has indeed happened, a fact proven by my subsequent scientific activity.

Based on the aspects presented above, the habilitation thesis titled Biofuels and road safety:

challenges and solutions in the context of sustainable mobility is structured in two main sections: (A) Abstract and (B) Scientific and professional achievements and the evolution and development plans for career development. The (B) section is also composed from three parts: (B-i) Scientific and professional achievements (B-ii) The evolution and development plans for career development and (B-iii) Bibliography.

In section (B-i) of the habilitation thesis, there are briefly presented significant scientific contributions related to the following topics: alternative fuels, the influence of road Infrastructure design over the traffic accidents and the influence of laser micro-perforation parameters over the airbag processing and on the efficiency of passengers' safety during an impact. This topics, as essential sustainable transportation systems by both point of view: energetic and ecologic performances of vehicles and traffic safety will be detailed in the following, in the present habilitation thesis.

In the third section (B-iii) the plan for the evolution and development of the professional, scientific and academic career is presented, based on the synthesis of teaching activity, professional experience and research activities, including the targeted research directions as well as ways to capitalize on the results presented in the habilitation thesis that have not been published.

Chapter 1. Alternative Fuels [DUM13], [DUM18a], [DUM21], [DUM24a]

In the present the world is facing two major challenges regarding the transportation systems of people and goods: fossil fuel depletion and an accelerated degradation of environment (local air pollution and global warming). These environmental problems are linked to the large-scale fossil fuel usage. Through increased alternative fuels usage, it can be diminishing the carbon emission and can also decrease pollutant emissions.

Thereby, alternative fuels are being considered to replace conventional ones in the transportation sector as power sources, consisting of liquid and gaseous fuels. Initially they had a limited use, with an experimental or demonstrative character due to the high production of cheap petroleum-based fuels. The constraints imposed by last years environmental legislation in order to curb the climate changes turned them into an increasingly attractive alternative, fact doubled by the limitations in electric propulsion field, and the need for sustainable energy.

Among the category of alternative fuels, the biofuels are receiving greater attention due to their renewable nature, being produced from biomass. The biofuels can contribute to the reduction and, in some regions, to eliminate the dependence on fossil fuels, to reduce emissions from internal combustion engines.

In the renewable energy category, the biofuels are able the retain CO_2 and generate O_2, contributing to maintain the environment ecology, other forms of renewable other energy not

having this feature.
In this chapter will be analyzed the main alternative fuels and some researches developed in this field by the author.

1.1 Biofuels

First generation of biofuels determined a food versus fuel conflict, while the second generation of biofuels are produced from waste biomass (e.g., plant materials and animal waste). The second-generation biofuels goal is to increase the amount of biofuels that can be produced sustainably by using biomass consisting of the residual non-food parts of current crops.
First-generation biofuels are produced from primary crops such as of sugar beet, sugarcane, corn, barley, wheat, rapeseed, sunflower, soybean, etc. If farmers decide to focus on growing energy crops rather than food crops, it may have an impact on food production and supply. Second-generation biofuels are produced from biomass waste or agricultural products, such as bagasse, rice straw, wheat straw, and cotton stalk. These biofuels are advantageous as they do not compete with food production.
It's important to note that while other renewable energy sources like solar, and wind do not contribute to air pollution, they may not offer the same widespread benefits to ecosystems as bioenergy does. Another aspect is that renewable energy can also impact the habitats of various organisms. For instance, solar powered systems require large land areas, leading to habitat reduction and the displacement of species. Because of these considerations, bioenergy stands out among renewable energy sources for its ability to support the sustainability of the environment and ecosystems.

Table 1.1 Biofuels classification

Biofuels classification	Feedstocks	Production technology	Fuels
First generation	Starch & sugar crops Vegetable oils	Fermentation Distillation Transesterification Hydrogenation Fischer-Tropsch Gasification Hydrolysis Pyrolysis Biotechnology	Biomethanol Bioethanol Butanol Biodiesel Vegetable oil Jet fuels (ATJ)
Second generation	Agricultural residues Forest residues Sawmill residues Wood waste Municipal solid waste		
Third generation	Algae		
Fourth generation	Engineered plants and microorganisms		

1.2 Alcohols and ethers

Alongside hydrogen, alcohols and their derivatives, ethers represent the main competitors from the energetic point of view (to replace fossil fuels). As mentioned before, the main attention is focused on their renewable version, i.e. bioalcohols, methanol and ethanol being considered two of the most promising alternative fuels.
In table 1.2 are presented the main properties of methanol, ethanol and isobutanol related to standard gasoline.

Table 1.2 Properties of 95 RON gasoline, methanol, ethanol and isobutanol [FOL22]

Fuel	Lower heating value (LHV) (MJ/(kg fuel))	h_{fg} (kJ/(kg fuel))	Density at NTP (kg/L)	RON/MON	Boling point at 1 bar (°C)	Stoich. AFR (mass) (−)	Stoich. AFR (mole) (−)	LHV (MJ/(kg stoich. air))	*hfg* (kJ/(kg stoich. air))	CO2 emission (g/MJ)
Gasoline 95	43.2	350	0.74	95.3/85.9	37–167	14.31	47.12	3.02	24.5	72.85
Methanol	20.09	1100	0.79	108.7/88.6	65	6.44	7.14	3.12	170.9	68.44
Ethanol	26.95	925	0.79	108.6/89.7	79	8.86	14.29	3.01	103.3	70.98
Isobutanol	33.08	585	0.81	106.3/90.4	118	11.14	28.57	2.97	52.5	71.90

Note that the properties of '95 RON gasoline' vary considerably depending on local refinery streams and other blend components; *LHV* = lower heating value, *NTP* = normal temperature and pressure, *hfg* = enthalpy ('heat') of vapourization.

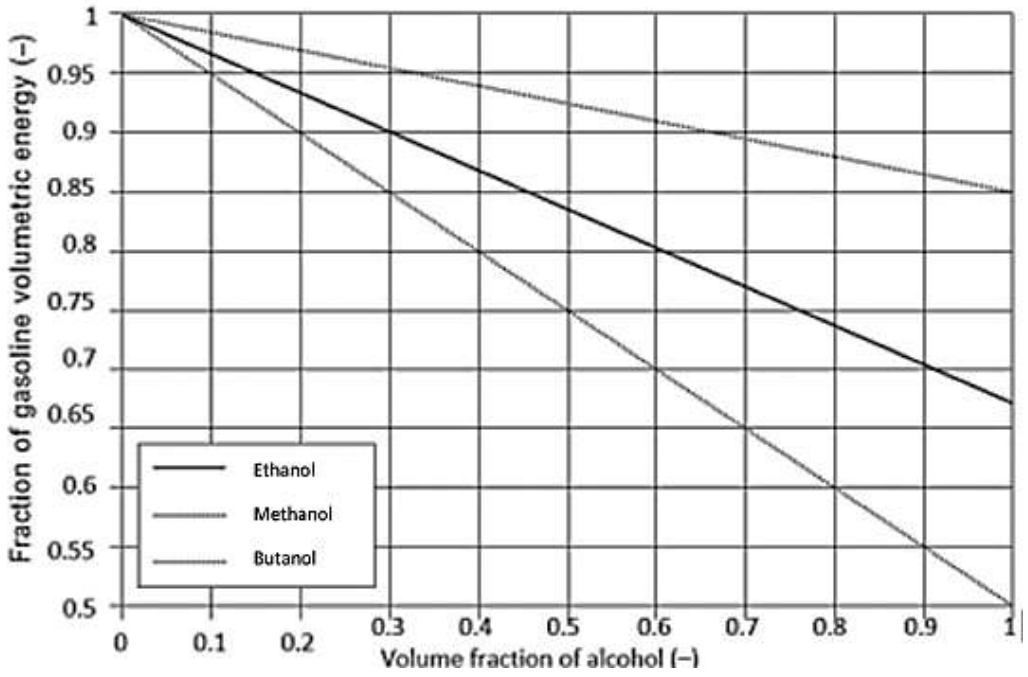

Fig. 1.1 Alcohol – gasoline blends: variation of volumetric energy density [FOL22]

In figure 1.1 is presented the influence of alcohol concentration over the volumetric energy density of alcohol – gasoline blends. For example, considering the case of 10% by volume alcohol concertation in gasoline, the volumetric energy density relative to gasoline is diminished by approximately 2% for butanol, 3,5% for ethanol and 5% for methanol. For 85% alcohol concentration the reduction of volumetric energy density is as follows: 13% for butanol,

28% for ethanol and 43% for methanol. This reduction of volumetric energy density implies engine optimization in order to overcame an increased fuel consumption.

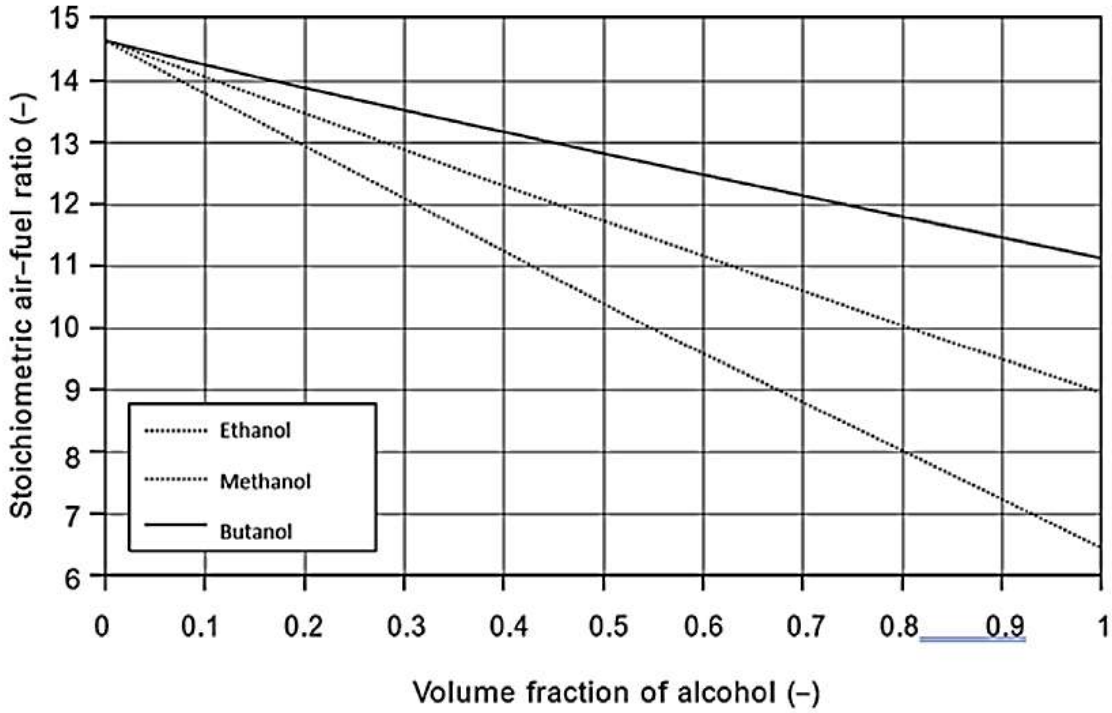

Fig. 1.2 Stoichiometric air - fuel ratio (AFR) of alcohol-gasoline blends [FOL22]

Figure 1.2 shows the stoichiometric air – fuel ration (AFR) of alcohol – gasoline blends. The graph above reveals that gasoline – butanol mixtures are closer to standard gasoline compared to ethanol / methanol – gasoline mixtures. The European standard for gasoline EN228 limits the oxygenates mass fraction to 2,7%. This has as equivalence of 7% volume of ethanol in blend (E7). This limit was increased to 10% (E10). Methanol is limited to 3% by volume. Regarding the ethers, the oxygenates 3,7% limit means approximately 22% methyl - tert-butyl-ether (MTBE) or ethyl-tert-butyl-ether (ETBE) by volume in gasoline.

1.2.1 Biomethanol

As a practical alternative to gasoline, biomethanol, CH_3OH has many benefits that help creating a more sustainable and ecologically friendly energy environment. Biomethanol is produced from renewable biomass feedstocks, like organic waste and agricultural residues, guaranteeing a permanent and sustainable energy source. Furthermore, being a carbon-neutral fuel, biomethanol has the ability to balance the CO_2 emissions produced during burning in ICE by using the carbon that is absorbed during the growth of biomass feedstock. As a result, greenhouse gas emissions are decreased, which helps to mitigate climate changes. Furthermore, burning biomethanol results in less pollutants than burning gasoline, which improves air quality and diminishes the harmful effects on human health.

Whether it is used in its pure form or mixed with gasoline, biomethanol demonstrates its

adaptability by directly replacing gasoline in modern internal combustion engines. This can be done without requiring significant changes to the current infrastructure. These aspects were demonstrated in extensive fleet testing in the `80s and `90s, and is now being reintroduced in a number of locations and uses.

Biomethanol is characterized by a high octane number, that determines a higher thermal efficiency. Also, being less volatile (high heat of vaporization 1100 kJ/kg) and burning at a lower temperature compared to gasoline, it is more difficult to start and warm up an engine in cold weather conditions. Due to its low specific energy (22 MJ/kg as opposed to 47 MJ/kg for gasoline), the fuel consumption is increased.

Methanol is characterized by a clean burning, reason for that it has been employed as a fuel involved in air quality improvement. Having only one carbon atom, it is difficult to produce the carbonaceous particulate matter typical of long-chain hydrocarbons. Second, methanol is the most basic liquid carbonaceous molecule at standard pressure and temperature.

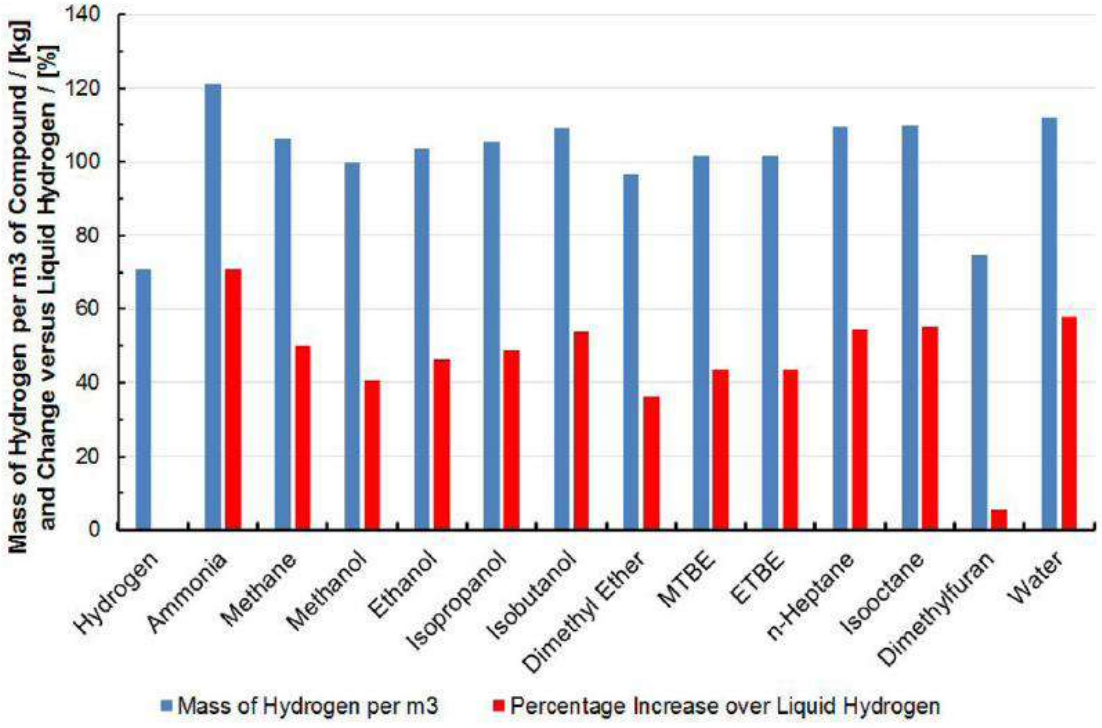

Fig. 1.3 Concentration of hydrogen in various fuel compounds (all in their liquid state) in terms of kilograms per cubic meter and change in this value relative to liquid hydrogen [VER19]

As mentioned before biomethanol can be produced from any carbonaceous stock through gasifying waste and using thermochemical processes (rather than biological ones). In this way, the process is quicker, the energetic yield is higher, and disruption induced to the food chain can be prevented. Another process is determined by using the existing industrial sources of hydrogen combined with atmospheric CO_2 or other available biogenic sources like pulp mills and bio-waste. In this case, the reaction is theoretically the following:

$$CO_2 + 3H_2 \rightarrow CH_3OH + H_2O \quad (1.1)$$

In this regard methanol can be seen as an excellent hydrogen carrier and from figure 1.3, it results that methanol contains 40% more hydrogen than liquid hydrogen.

Renewable methanol production at commercial scale is represented Carbon Recycling International plant in Iceland being the global leader in CO_2 to methanol technology, with over 200000 tonnes per year of installed sustainable methanol production capacity (captured CO_2 about 310000 tonnes/year and methanol production 214000 tonnes/year).

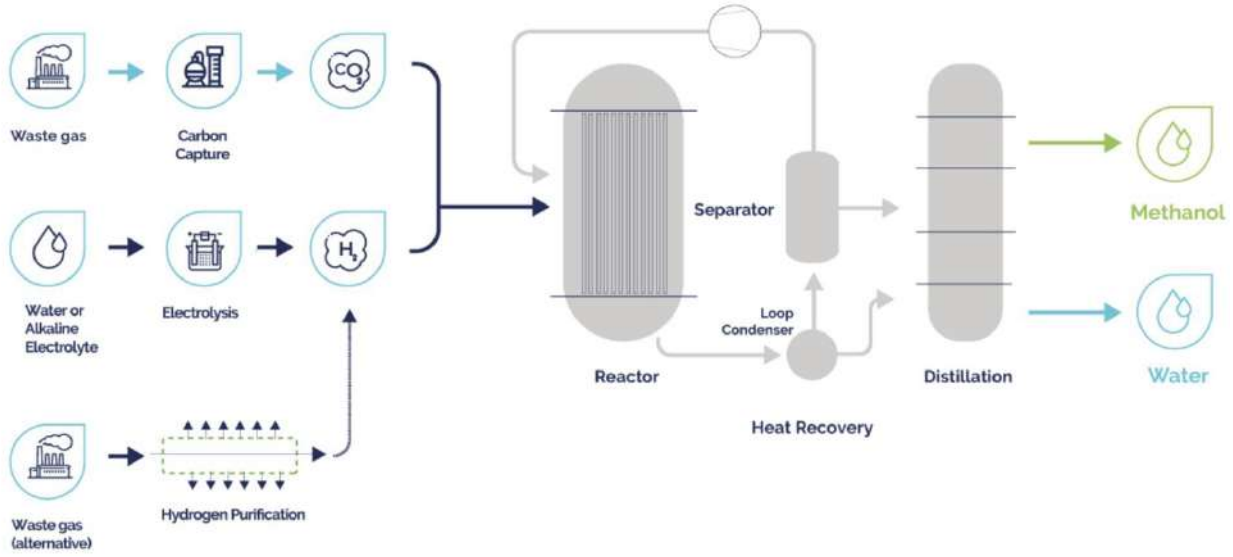

Fig. 1.4 CRI's emissions-to-liquids, renewable methanol process "ETL" [CRI24]

Methanol as fuel in ICE

Methanol is mostly regarded as a SI engine fuel because of its high heat of vaporization and great autoignition resistance. Methanol can be utilized as a blend ingredient or as a fuel in its pure form. Also, methanol can be added to gasoline separately and employed as an octane booster only when it's necessary to avoid knocking due to its high octane number and charge cooling effect. Therefore, a higher compression ratio or an increased boost pressure can be adopted, together with an improvement in the vehicle fuel consumption. Ideally, the overall alcohol consumption is lower compared to the situation on a methanol-gasoline blend.

Another application is in naval engines where methanol is used as a source of ignition. In Diesel engines it was adopted the Diesel methanol compound combustion (DMCC), where two combustion modes are considered: a diffusion combustion with Diesel fuel and the other is a premixed air/methanol mixture ignited by the Diesel fuel.

The methanol high oxygen content lowers the energy level (heating value). Fuel tank and the design of fuel injection system depend on the volumetric energy content. The volumetric energy content of methanol is half that of gasoline, despite its higher density the heating value is less than half that of gasoline. As a result, injection durations must be doubled to deliver the same amount of fuel/energy to the engine, which implies for appropriate injectors.

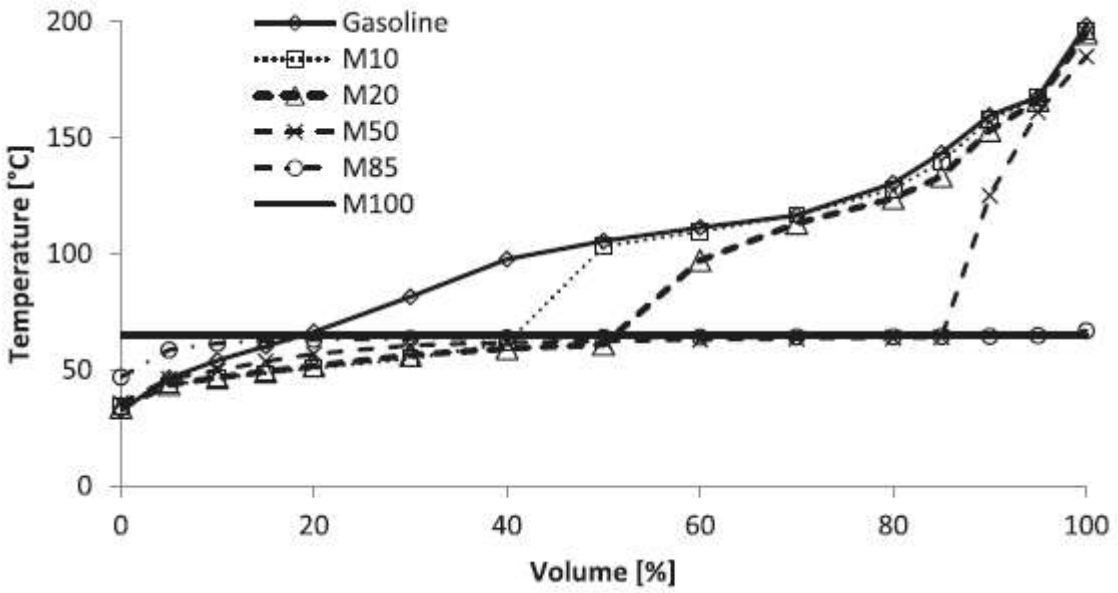

Fig. 1.5 Distillation curve of methanol-gasoline blends [SIL15]

Methanol also is characterized by a low vapor pressure. This lower volatility, correlated with a superior lower flammability limit in air (a flammable mixture is obtained only with a higher concentration of vapors), leads to a more challenging cold start. Methanol-gasoline blends have near-azeotropic behavior, which is demonstrated by a slower-rising distillation curve that shows less volatility than that of the base gasoline.

In the case of spark ignition (SI) engines, the danger of autoignition/knocking is lower, thus some technical solutions can be used: a higher compression ratio (increasing engine efficiency), a superior boost pressure, an optimal spark timing throughout the engine operating map Additionally, the cooling impact raises intake air density, which boosts volumetric efficiency. This improves the engine's power density. A low temperatures disadvantage is represented by the challenge to obtain a fast catalyst warm up.

In the case of SI direct injection engines, the high heat of vaporization, correlated with low stoichiometric air/fuel ratio, determines a high degrees of intake charge cooling as the fuel evaporates (latent heat), with direct impact on engine efficiency, avoiding in the same time the knock tendency in some conditions (e.g., high pressure and compression ratio).

Because of its extremely low cetane number, methanol requires accurate solutions in order to be used in compression ignition (CI) engines. However, in order to guarantee fuel autoignition, the majority of solutions use a high cetane number fuel, primarily diesel fuel. An alternative for pure diesel is to inject a methanol-diesel mixture. However, because mixing diesel and alcohol is problematic, emulsifier agents being required, and even then, the methanol fraction is limited. This is determined due to fact that an increased methanol fraction will induce a reduced fuel's volumetric energy content, injection systems must be optimized, considering too, the methanol low lubricity compared to diesel fuel (lubrication additives must be added). An appropriate technical solution is the dual fuel one, in which diesel and methanol are

introduced separately into the cylinder. Like diesel direct injection, methanol can be injected into the combustion chambers, then methanol is then ignited using the diesel fuel as a pilot injection.

Reducing NO_X and PM, the two primary pollutants emitted by diesel engines, represents the goal of converting the base diesel engine to dual fuel operation with methanol. The dual fuel operation generates, in general a decrease in NO_X emissions across the engine load and speed range. Considering the engine load and the amount of methanol fraction, this reduction can range from 6% to over 50% [CHE09, YAO08]. By raising the substitution ratio, the diminish becomes more noticeable, due to the cooling effect of the methanol injected into the engine's intake. It significantly reduces thermal NO_x generation by lowering in-cylinder temperatures. The premixed combustion of methanol reduces the combustion duration, and peak in-cylinder temperature determining a less time for NO_x formation. Also, the soot emissions are suppressed due to this dual fuel system, diesel fuel being replaced by methanol that is C-C bonds and aromatics free.

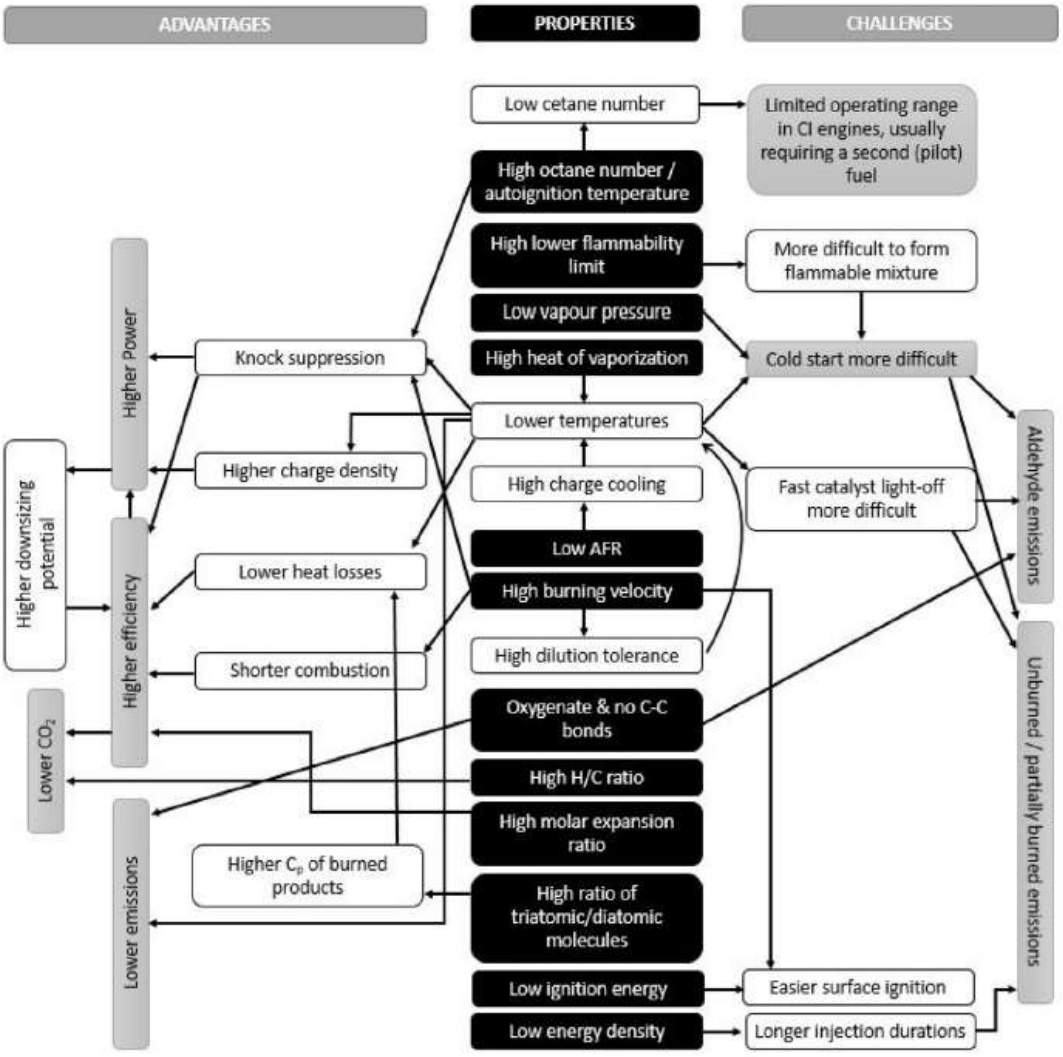

Fig. 1.6 Methanol properties effect over the engine performance [VER19]

Previously, some of the advantages and challenges of using biomethanol in internal combustion engines were presented.

In the present all vehicles equipped with SI engines, are able to run-on low-level blends, i.e., where the methanol fraction falls within current gasoline specifications (e.g., in the case of EN228, up to 3 vol% of methanol).

Methanol is promoted as a long-term renewable fuel that is burning cleaner and enhancing air quality. It is the most straightforward fuel that is liquid under air conditions among those that can be produced from renewable resources. As a result, it has the potential to have zero net carbon emissions.

1.2.2 Bioethanol

In the present ethanol (C2H5OH is the most important biofuel, with an increasing global annual production, that is represented in figure 1.7. From the ethanol consumed by the road transport sector in 2023, the United States produced 53%, with Brazil producing 28% and the EU 5% [ETH23]. In EU the ethanol production feedstock is represented by wheat, corn, sugar beet, rye and barley. Approximately 70% of the world's biofuels production is represented by ethanol.

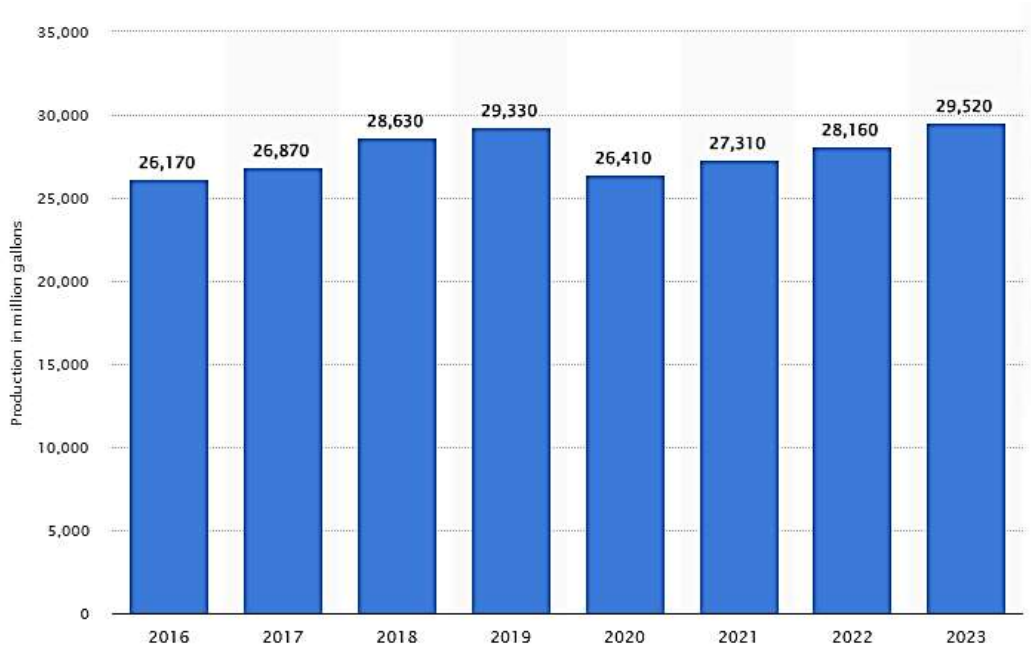

Fig. 1.7 Annual production of bioethanol [STA23]

Fermentation followed by distillation is the most common method for turning biomass into ethanol. Fermentation is a biochemical conversion process that uses microorganisms (enzymes or bacteria) to decompose biomass. A wide variety of biomass feedstocks can be utilized with this method. In the case of starch and lignocellulose that are polymers, the hydrolysis is the process that produce sugars for fermentation.

The use of a gasification method to produce ethanol from waste materials has been the focus of recent efforts. The whole procedure involves thermochemically converting the synthesis gas, followed by a catalytic process that transforms it into higher molecular weight alcohols, and finally distillation to isolate the high purity ethanol.

The procedure is comparable to the gas-to-liquids and methanol operations of today. The catalysts and their working conditions are the primary differentiators.

Ethanol purity needs to be almost 100% for fuel uses. This implies that there must be a significantly reduced water content.

Due to the lack of competition with food production, the use of lignocellulosic biomass for second-generation ethanol production is preferred over first-generation ethanol production based on sugar and starch. The lignocellulosic biomass consists of agricultural wastes (corn stover, wheat, or rice straw), sugarcane bagasse, grass, household trash, and energy crops.

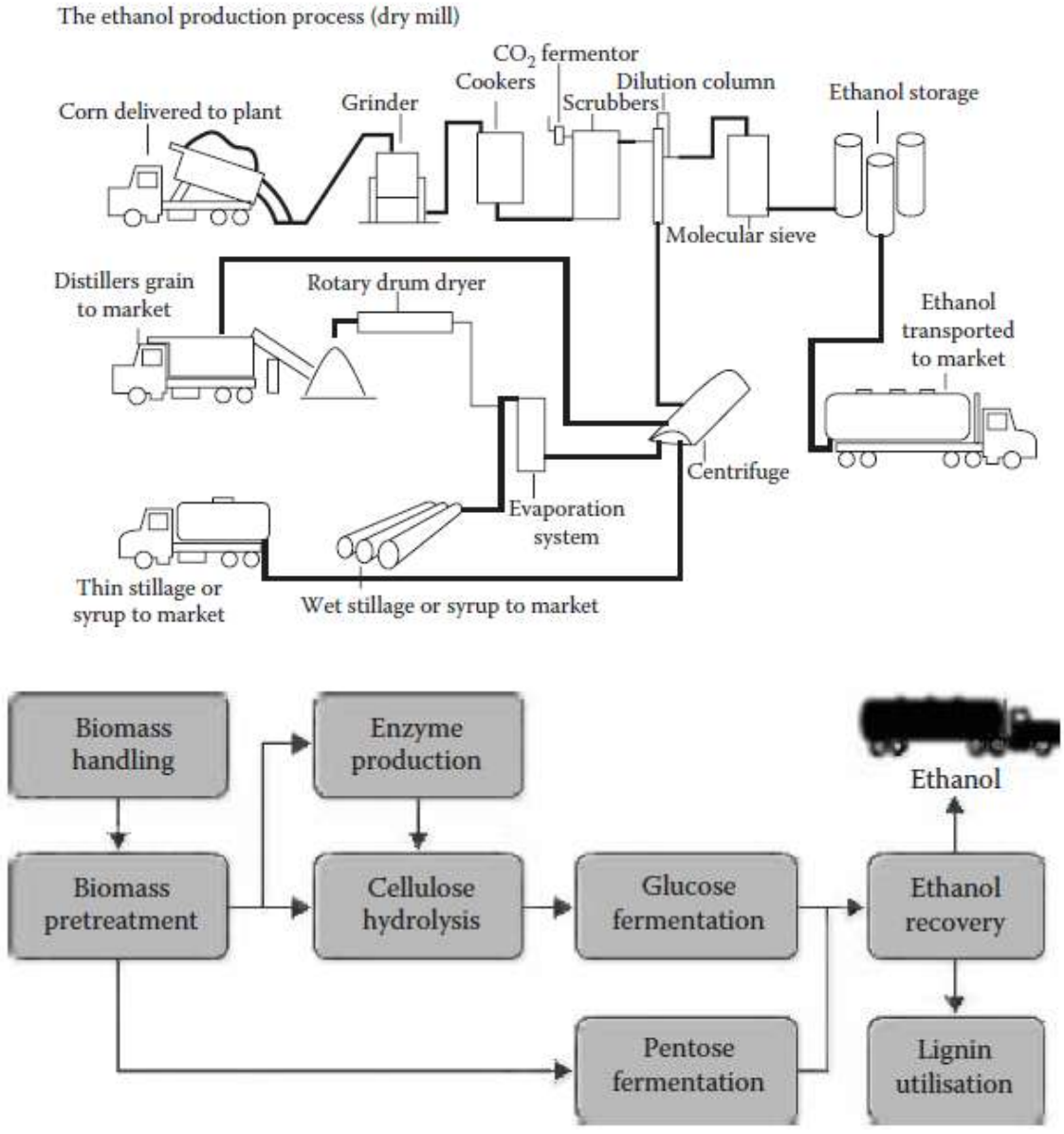

Fig. 1.8 Ethanol production: process from corn feedstock and biochemical conversion

Ethanol as fuel in ICE

Ethanol is added to gasoline fuels as a blending agent. Its amount varies greatly, ranging from E5 to E85 (E5, 5% of ethanol in the blend). Also, E95 and E100 blends are used. In EU ethanol is used as a 10% by volume blended with gasoline without need for any engine modification. It has been gradually implemented throughout Europe, being available in 19 countries.
Modern flex-fuel vehicle (FVV) engines can now burn any percentage of the resulting gasoline and ethanol mixture. An additional fuel mixture composition sensor detects the actual blend, and fuel injection and spark timing are changed accordingly.

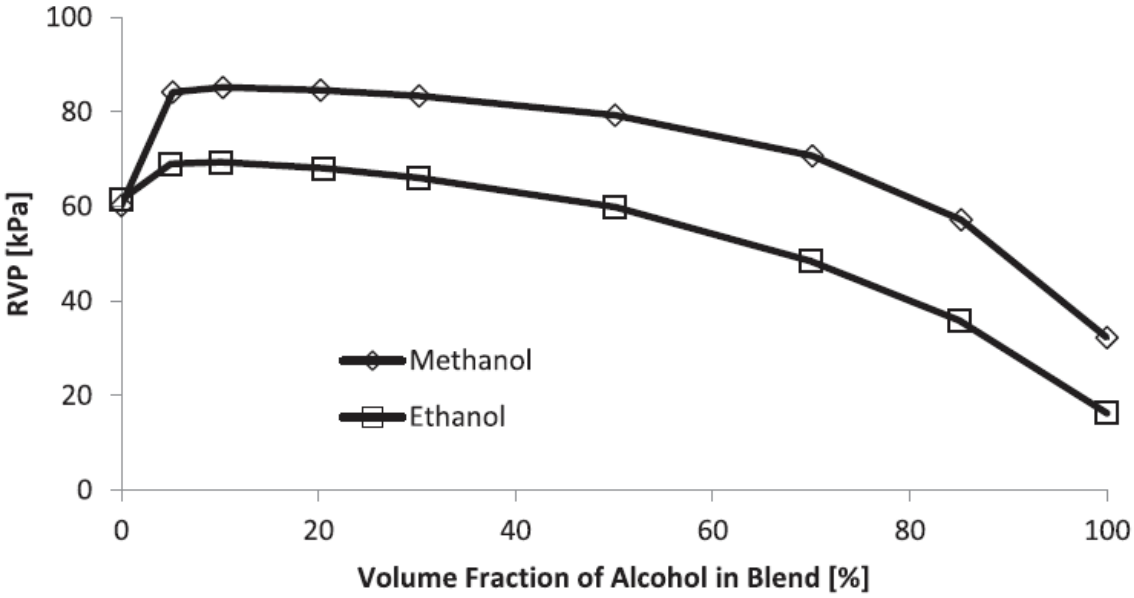

Fig. 1.9 Methanol, ethanol Reid vapor pressure (RVP) [SIL15]

Figure 1.9 characterizes the Reid vapor pressure variation depending on the alcohol concentration by volume in gasoline mixture. Methanol / ethanol – gasoline mixtures register a peak value around 10 % by volume of alcohol, then this trend diminishes with increasing alcohol concentration. Also, the RVP evolution in case of ethanol mixtures is less pronounced compared to methanol addition (the ethanol vapor pressure is lower).
Methanol and ethanol are single component fuels with a single, defined boiling point. Unlike gasoline they do not contain volatile components that can improve cold start ability.
Compared to gasoline, ethanol has a higher octane number, wider flammability limits, superior flame speed, and greater heat of vaporization. Theoretically, these characteristics give internal combustion engines an efficiency advantage over gasoline by enabling a greater compression ratio, shorter burn period, and leaner burning process.
However, the drawbacks of ethanol include its low flame brightness, low vapor pressure, corrosiveness, miscibility with water, and lower energy density than gasoline.
Ethanol has a weight percentage of 35% oxygen, whereas gasoline has no oxygen. Because oxygen determines a more thorough burning, there are fewer tailpipe emissions. Ethanol

combustion significantly lowers emissions of carbon monoxide, volatile organic compounds, particulate matter, and greenhouse gasses when compared to gasoline combustion. In terms of energy, a liter of ethanol contains about 32% less than a liter of gasoline, and this must be compensated in a certain extent through engine functioning parameters setup, based on high ethanol high octane rating.

Two factors must be taken into account when using ethanol in a spark ignition engine: the first is that ethanol has a far lower calorific value than gasoline, and the second is that significantly less air is needed to generate a stoichiometric air – fuel mixture (1/9 vs. 1/14.7). Accordingly, the engine uses more ethanol, but because of the reduced air – fuel ratio, the engine's maximum power can be raised. And this because for the same engine displacement, more fuel may be injected into the cylinder.

The increased thermal efficiency of ethanol and its mixtures can be explained through the superior heat of vaporization, that consumes more energy. Also due to the cooling effect the engine volumetric efficiency increases in the case when the ethanol injection is made in the intake manifold.

Ethanol also improves the combustion process efficiency through heavy fraction free content, compared to gasoline.

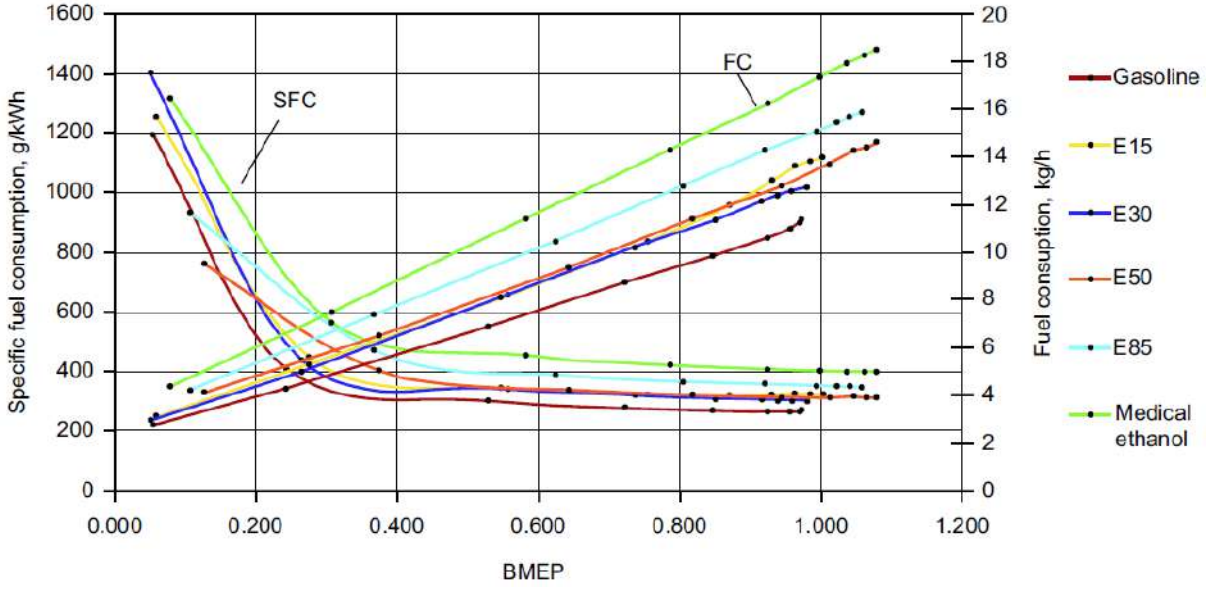

Fig. 1.10 Specific fuel consumption and fuel consumption at different values of effective pressure. FC – fuel consumption; SFC – specific fuel consumption [BAS19]

As can be seen from figure 1.10 the specific fuel consumption is higher int the case of ethanol mixtures, especially when E50 – E100 fuels are used. In order to decrease the specific fuel consumption, it is necessary to make changes in engine mapping.

By ecological point of view, in spark ignition engines running on ethanol, the amount of nitrogen compounds, carbon monoxide, and hydrocarbons in the exhaust gases is reduced.

The percentage of nitrogen compounds typically tends to decrease, the degree of reduction

depends on ethanol proportion in the blend. This reduction is determined by the high evaporation heat of ethanol.

The increase in ethanol heat of vaporization is caused by its water content, which slows the evaporation process and may leave some fuel drops in the air-fuel mixture unvaporized. It takes longer for unvaporized blend to burn, and the amount of carbon monoxide in the exhaust gases rises as well. However, because of the more effective combustion process compared to standard gasoline, the amount of carbon dioxide in engine exhaust gases generally increases while the amount of carbon monoxide reduces. In contrast, incomplete combustion is characterized by carbon monoxide. The amount of carbon dioxide in the exhaust gases rises in proportionally with the combustion process' efficiency increasing.

Additionally, the percentage of unburned hydrocarbons decreases as combustion efficiency rises. The exact engine adjustment is essentially responsible for the drop in the percentage of hydrocarbons in the exhaust flow. The percentage of hydrocarbons rises when an engine runs on rich air – fuel mixture.

In the case of diesel engine, functional adjustments are necessary when ethanol is added to diesel fuel, because the low calorific value of ethanol influences the engine's power loss if it is not adjusted.

In the ecological field when using ethanol and diesel fuel, the exhaust compounds CO, CO_2, NO_x and soot decrease in both cases as blend or as additional fuel (ethanol is injected in the intake manifold). The decrease of NO_x emissions is determined by the ethanol high vaporization heat, that lowers the peak temperature in the cylinder. Soot diminish is conditioned by the decrease of diesel fuel proportion in the air – fuel mixture. Developed studies also reveal that level of water content in ethanol influences the soot emission in a negative manner, fact that determines a worsening of the combustion process.

However, the percentage of hydrocarbons rises when ethanol is utilized. In engines using a common rail fuel supply system, the percentage of hydrocarbons drops at low loads, but only if ethanol accounts for less than 30% of the air fuel mixture [BAS19]. The amount of hydrocarbons in the exhaust gas rises in tandem with the amount of ethanol in the air – fuel mixture.

The lengthening of the combustion process is the primary source of the hydrocarbons increase in the exhaust gases. In particular, ethanol lengthens the ignition delay and lowers the cylinder's combustion pressure, which means the air – fuel mixture takes longer to burn. On the other hand, controlling the injection timing can solve this problem. A partial drop in combustion pressure determines a lower of combustion temperature with effect in reduction of nitrogen compounds.

The combustion pressure is a major parameter in the examination of an engine's combustion process. The effect of ethanol over the combustion process and heat release rate is seen in fig. 1.11. The data are collected from a normally aspirated engine. The difference in combustion pressure evolution, can be observed especially between 370 and 390 degrees. The pressure

magnitude is proportionate with the amount of ethanol in the air - fuel mixture, the increase of ethanol quantity determines a pressure drop in the engine cycle. Regarding the heat release rate, it is evident that the rise in ethanol in the air - fuel mixture causes a corresponding delay in energy release. Furthermore, the heat release rates graphs make it clear that burning an ethanol-containing air - fuel mixture takes longer.

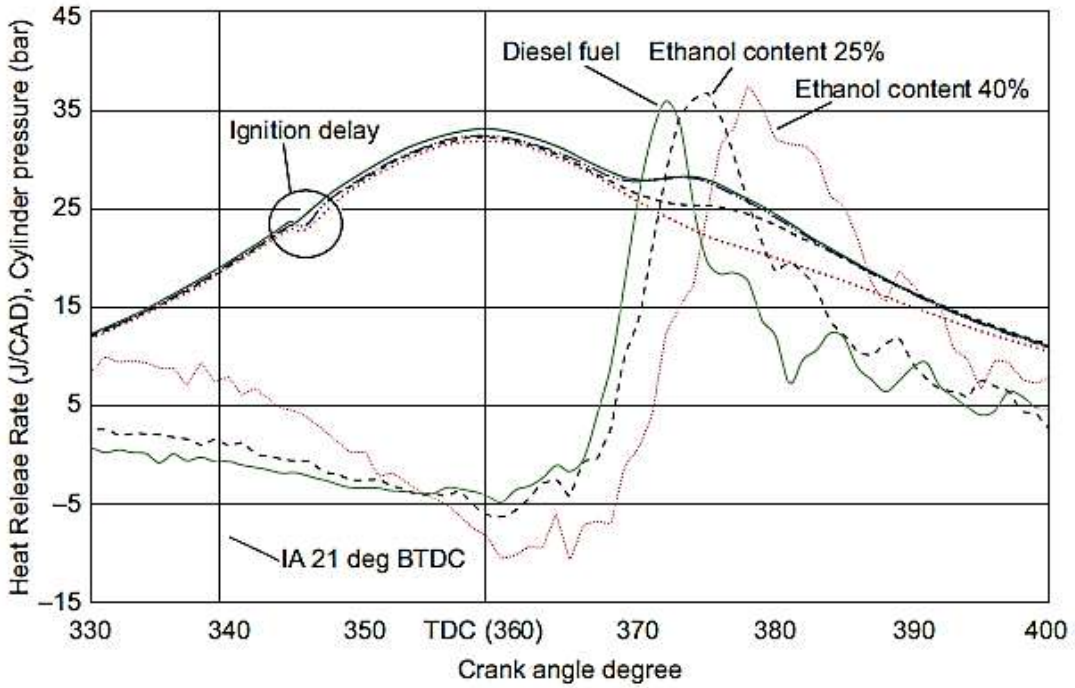

Fig. 1.11 Combustion of diesel and ethanol blends [BAS19]

A major problem in ethanol usage in diesel engines is represented by the lack of lubrication properties and the corrosion effect on engine parts. Additives must be added in order to solve this aspect and to avoid wearing, corrosion of the fuel supply system (nanocomposite materials and special alloys).

1.2.3 Ethers

Ethers are functional derivatives of hydroxyl compounds, formally resulting from two alcohol molecules by eliminating a water molecule.

$$R'\text{-}OH + R\text{-}OH \rightarrow R'\text{-}O\text{-}R + H_2O \quad (1.2)$$

High-octane fuel manufacturing relies heavily on fuel ethers, such as MTBE, bio-MTBE, bio-ETBE, TAME, bio-TAME, and TAEE. They are a safe and effective substitute for substances that have been shown to be harmful to both human health and the environment, including toxic lead. Fuel ethers have a higher energy density than alcohols, regardless of whether they are made from conventional hydrocarbons or renewable biomass. As a result, they improve the performance of gasoline while lowering CO_2 and air pollution emissions throughout their entire cycle.

Currently the following products are used as fuel components:

- ✓ MTBE - methyl tert-butyl ether – CH_3-O-C_4H_9;
- ✓ ETBE - ethyl tert-butyl ether – C_2H_5-O-C_4H_9;
- ✓ TAME - tert-amyl methyl ether – C_5H_{11}-O-CH_3;
- ✓ TAEE - tert-amyl-ethyl-ether – C_5H_{11}-O-C_2H_5.

In general, ethers' properties are more like those of gasoline than alcohols. Ethers do not undergo phase separation in the presence of water, unlike methanol and ethanol. They have no harmful effects over the elements of the fuel supply system and are miscible in gasoline.

MTBE, ETBE are mainly used as blending components for gasoline due to their high octane number (octane booster).

The chemically accessible oxygen in ethers lowers the production of carbon monoxide and other toxic pollutants when they are mixed into gasoline.

Table 1.3 Physical and blending properties of ethers [ELV22]

	MTBE	ETBE	TAME	TAEE
Molecular mass	88	102	102	116
Oxygen, (wt%)	18.2	15.7	15.7	13.8
Boiling point, (°C)	55	72	86	102
RVP[a] blending, (kPa)	55.2	27.6	10.4	9.0
Density, (kg/l)	0.74	0.75	0.77	0.77
RON, blending	117	119	110	108
MON, blending	102	103	99	95

a) Reid vapor pressure.

Because of its excellent blending qualities, low volatility, complete miscibility with gasoline, low susceptibility to phase separation, MTBE emerged as the compound most likely to dominate the oxygenates market right away. Moreover, it is inexpensive and easy to synthesize.

In EU countries MTBE, ETBE are used as high-octane components for gasoline according to the different legislations (e.g. some national norms).

The synthesis of TAME/TAEE can be used to enhance the overall characteristics of the fuel blend. These etherification processes actually enable the reduction of Reid vapor pressure, olefin and sulfur content, dilution of aromatic compounds, and the addition of some oxygen to the final product.

The advantage of ethers over alcohols becomes much clearer when volatility is taken into account, even if the density and knocking resistance of oxygenates are fairly equal. The RVP and the form of the neat gasoline distillation curve are essentially unaffected by ethers (no significant distortion of the distillation curve). However, when blended with gasoline, alcohols,

which have better volatility properties when viewed as neat compounds, behave nonlinearly. This is because the alcohols have very high blending RVP values that are typically outside of the gasoline specifications because of the formation of azeotropes with the light hydrocarbon components.

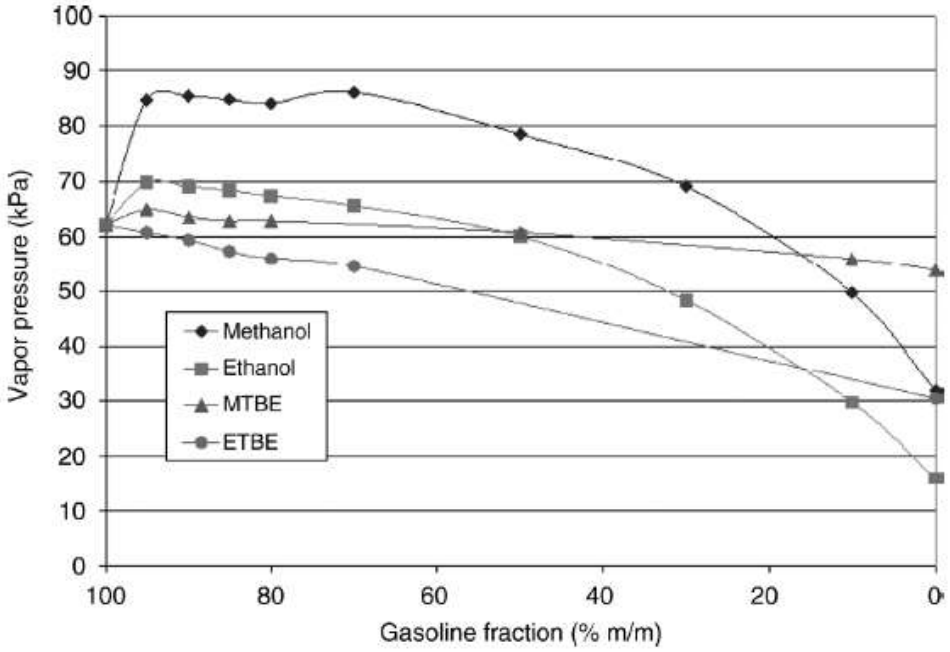

Fig. 1.12 Vapor pressure by mixing of methanol, ethanol, MTBE, and ETBE in gasoline according to EN 228 [LAC10]

Another significant benefit of ethers is their total miscibility with hydrocarbons, which removes the need for specific storage and distribution protocols for etherified gasoline. On the other hand, when modest amounts of water are present, alcohols—methanol in particular—have a significant tendency to phase separate, losing their octane quality and creating issues with network distribution.

Also, ETBE has a positive economic impact by mitigating the need to remove light components such as butanes/pentanes from neat gasoline, like the scenario when ethanol is used.

To meet the volatility specification limit, especially during summer time, gasoline containing ethanol (E5 or E10) requires adjusting the neat gasoline formulation and removing light, inexpensive gasoline components like butanes and pentanes. Additionally, in Europe, under specific circumstances, an additional vapor pressure waiver may be granted to facilitate the ethanol usage.

Compared to alcohols, the ethers offer a better compatibility with seals and gaskets.

Compared with other oxygenated fuels, ether have some important advantages, including the ability to burn in existing IC engine and the property to reduce pollutants (e.g. lower VOCs emission) and greenhouse gas emissions.

1.2.4 Biodiesel

Biodiesel represents a renewable fuel for diesel engines that can be manufactured from vegetable oils, animal fats or recycled restaurant grease. There are numerous feedstocks from which it can be made. Animal fats (usually tallow), algae biomass or waste oils (frying and cooking oils) can also be utilized, but vegetable oils (such as rapeseed, soybean, cottonseed, palm, peanut, sunflower, sunflower, and coconut) are used most frequently.

Biodiesel can be classified according to the type of feedstock used for its production. By this criterion it can be:

- ✓ first generation biodiesel: it is produced from vegetable oil such as rapeseed, soybeans, palm oil, sunflower, rapeseed, and peanut;
- ✓ second generation biodiesel: are typically made from nonfood crops, forestry wastes, biomass sources, waste vegetable oils and fats, and other inedible feedstocks.
- ✓ third generation biodiesel: is obtained from algae.

When used as fuel, biodiesel significantly lowers harmful pollutants while also being nontoxic and biodegradable. Technically, biodiesel is a fuel for diesel engine that satisfies ASTM D6751 standards and is made up of monoalkyl esters of long-chain fatty acids obtained from vegetable or animal fats.

In the presence of a catalyst, biodiesel is usually made by reacting vegetable or animal fat with methanol or ethanol to generate glycerin and methyl or ethyl esters of fatty acid (biodiesel, FAME). Since methanol is less expensive than ethanol, it is typically chosen for transesterification.

Biodiesel is compatible with fossil diesel fuel in all ratios; in fact, in many nations worldwide, it is more frequently utilized in blends with regular diesel than as pure biodiesel. A most common one is B20, a combination of 20% FAME and 80% pure diesel. Thus, a B0 fuel would be a clean fossil diesel fuel, while a B100 fuel would be a clean biodiesel. The percentage represents volume percentage rather than mass percentage. In Europe EN 16709:2024 represents the standard that specifies requirements and test methods for marketed and delivered high FAME (B20 and B30).

The vehicle manufacturer's clearance is need for the use of biodiesel as neat fuel or in blends that contain more than 7%. Biodiesel. It may cause issues, such as attacking rubber and plastic parts. Particle filters are no exception. Verifying that the particle filter and vehicle engine are authorized for the use of biodiesel is essential.

When used biodiesel generates a higher consumption than neat diesel fuel, a little less power and torque. But when it comes to sulfur level, flash point, aromatic content, and biodegradability, biodiesel outperforms diesel fuel. Because biodiesel may gel more quickly than diesel in cold climates.

Table 1.4 Biodiesel properties

				First-Generation Biodiesel				Second-Generation Biodiesel			Third-Generation Biodiesel
ıperty	Units	Diesel	ASTM Biodiesel D6751	Palm	Linseed	Rapeseed	SOY	Karanja	Jatropha	Waste Palm Oil	Algae
ısity	kg/m³	837.8	–	878.4	865	884.9	885.2	860	897	875	872
cosity	mm²/s	3.275	1.9–6.0	4.698	4.2	4.585	4.057	6.87	5.65	4.4	5.82
tane number	–	50.6	≥47	62	48	54.5	51.3	50	49	60.4	–
lorific value	MJ/kg	45.85	–	39.91	40.759	39.9	39.66	38.5	37.9	38.73	40.8
sh point	°C	68	130	189	161	177	173	175	187	70.6	–
ır point	°C	–35	–	–	–18	–	–	–	–	–	–16
stillation 0% volume)	°C	–	–	–	–	320	319	–	–	331	–
stillation 0% volume)	°C	–	–	–	–	339	337	–	–	348	–
fur	–	0.0019	–	0.0005	–	0.0001	0.0003	–	–	–	–

rce: Lin, B.-F., Huang, J.-H. and Huang, D.-Y. (2009), Experimental study of the effects of vegetable oil methyl ester on DI diesel engine performance characteristics and pollutant emissions, *Fuel*, 88(9), 1779–1785; Nautiyal, P., Subramanian, K. A. and Dastidar, M. G. (2014), Production and characterization of biodiesel from algae, *Fuel Processing Technology*, 120, 79–88.

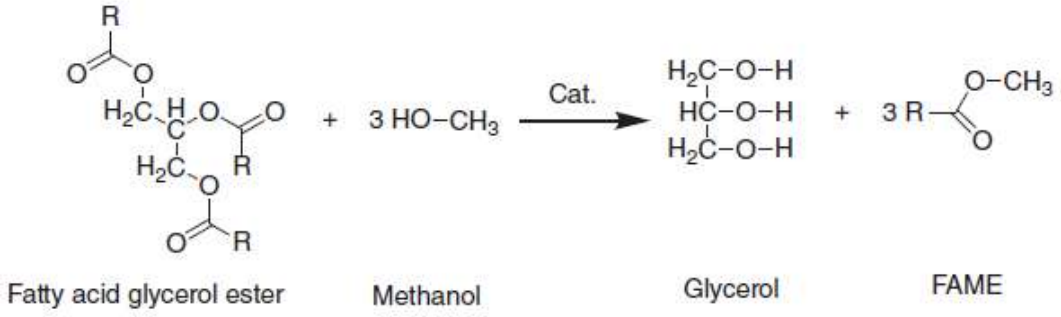

Fig. 1.13 The transesterification reaction – biodiesel production [ELV22]

The reaction that is the basis of the transformation of vegetable oil into biodiesel is represented in figure 1.13. The fatty acids in oils are under the form of triglycerides. In transesterification process, the triglyceride reacts with an alcohol to form esters and glycerol. A catalyst (e.g., KOH, NaOH) is usually used to enhance reaction rate and yield. Excess alcohol is utilized to move the equilibrium to the product side because the reaction is reversible.

Transesterification is one of the most popular ways to reduce the viscosity of fatty acids, that represents a significant issue with the usage of pure fatty acids and vegetable oils. For the simple reason that methanol is the least expensive alcohol, the methyl esters are usually manufactured.

Through transesterification of a vegetable oil and its transformation into methyl ester of the vegetable oil, the size of the component molecules was reduced by about 3 times and as a result the viscosity was substantially reduced by about 7-8 times, coming very close to that of diesel fuel. In addition, a much better behavior in the cold condition is obtained. Generally, through esterification a rise in cetane number, a decrease in viscosity, and a decrease in the boiling point is obtained. Biodiesel's viscosity is an essential characteristic since it affects how injection system works, particularly at low temperatures when the fuel's fluidity is impacted by the viscosity increase. A high viscosity causes the fuel spray to be poorly atomized, which makes the fuel injectors operate less precisely. It is easier to pump and atomize biodiesel to produce finer droplets for combustion when its viscosity is lower.

The cetane number (CN) is a measure of autoignition quality of diesel fuels; high CN value determines short autoignition delay, giving more time for combustion to finish. High CN fuels are more efficient for high-speed diesel engines. The biodiesels CNs are generally higher than conventional diesel (CN values in the range of 40–45).

For operation in cold climates, cloud point (CP) and pour point (PP) of the fuel are also important parameters. Biodiesels have both higher CP and PP compared with conventional diesel.

Another problem that must be considered in the case o biodiesel is the diesel particulate filter (DPF) regeneration. The energetic content of biodiesel being lower it is more difficult to reach regeneration temperatures. This makes it necessary to do more prolonged post-injections, and in some circumstances determines an increased level of engine oil dilution.

Biodiesel blends in Diesel engines

The effect of using biodiesel as fuel for compression-ignition engines' combustion performance, and emissions characteristics must be considered.
Compared to base diesel, biodiesel has a greater cetane number, making it a better fuel for compression-ignition engines.
Injection parameters (e.g. pressure, timing), spray configuration, autoignition delay, combustion characteristics influence the engine's performances and the pollutant emissions type. Due the fact that biodiesel physicochemical properties (e.g. viscosity, surface tension, density, distillation curve) are not exactly the same as those of diesel fuel, the injection and spray characteristics will differ for an engine running on biodiesel.
The fuel's compressibility is shown by the bulk modulus. Because biodiesel has a larger bulk modulus (1500 MPa) than base diesel fuel (1350 MPa), the diesel engine's injection timing advances when it is powered by biodiesel. Biodiesel's higher fuel density accelerates the injection timing start. As the proportion of biodiesel in diesel fuel increases, the injection pressure, injection timing, and duration will increase, too.
Because biodiesel has a larger density than base diesel, its breakup length is superior. This is primarily due to density. Reducing the nozzle hole diameter and raising the injection pressure will shorten the breakup length.
Because biodiesel has a higher density than diesel fuel, its breakup length is longer. This is primarily due to superior density of biodiesel. Reducing the nozzle hole diameter and raising the injection pressure will shorten the breakup length. The fuel droplet mean diameter influences the mixing rate. For droplet's larger size due to a poor heat transfer rate from air, the vaporization rate will be poor, too.
Because biodiesel has a larger density, viscosity, and surface tension, its droplet mean diameter is higher. Compared to neat diesel, all biodiesel-diesel blends have a higher spray penetration rate. Increased spray penetration can cause wall impingement but is good for air entrainment. On the other hand, excessive spray penetration would cause wall impingement on the cylinder wall and piston bowl, while insufficient spray penetration would result in inefficient air use in fuel spray. The superior spray penetration with biodiesel is determined by the higher injection pressure. A way to improve spray penetration is to optimize the injector nozzle hole diameter. The injection pressure, hole diameter, air pressure and movement influence spry penetration and cone angle. Depending on engine speed and load the penetration must be optimal in order to avoid inappropriate air usage and wall impingement. The droplet wall impingement may be either dry or wet impingement. The phenomenon will affect mixture preparation and will also generate deposits in the combustion chamber with direct effects over engine durability, performances and emissions.

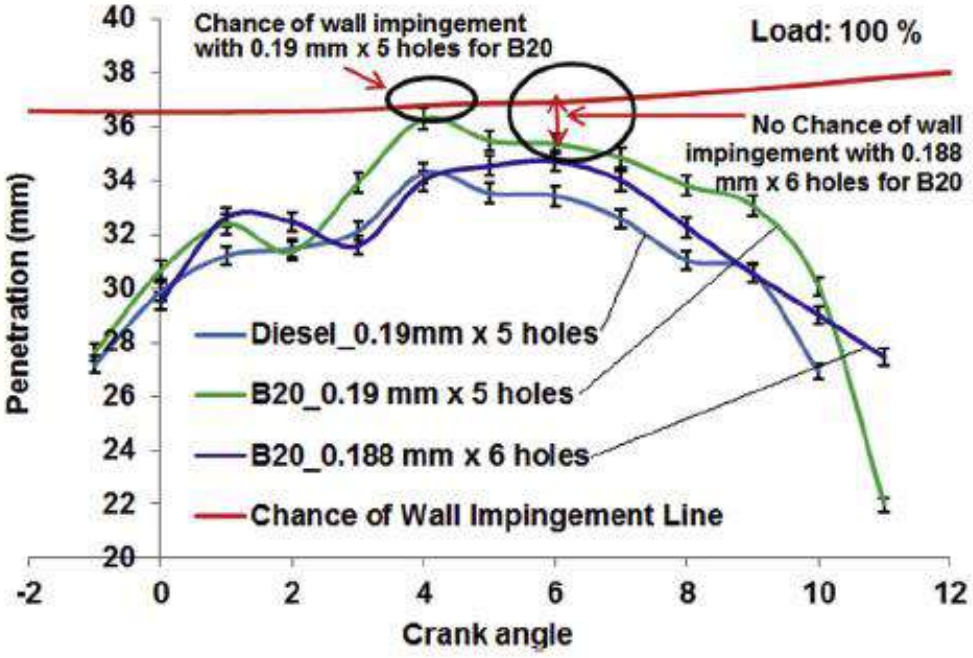

Fig. 1.14 Variation of spray penetration and wall impingement for diesel and B20 [LAH14]

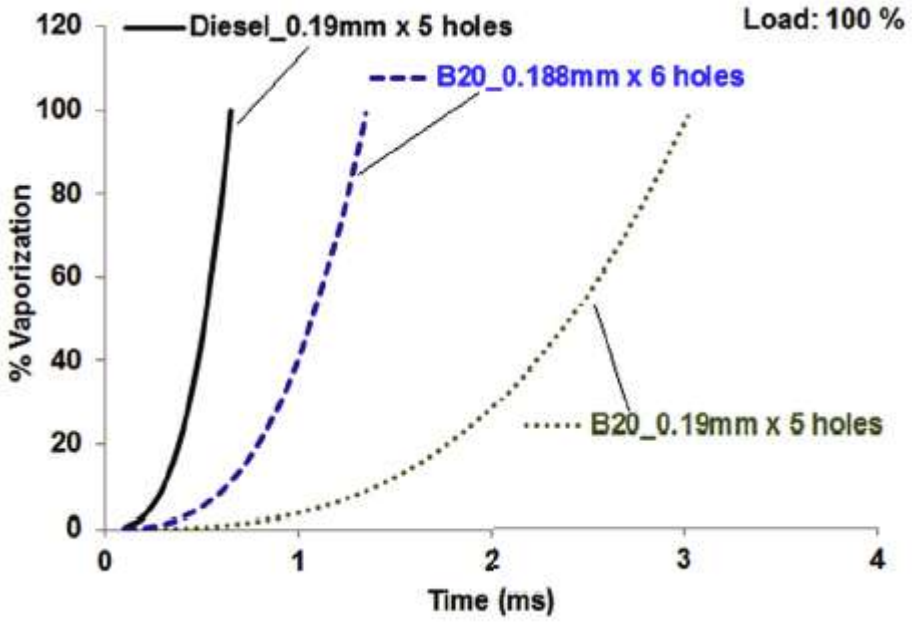

Fig. 1.15 Vaporization percentage variation for diesel and B20 [LAH14]

Figure 1.14 shows that in the case of smaller diameter of nozzle hole the penetration distance decrease and the chances of wall impingement is reduced. It is an example of an injector optimization including total number of nozzle holes and their diameter, solution that reduces the chance of wall impingement in the case of a diesel engine fueled with biodiesel blend (B20).

The vaporization percentage of biodiesel is influenced by the nozzle holes diameter. By reducing the diameter of the nozzle holes is obtained a smaller Sauter mean diameter (SMD). Anyway, the vaporization biodiesel blends compared to pure diesel is still lesser.

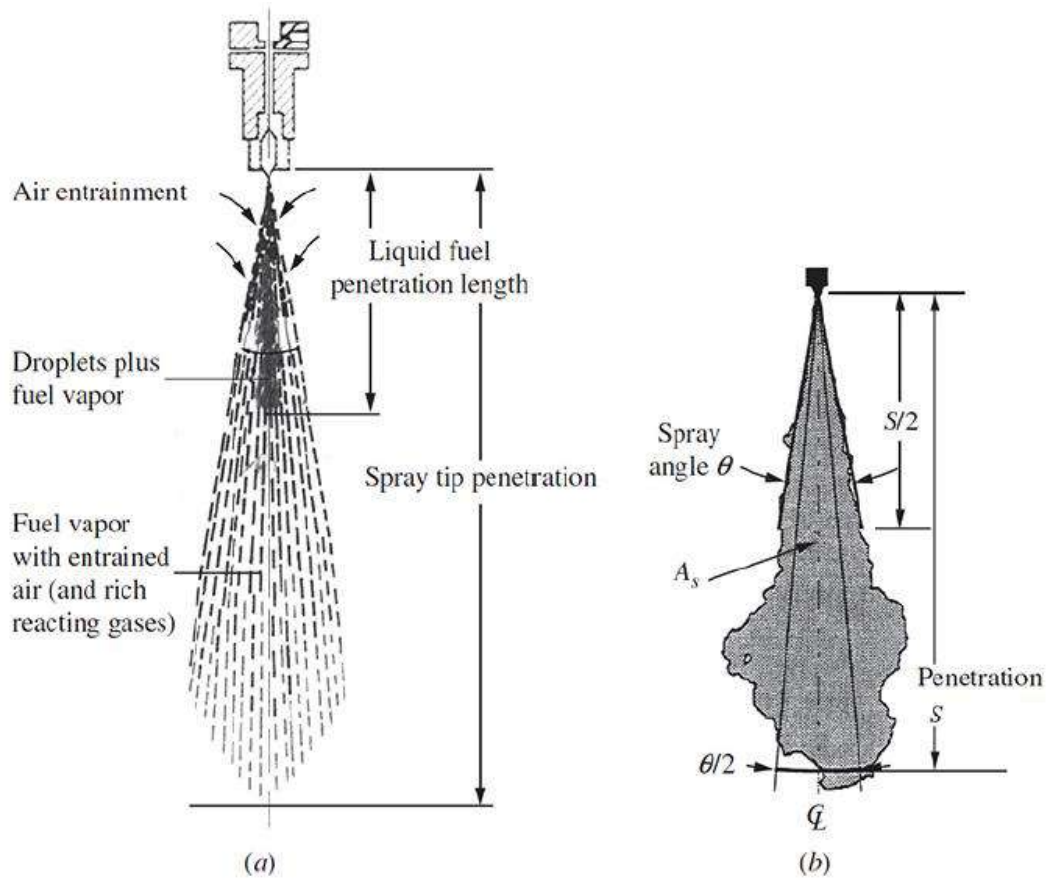

Fig. 1.16 Schematic of diesel fuel spray [HEY18]
(a) its major features and (b) its key parameters: spray axis, CL; penetration distance S; full core angle ϴ; projected spray area (grey) A_s.

Figure 1.16 illustrates the basic features of a typical DI engine fuel spray, model that is applied to biodiesel blends, too. As the liquid jet leaves the nozzle it atomizes into fine drops whose momentum creates a spray, and spreads out as the spray entrains the surrounding air. As the liquid column exiting the nozzle rapidly disintegrates, the outer surface of the liquid jet breaks up into drops of order 10 μm diameter or smaller, near the nozzle exit. The mass of air entrained into the spray increases, the spray diverges, its width increases, and its velocity reduces as the injected fuel moves away from the nozzle. As this hot air entrainment process continues, the fuel drops evaporate.

Air swirl has a significant impact on spray penetration. Figure 1.17 illustrates how the spray shape and position alter as swirl increases. Also, the spray tip penetration changes with time. Swirl have two effects: reduce the spray radial penetration and spreads out the spray in the swirl direction proportional to swirl movement intensity. Due the fact that biodiesel blends evaporation is lower (compared to pure diesel) it becomes essential that atomization of the liquid fuel blend into numerous tiny, fast-moving droplets is also required to produce a large surface area across which liquid fuel can evaporate.

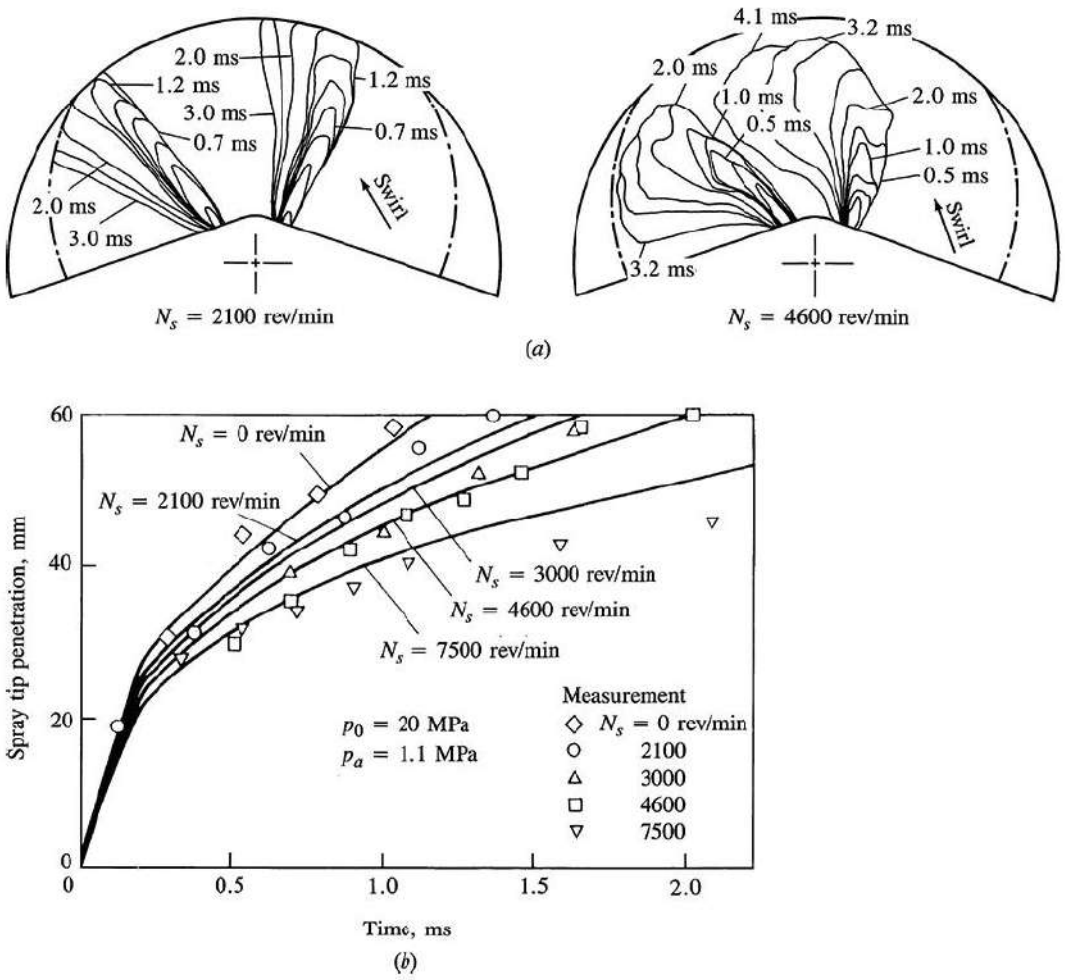

Fig. 1.17 The effect of air swirl on spray penetration [HEY18]
(a) measured outer boundary of sprays injected into swirling airflow and (b) spray tip penetration as a function of time for different swirl rates

While cetane number affects the chemical ignition delay of diesel engines, fuel quality characteristics like density, viscosity, air temperature, SMD, and droplet velocity are the primary determinants of the physical delay period.

When compared to pure diesel, biodiesel has a greater cetane number, which reduces the ignition delay in diesel engines. Also, the ignition delay can be decreased by increasing the compression ratio.

Due to its higher oxygen content (11–15 wt.%), biodiesel heat release rate more is superior to diesel fuel. Due to biodiesel higher bulk modulus the dynamic fuel injection timing is advanced and the combustion started earlier in a diesel engine using biodiesel. By retarding the injection timing, the in cylinder peak pressure decrease with direct effect in NO_x emission reduction, but the overall combustion duration increased. Because biodiesel has a lower calorific value (about 38 MJ/kg) than pure diesel (approximately 44 MJ/kg), more fuel must be injected to maintain the same power output and the necessary energy rate. Therefore, a longer fuel injection time is required, which generates a longer combustion duration.

In the ecological field, the amount of exhaust emissions can be significantly reduced by switching from diesel to biodiesel. FAME is well acknowledged to have a positive effect on emissions of hydrocarbon (HC), carbon monoxide (CO), and fine particulate matter (PM), while nitrogen oxide (NO_X) emissions level may somewhat rise or decrease, depending on the engine family and testing methods. The main factor influencing NOx in the combustion of biodiesel seems to be the addition of oxygen to the fuel, which raises the flame temperature by bringing the oxygen equivalency ratio in the rich autoignition zones of the flame closer to a value of 1. Because pure diesel has a sulfur concentration 20–50 times higher than biodiesel, this one emits very little sulfur dioxide. Additionally, using biodiesel can lower net emissions of carbon dioxide (CO_2).

Also, the increase of biodiesel content determines a reduction in DPF regeneration frequency with benefits in fuel economy.

An important property of biodiesel is represented by its lubricity that is excellent. Modern diesel injection systems require an adequate lubricity in order to avoid excessive wear of its moving parts. Today's low sulfur diesel fuels are characterized by poor lubricity capabilities, that must be enhanced through additives. The addition of small quantities of biodiesel (<1%) to pure diesel fuel generates significant improvements in lubricity capacity.

Higher viscosity, lower energy content, higher CP and PP, higher nitrogen oxide (NO_x) emissions, reduced engine speed and power, and injector coking are the main drawbacks of biodiesel when compared to diesel.

1.3 Researches regarding the performances of a turbocharged GDI engine fueled with E10

Fuel type and quality, in terms of physical and chemical properties became essential for engine's power performances and emissions. These aspects were pushed forward by the EU regulations regarding emissions.

Thus, the internal combustion engines evolved, adopting a series of strategies in order to improve their efficiency and reduce the pollutant emissions. So, these solutions were: downsizing combined with supercharging or/and turbocharging, lean burn, higher compression ratios, variable compression ratios. All these technical solutions also involve the improvement of fuels properties in order to avoid abnormal, destructive operating regimes, such as knock, which consists in autoignition of portions of the unburned mixture ahead of the flame front. Then one or more specific regions in the end gas are compressed to a high pressure and temperature that generate spontaneously autoignition. This abnormal combustion – knock – limits engine's compression ratio and boost pressure and therefore engine performance and efficiency.

The tendency to knock depends on:

- ✓ constructive and functional parameters such as engine design and operating values which influence end-gas temperature, pressure and duration, before flame front arrival;
- ✓ antiknock property of the gasoline is defined by the fuel's octane number which is an indicator of a gasoline's resistance to autoignition.

It became obvious the dependency between engine operating parameters, compression level and gasoline octane number. Considering this aspect, the higher the octane number, the better the resistance to autoignition and knock. Ethanol through its properties can improve the performances and knock behavior of a downsized turbocharged DI SI engine focusing on octane numbers and latent heat of vaporization. The vaporization process for ethanol-gasoline fuel blends has a charge cooling effect, ethanol having a vaporization enthalpy (845 kJ/kg) much higher than gasoline (420 kJ/kg). This cooling effect decreases the tendency to knock, allowing an increase in compression ratio with direct impact on efficiency.

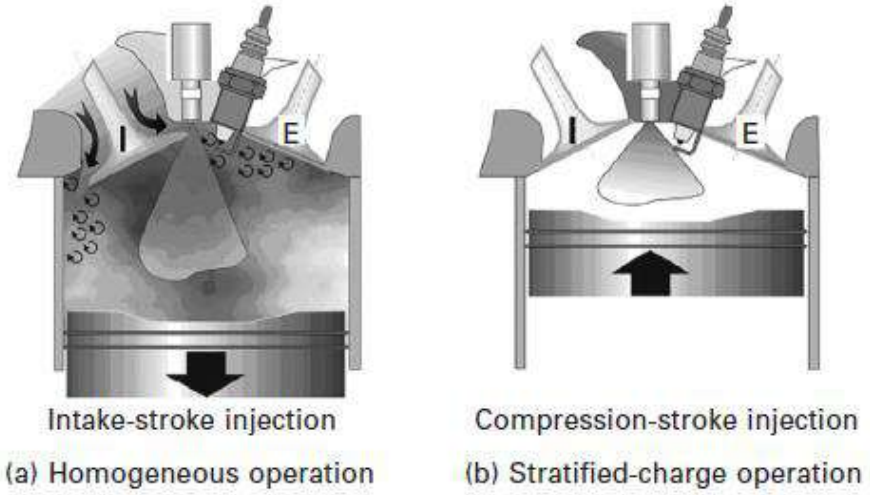

Fig. 1.18 Operating modes for GDI engines [HUA10]

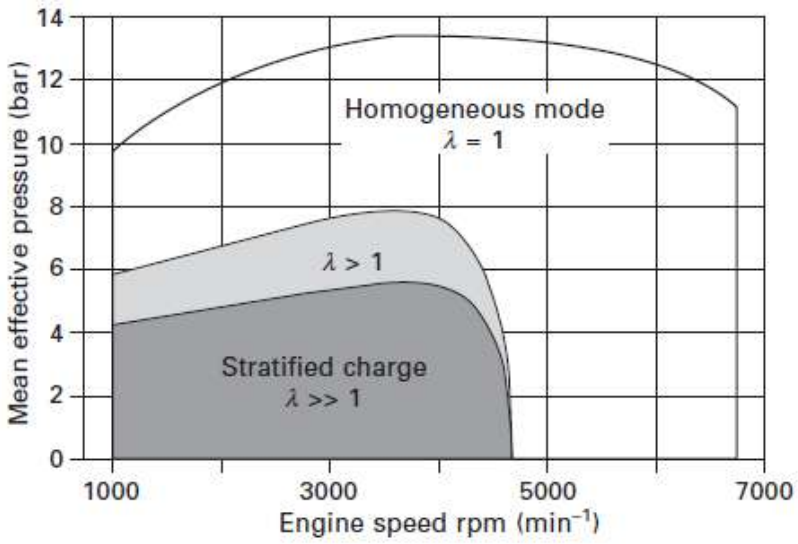

Fig. 1.19 GDI engines operating maps [HUA10]

Considering the operating modes presented in figure 1.18 when fuel blend is injected during intake stroke, the charge cooling effect improves the engine volumetric efficiency (more air enters into cylinder), with minimal or no effect over the cylinder pressure. When the fuel blend is injected in the combustion chamber at the end of compression stroke, cylinder pressure will register a drop (cooling effect). The ignitable mixture is formed in the middle of combustion chamber, surrounded by extra air.

Figure 1.19 indicates the zones of the operating modes for GDI engines that can run either with pure gasoline or with mixtures of gasoline and alcohol.

The vehicle & engine

The tests were performed with a Ford Focus equipped with an EcoBoost gasoline direct-injection turbocharged 1.6-liter four in line cylinder engine, power 134 kW, at 6000 rpm. The EcoBoost engine features double overhead belt-driven camshafts and variable intake and exhaust valve timing. Displacement: 1,596 cm^3; bore x stroke: 79 x 81,4 mm.

Fig.1.20 The test car on the dynamometric MAHA LPS 3000 test bench

The dynamometric MAHA LPS 3000 test bench

The research was carried out on the dynamometric MAHA LPS 3000 stand. The dynamometer consists of:

- ✓ communication desk with PC;
- ✓ a remote control;
- ✓ a roller set.

The LPS 3000 is available in various versions for performance testing of cars. Depending on

the version, wheel power from 260 kW to 520 kW with a max. test speed of 260km/h can be tested. The dyno load simulation is done with an eddy-current brake.
The LPS 3000 enables engine power measurements to be made on cars with Otto and diesel engines. Testing of four-wheel drive vehicles is possible if the LPS 3000 is equipped with the appropriate roller set and the corresponding control electronics. A cooling air fan which is connected to the communication desk and is operated via the radio remote control.

Test results obtained with E10

For tests standard E10 with available 95 RON, respectively 100 RON was used. The test aims to analyze the differences in power performance of a turbocharged engine in the case of fueling with E10, regular and premium. Generally, on turbocharged gasoline engines higher octane fuels are typically recommended.

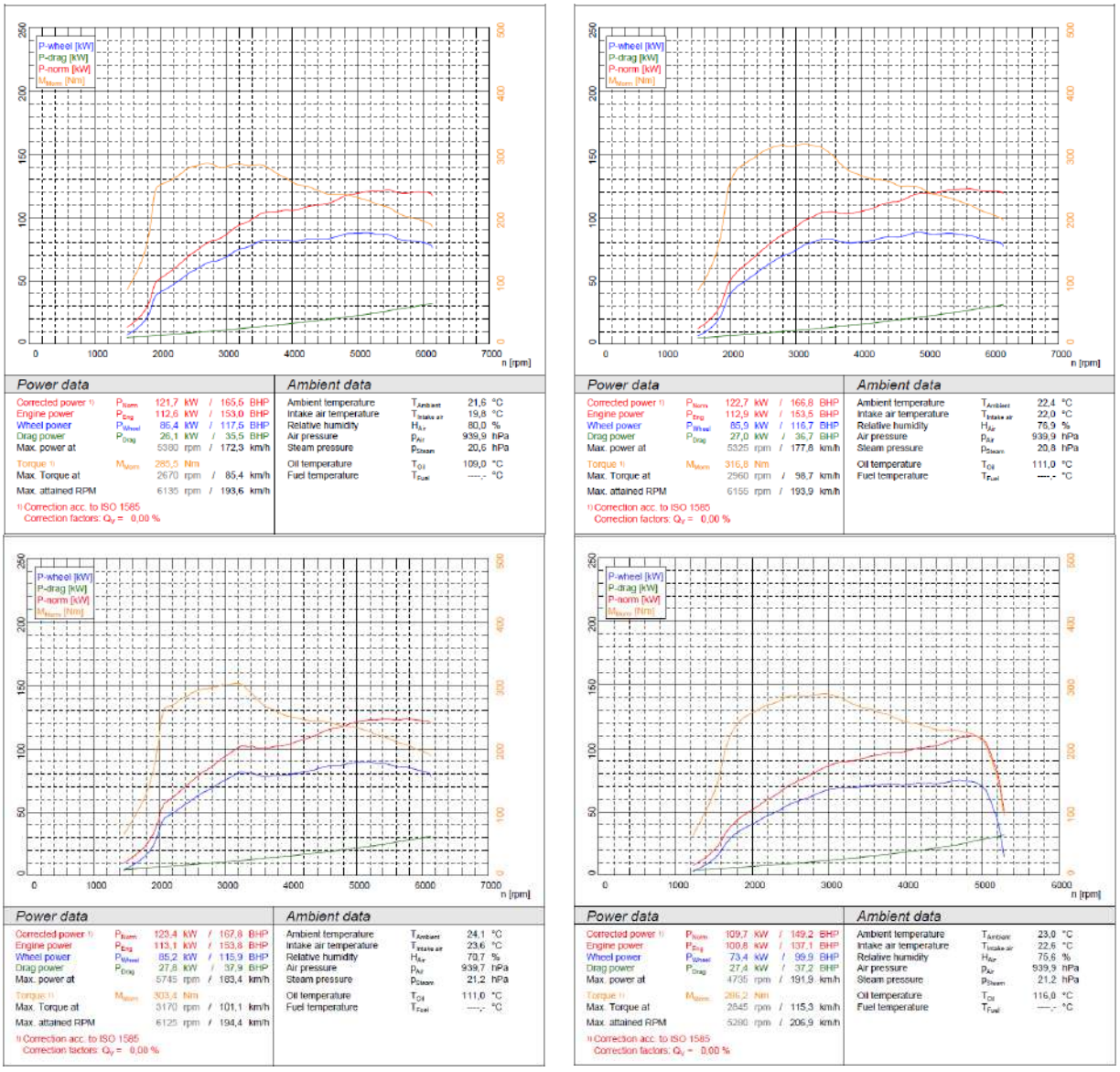

Fig.1.21 Test results for E10, RON 95

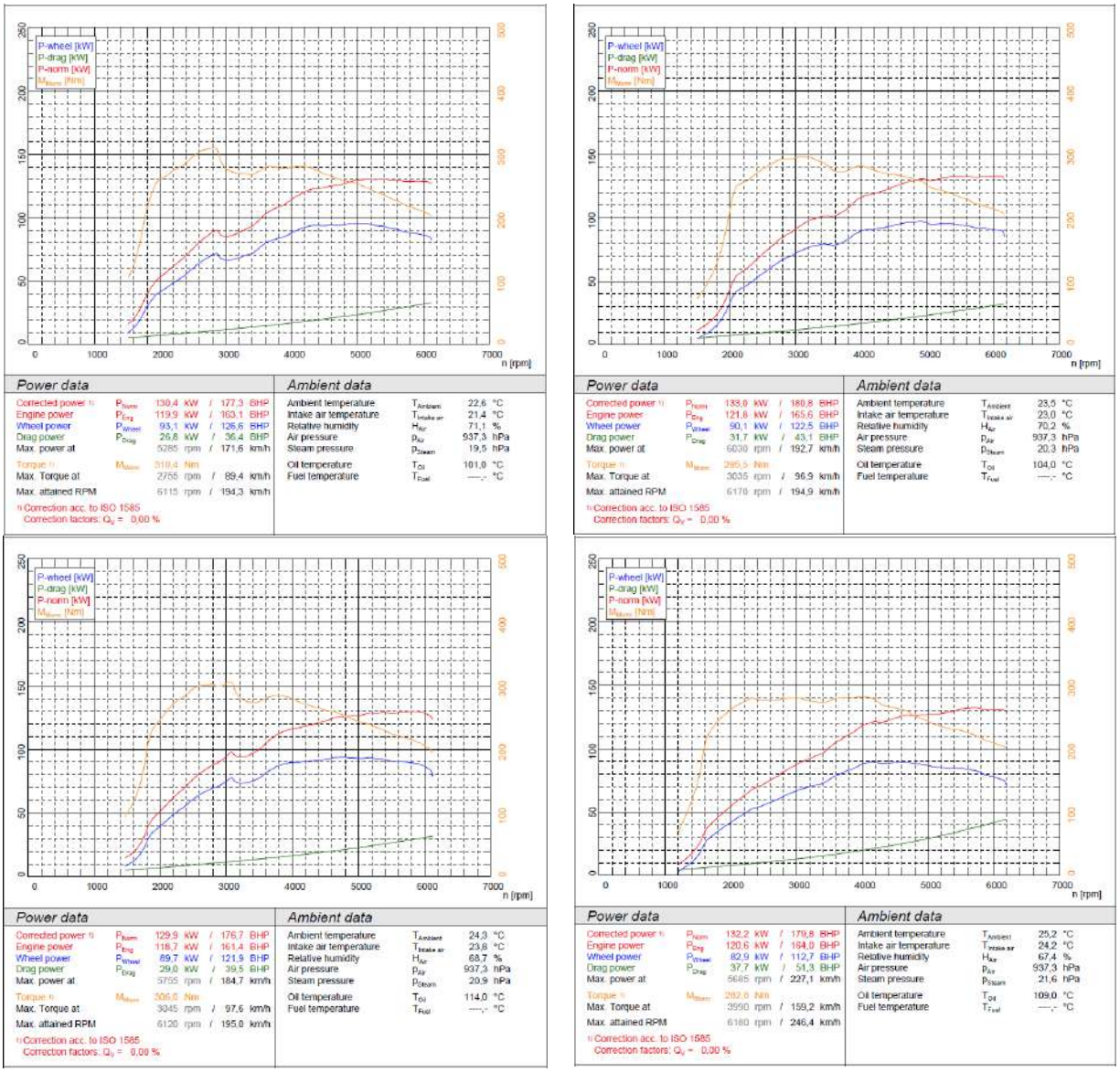

Fig.1.22 Test results for E10, RON 100

A fuel with higher octane number, typically, will boost performance in the case of supercharged or turbocharged engines, considering and adequate engine's mapping, too. Nowadays, the oxygenated compounds are used to increase the octane number, ethanol being one of them, as a renewable source of energy.

During the test all the characteristic parameters, such as the power and torque curves, have to be recorded and comparatively assessed.

In figure 1.21 and 1.22 are presented the results obtained for E10 (RON 95 and 100) and in figure 4 is represented the comparative analyses between them.

The tests were performed in the fourth gear of the gearbox where the power and torque are maximum.

From the tests data, a comparative analysis is presented in figure 1.23, for E10 with both RON values, 95 and 100, considering the medium 11values.

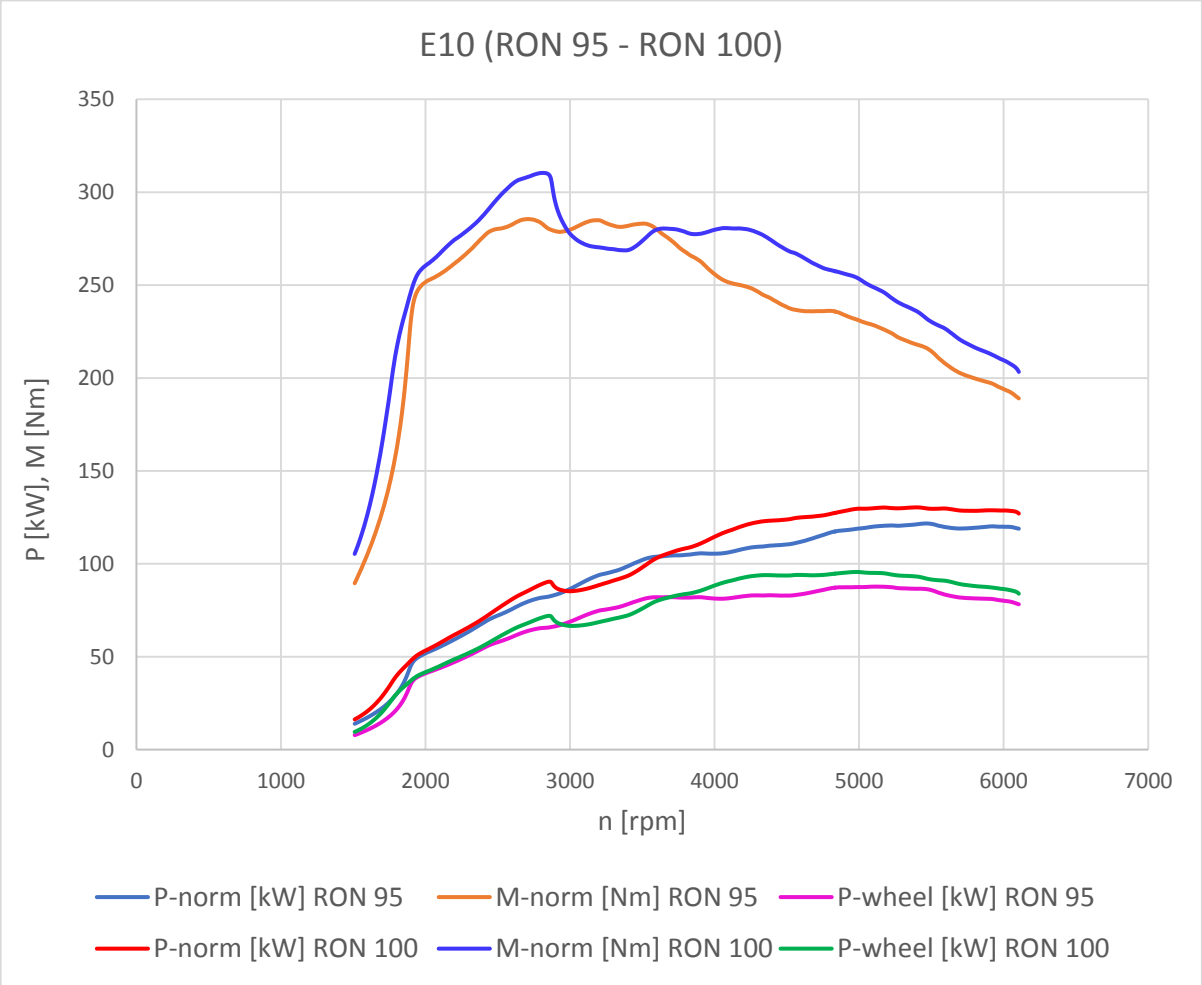

Fig.1.23 Comparative analyses for E10, RON 95 – RON 100

1.4 Conclusions

From the data presented above it can be seen that engine maximum power, as medium value is around 112 kW for E10, RON 95 and about 120 kW for E10, RON 100. In terms of power an increase of about 6 % was recorded and this above 4000 rpm.

In the speed range between 2000 and 3000 rpm the differences between the registered power values for the two types of E10 are insignificant, the curves overlapping almost on the entire interval. In this case a higher-octane level doesn't increase the vehicle performance.

In the speed range between 3000 and 3500 rpm the power values for 95 RON E10 are superior compared to 100 RON E10, the usage of a superior octane number decreased the engine energetical performance.

Only after the speed of 3600 rpm the power values become superior in the case of the 100 RON E10, in other words after this speed, the 100 RON E10 makes its presence felt. Between 3600 rpm and 6000 rpm the engine power level become superior, compared with the case of 95 RON E10.

Maximum torque and maximum speed were obtained at about the same points for both types of octane numbers, these aspects can be seen on the related diagrams.
In the case of this type of turbocharged engine, higher octanes can improve performance and can reduce emissions during some average to severe duty operations, above 3600 rpm. However, under normal driving conditions, it will do minimal to no gain in vehicle performance.
Extrapolating the research results, it can be concluded that in a large number of cases a higher-octane level may not necessarily increase the vehicle's performance, but only paying extra for premium gasoline ethanol blend, E10. This become more obvious for naturally aspirated engines, which clearly do not have a mapping that can capitalize the benefits of a higher-octane number.
This can be contradicted, for example, by the corresponding increase of the compression ratio value for the naturally aspirated engines, in order to increase their performance and efficiency.

1.5 The influence of ethanol concentration over the engine fuel consumption

Like it was specified above, generally at EU level for the most part, ethanol to gasoline ratio is 1:9 as an initiator of environmental negative effects inhibitor. The chemical properties of ethanol must be capitalized in order to maintain engine performance, fuel economy, emissions, and drivability under all operating conditions.
Ethanol fuel's high octane number may lessen the likelihood of engine knocking. Because ethanol has a higher octane number, boosting the engine's compression ratio could improve its thermal efficiency. The octane number of gasolines rises when ethanol is added at varying quantities, while the fuel's calorific value falls. Compared to neat gasoline, this requires supplying a larger amount of fuel per cycle.
Performance and emissions may be impacted by the increased latent heat of vaporization in both good and negative ways. An ethanol-gasoline mixture's charge cooling effect would boost volumetric efficiency at high loads. This would contribute to the engine's increased output of power and torque.

The test engine and blends

For tests a port fuel injection gasoline engine was used. It's a Renault 1.6-liter four inline cylinder engine, power 66 kW, at 5500 rpm, torque 128 Nm at 3000 rpm, code K7M 710.
The gasoline – ethanol blends used for tests were the following: E10 (95, 100 RON), E20 (95, 100 RON), E30 (95 RON), E100.
The full equipped engine was coupled to a hydrodynamic pin brake VEB – Shönebeck and the tests were performed for engine speed between 2000 and 3000 rpm at partial load.
In order to make the comparative analyses of fuel blends consumption, the hydrodynamic break load applied to engine for the entire range speed was 8 kgf, 78 N.

Fig.1.24 Renault K7M 710 engine on the test bed

The gasoline – ethanol blends

Considering the gasoline – ethanol blends of different concentrations, for alcohol the mass fractions of its elements carbon, hydrogen and oxygen must first be defined. The same iteration must be applied for gasoline, too. Mass fractions formula is the following:

$$x_i = \frac{m_i}{\Sigma m_i}. \quad (1.4)$$

In the following, the mathematical modeling of the elementary quantities, respectively of the air necessary for combustion for each mixture, will be presented.

Table 1.5 Molar mass and mass fractions for gasoline

Gasoline	C_8H_{18}	Atom no.	Atomic mass	Mass	x_i
		-	[g]	[g/mol]	
	C	8	12	96	0.842
	H	18	1	18	0.158
$\sum m_i$				114	

Table 1.6 Molar mass and mass fractions for ethanol

Alcohol	C_2H_5OH	Atom no.	Atomic mass	Mass	x_i
		-	[g]	[g/mol]	
	C	2	12	24	0.5217
	H	6	1	6	0.1304
	O	1	16	16	0.3478
$\sum m_i$				46	

Ethanol density is $\rho_{ethanol}$=0.789 kg/dm^3 and for the gasoline $\rho_{gasoline}$=0.752 kg/dm^3.
Mass fractions for carbon and hydrogen in the case of gasoline are presented in table 1.7.

Table 1.7 Mass fraction for carbon and hydrogen in the case of gasoline

Element	x_i
C	0.842
H	0.158

In the next section will be detailed each considered blend as follows:

a) E10 blend

For one liter of blend, the amounts of carbon and hydrogen for gasoline that represents 90% of the mixture will be determined as follows:

$$m_{C,gasoline} = 0.9 \cdot x_c \cdot \rho_{gasoline} = 0.9 \cdot 0.842 \cdot 0.752 = 0.569\ kgC,$$
$$m_{H,gasoline} = 0.9 \cdot x_H \cdot \rho_{gasoline} = 0.9 \cdot 0.158 \cdot 0.752 = 0.106\ kgH.$$

For one liter of blend, the amounts of carbon, hydrogen and oxygen for gasoline that represents 10% of the mixture will be determined as follows:

$$m_{C,ethanol} = 0.1 \cdot x_c \cdot \rho_{ethanol} = 0.1 \cdot 0.521 \cdot 0.789 = 0.041\ kgC,$$
$$m_{H,ethanol} = 0.1 \cdot x_H \cdot \rho_{ethanol} = 0.1 \cdot 0.130 \cdot 0.789 = 0.0102\ kgH,$$

$m_{O,ethanol} = 0.1 \cdot x_O \cdot \rho_{ethanol} = 0.1 \cdot 0.347 \cdot 0.789 = 0.0274\ kgO.$

By masses summation of each component from the mixture, carbon, hydrogen and oxygen, it results the density of the mixture and the mass fraction of each component.

Table 1.8 Mass fraction - E10

Element	m_i [kg/l]	x_i
C	0.611	0.809
H	0.116	0.155
0	0.027	0.036

To determine the amount of air required for combustion, the minimum amount of air for burning gasoline must first be determined.

$$L_{min} = \frac{1}{0.21}\left(\frac{C}{12} + \frac{H}{4}\right) = 0.522\ kmol_{air}/kg_{gasoline}$$

Air molar mass being M_{air} = 28,958 kg/kmol it results that minimum amount of air to burn a kg of gasoline is:

$L'_{min} = L_{min} \cdot M_{air} = 15.117\ kg_{air}/kg_{fuel}$

For E10 blend the air quantity is:

$L_{min,E10} = \frac{1}{0.21}\left(\frac{C}{12} + \frac{H}{4} - \frac{O}{32}\right) = \frac{1}{0.21}\left(\frac{0.809}{12} + \frac{0.155}{4} - \frac{0.036}{32}\right) = 0.5001\ kmol_{aer}/kg_{E10}$

$L'_{E10} = L_{min,E10} \cdot M_{aer} = 14.483\ kg_{aer}/kg_{E10}$

Air–fuel equivalence ratio:

$\lambda_{E10} = \frac{L_{min}}{L_{min,E10}} = \frac{15.117}{14.483} = 1.043$

b) E20 blend

For one liter of blend, the amounts of carbon and hydrogen for gasoline that represents 80% of the mixture will be determined as follows:

$m_{C,gasoline} = 0.8 \cdot x_c \cdot \rho_{gasoline} = 0.8 \cdot 0.842 \cdot 0.752 = 0.506\ kgC,$

$m_{H,gasoline} = 0.8 \cdot x_H \cdot \rho_{gasoline} = 0.8 \cdot 0.158 \cdot 0.752 = 0.095\ kgH.$

For one liter of blend, the amounts of carbon, hydrogen and oxygen for ethanol that represents 20% of the mixture will be determined as follows:

$m_{C,ethanol} = 0.2 \cdot x_c \cdot \rho_{ethanol} = 0.2 \cdot 0.521 \cdot 0.789 = 0.0823\ kgC,$
$m_{H,ethanol} = 0.2 \cdot x_H \cdot \rho_{ethanol} = 0.2 \cdot 0.130 \cdot 0.789 = 0.0205\ kgH,$
$m_{O,ethanol} = 0.2 \cdot x_O \cdot \rho_{ethanol} = 0.2 \cdot 0.347 \cdot 0.789 = 0.0548\ kgO.$

By masses summation of each component from the mixture, carbon, hydrogen and oxygen, it results the density of the mixture and the mass fraction of each component.

Table 1.9 Mass fraction - E20

Element	m_i [kg/l]	x_i
C	0.588	0.7755
H	0.1155	0.1521
0	0.0548	0.0722

For E20 blend the air quantity is:
$L_{min,E20} = \frac{1}{0.21}\left(\frac{C}{12} + \frac{H}{4} - \frac{O}{32}\right) = \frac{1}{0.21}\left(\frac{0.775}{12} + \frac{0.152}{4} - \frac{0.0722}{32}\right) = 0.4777\ kmol_{aer}/kg_{E20}$
$L_{E20} = L_{min,E20} \cdot M_{aer} = 13.834\ kg_{aer}/kg_{E20}$

Air–fuel equivalence ratio:
$\lambda_{E20} = \frac{L_{min}}{L_{min,E20}} = \frac{15.117}{13.834} = 1.092$

b) E30 blend

For one liter of blend, the amounts of carbon and hydrogen for gasoline that represents 70% of the mixture will be determined as follows:

$m_{C,gasoline} = 0.7 \cdot x_c \cdot \rho_{gasoline} = 0.7 \cdot 0.842 \cdot 0.752 = 0.4432\ kgC,$
$m_{H,gasoline} = 0.7 \cdot x_H \cdot \rho_{gasoline} = 0.7 \cdot 0.158 \cdot 0.752 = 0.0831\ kgH.$

For one liter of blend, the amounts of carbon, hydrogen and oxygen for ethanol that represents 30% of the mixture will be determined as follows:

$m_{C,etanol} = 0.3 \cdot x_c \cdot \rho_{etanol} = 0.3 \cdot 0.521 \cdot 0.789 = 0.1233\ kgC,$
$m_{H,etanol} = 0.3 \cdot x_H \cdot \rho_{etanol} = 0.3 \cdot 0.130 \cdot 0.789 = 0.0307\ kgH,$
$m_{O,etanol} = 0.3 \cdot x_O \cdot \rho_{etanol} = 0.3 \cdot 0.347 \cdot 0.789 = 0.08213\ kgO.$

By masses summation of each component from the mixture, carbon, hydrogen and oxygen, it results the density of the mixture and the mass fraction of each component.

Table 1.10 Mass fraction – E30

Element	m_i [kg/l]	x_i
C	0.567	0.743
H	0.114	0.149
O	0.082	0.108

For E30 blend the air quantity is:

$$L_{min,E30} = \frac{1}{0.21}\left(\frac{C}{12} + \frac{H}{4} - \frac{O}{32}\right) = \frac{1}{0.21}\left(\frac{0.743}{12} + \frac{0.149}{4} - \frac{0.108}{32}\right) = 0.4561\ kmol_{aer}/kg_{E30}$$

$$L'_{E30} = L_{min,E30} \cdot M_{aer} = 13.2077\ kg_{aer}/kg_{E20}$$

Air–fuel equivalence ratio:

$$\lambda_{E30} = \frac{L_{min}}{L_{min,E30}} = \frac{15.117}{13.207} = 1.144$$

d) Ethanol E100

For one liter of pure ethanol E100, the amounts of carbon, hydrogen and oxygen will be determined as follows:

$$m_{C,etanol} = 1 \cdot x_c \cdot \rho_{etanol} = 1 \cdot 0.521 \cdot 0.789 = 0.411\ kgC,$$
$$m_{H,etanol} = 1 \cdot x_H \cdot \rho_{etanol} = 1 \cdot 0.130 \cdot 0.789 = 0.1025\ kgH,$$
$$m_{O,etanol} = 1 \cdot x_O \cdot \rho_{etanol} = 1 \cdot 0.347 \cdot 0.789 = 0.2737\ kgO.$$

For E100 the air quantity is:

$$L_{min,E30} = \frac{1}{0.21}\left(\frac{C}{12} + \frac{H}{4} - \frac{O}{32}\right) = \frac{1}{0.21}\left(\frac{0.522}{12} + \frac{0.130}{4} - \frac{0.347}{32}\right) = 0.311\ kmol_{aer}/kg_{E100}$$

$$L'_{E30} = L_{min,E30} \cdot M_{aer} = 9.0059\ kg_{aer}/kg_{E100}$$

Air–fuel equivalence ratio:

$$\lambda_{E100} = \frac{L_{min}}{L_{min,E100}} = \frac{15.117}{9.0059} = 1.678$$ (compared to neat gasoline)

In figure 1.25 is represented the variation of the elementary content of pure ethanol and of some gasoline ethanol blends. From this graph it can be observed that the oxygen content increases correspondingly with the rise in the ethanol content in the mixture, reaching up to 35% in the case of E100. In contrast, the carbon content decreases with increasing ethanol content. These aspects highlight the low energy content of ethanol due to both the presence of oxygen and the reduction in carbon content. This aspect is also reflected in the lower calorific value that is decreasing with rising the ethanol content in the blend.

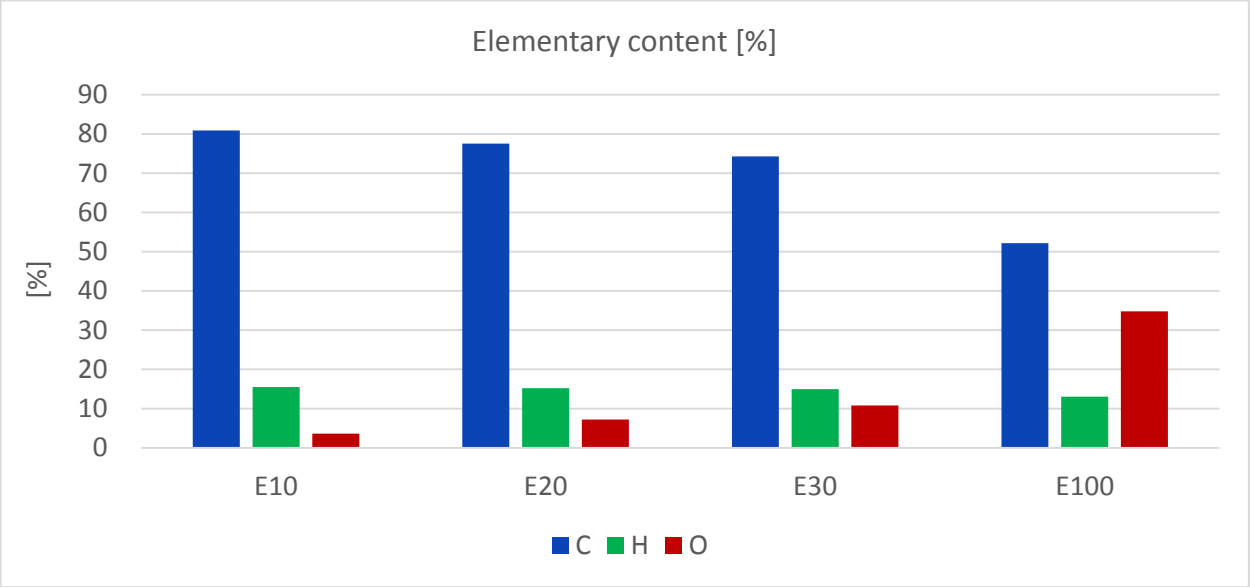

Fig.1.25 Elementary content of pure ethanol and blends

Test results

For the considered engine load and speed range, initially was determined the hourly fuel consumption, and then the specific fuel consumption as a measure of engine efficiency fueled with gasoline - ethanol blends and neat ethanol.
Another parameter to evaluate the engine efficiency is the ratio of energetic efficiency M_{ef} defined as ratio between effective mechanical work L_{ef} [J] and mass flow rate of injected fuel per cycle and cylinder q_{inj} [mg/cycle].

$$M_{ef} = \frac{L_{ef}}{q_{inj}} \tag{1.5}$$

Conclusions

Analyzing the results, it can be mentioned the following conclusions:

- ✓ the engine speed range and load were chosen specific to urban traffic conditions, where there are major challenges regarding the energy and ecological efficiency of engines;
- ✓ in figure 1.25 it can be observed that the best hourly fuel consumption values were obtained for E10 blends, poorest ones for E100, with slightly advantage above 2400 rpm for E10 RON 95 blend;

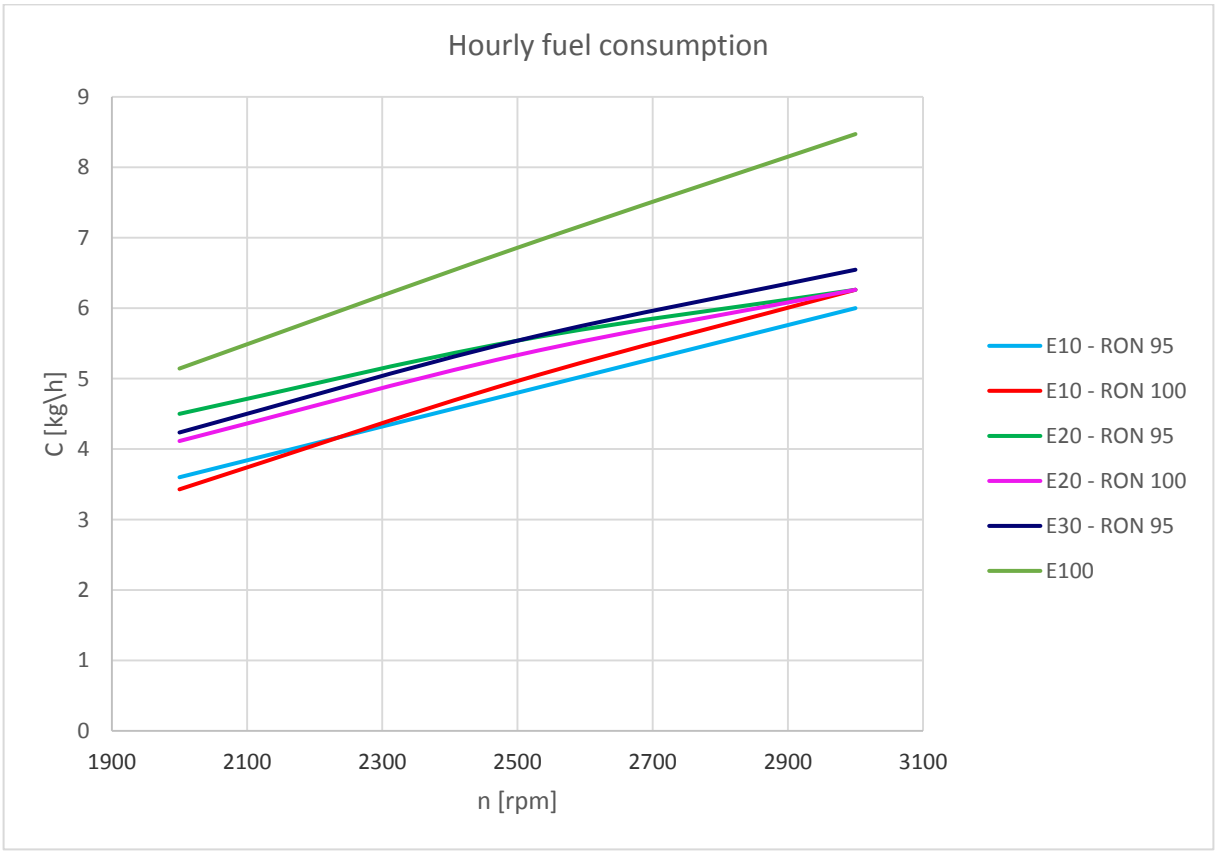

Fig.1.26 Hourly fuel consumption

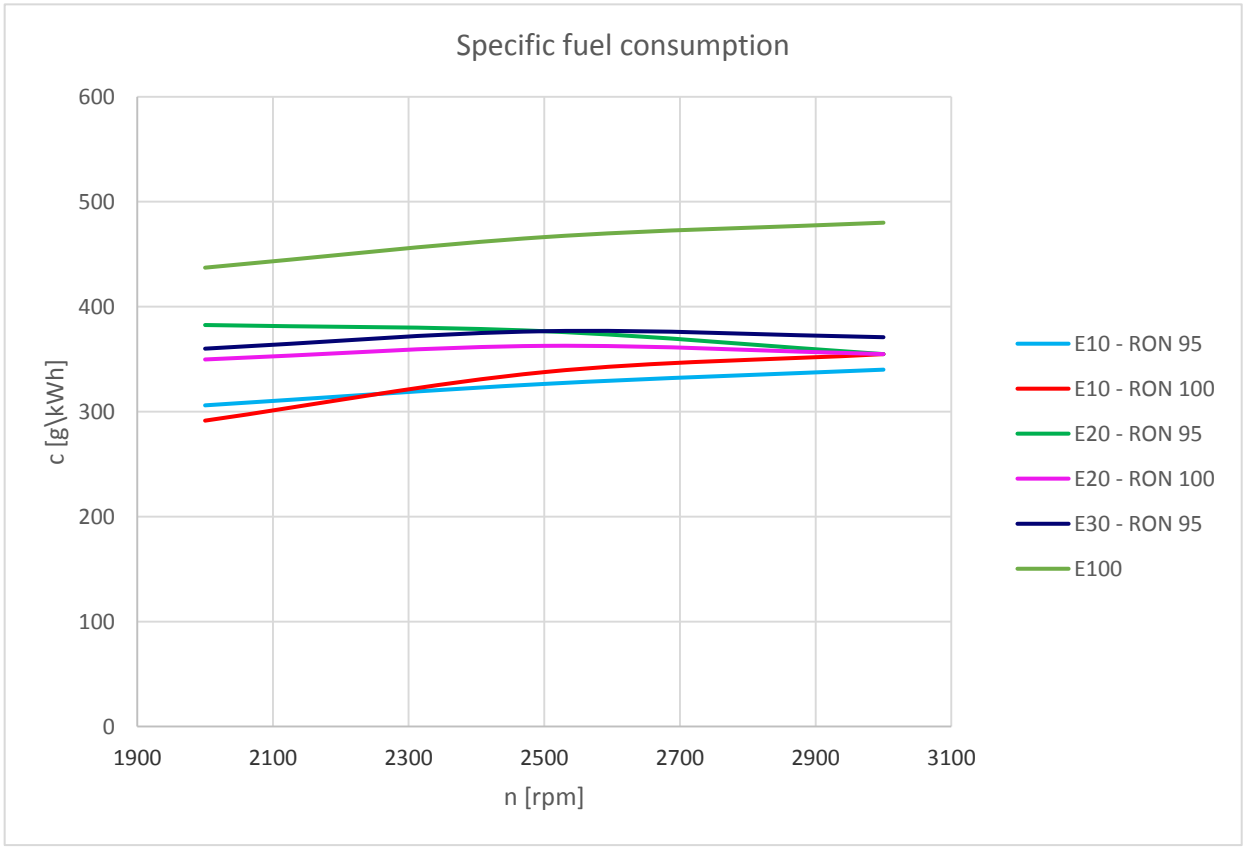

Fig.1.27 Specific fuel consumption

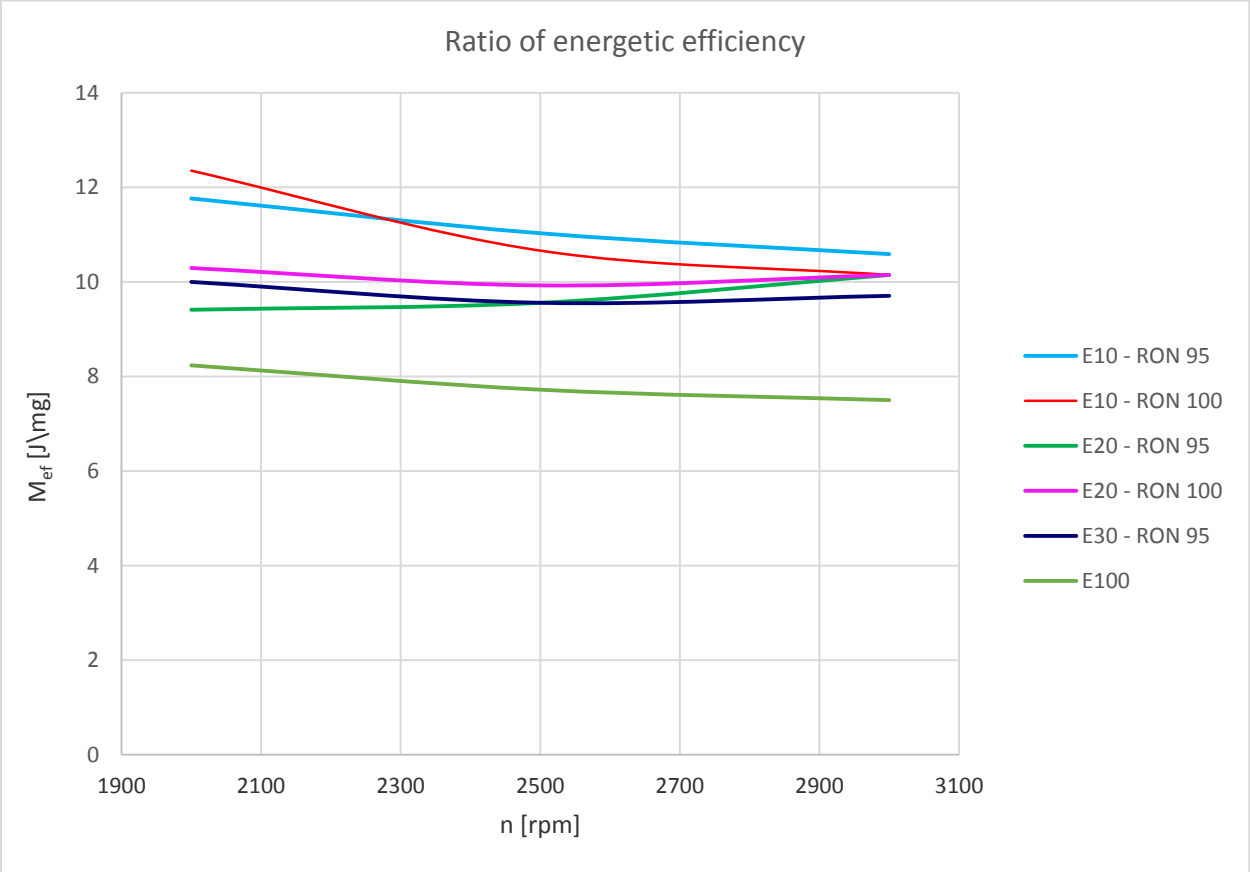

Fig.1.28 Ratio of energetic efficiency

- ✓ the lowest values for specific fuel consumption resulted for E10 blends, especially for the RON 95 above 2300 rpm that indicates that engine mapping was optimized for gasoline with 95 octane rating;
- ✓ the results are explained through fuel's calorific value, that's decreasing with rising the amount of ethanol in the blend (characterized by low energy density, due to oxygen content);
- ✓ in order to maintain the same engine power output on tested speed range, fuel consumption increases in the case of superior ethanol participation percent in the blend.
- ✓ the specific fuel consumption, for tested speed range and all fuel blends vary between 280 g\kWh and 480 g\kWh; in the case of E100 were obtained the highest values for specific fuel consumption in an interval between 437 g\kWh at 2000 rpm and 480 g\kWh at 3000 rpm;
- ✓ E100 (neat ethanol) represents a drawback by energetical point of view, functional optimizations of the engine maps being necessary and, depending on the results, constructive changes;
- ✓ by energetic efficiency ratio the same aspects are obvious, the most attractive option is E10 on a stock engine, without engine maps optimizations;
- ✓ on current engines in order to increase efficiency functional optimizations are need in order to compensate the ethanol lack of energy density.

1.6 Researches regarding energetical and ecological performances of D.I. diesel engine fueled with biodiesel

Biodiesel, due to its renewable feature, greenhouse gas emission reduction became an attractive alternative to replace fossil diesel fuel in order to fulfill future demands for sustainable transport development. The physical and chemical properties of biodiesel make it suitable to be used in pure form (B100) or may be blended with petroleum diesel at different concentration.

The aim of this research is to present some aspects regarding the energetical and ecological performances obtained with a compression ignition engine fueled with biodiesel.

Compared to petroleum diesel, biodiesel is characterized by:

- energy content is about 10% less on a mass basis;
- reduced level of some exhaust emissions (although it may, in some conditions, increase others);
- no sulfur content;
- lower heating value;
- no aromatics content;
- oxygen content up to 11%;
- higher cetane number;
- higher flash point;
- higher freezing temperature;
- higher viscosity;
- less toxic;
- superior lubricity;
- biodegradable;
- tends to deteriorate some types of natural rubber of which are made the fuel system parts found in some older engine.

Some characteristics, such as higher cetane number, superior lubricity, sulfur and aromatics free content, flash point, etc. are advantages of biodiesel, while others, including flow proprieties at low temperature, lower heating value, higher viscosity, corrosion properties are inconveniences.

Experimental research data

During the experimental phase, it was used pure petroleum diesel fuel and blended with biodiesel obtained from sunflower oil and waste oil. The proportion of biodiesel used during experiments was 10%.

Renault K9KP732 engine characteristics are the following:

- ✓ displacement: 1451 cm^3;
- ✓ bore x stroke: 76 x 80,5 mm;
- ✓ 4 inline cylinders, turbocharged;
- ✓ common rail direct injection;
- ✓ power: 78 kW / 4000 rpm;
- ✓ torque: 240 Nm / 2000 rpm.

Experimental test bench is represented by a Horiba Titan T250 test stand that is optimized for steady state and transient testing of light and heavy-duty gasoline and diesel engines. The main characteristics of the Horiba Titan T250 test stand are:

- ✓ maximum torque: 400 Nm
- ✓ maximum speed: 8000 rpm
- ✓ moment of Inertia: > 0.3 kgm^2
- ✓ dynamometer: Dynas3 HT250
- ✓ response time: 4 ms
- ✓ maximum absorbed power: 250 kW

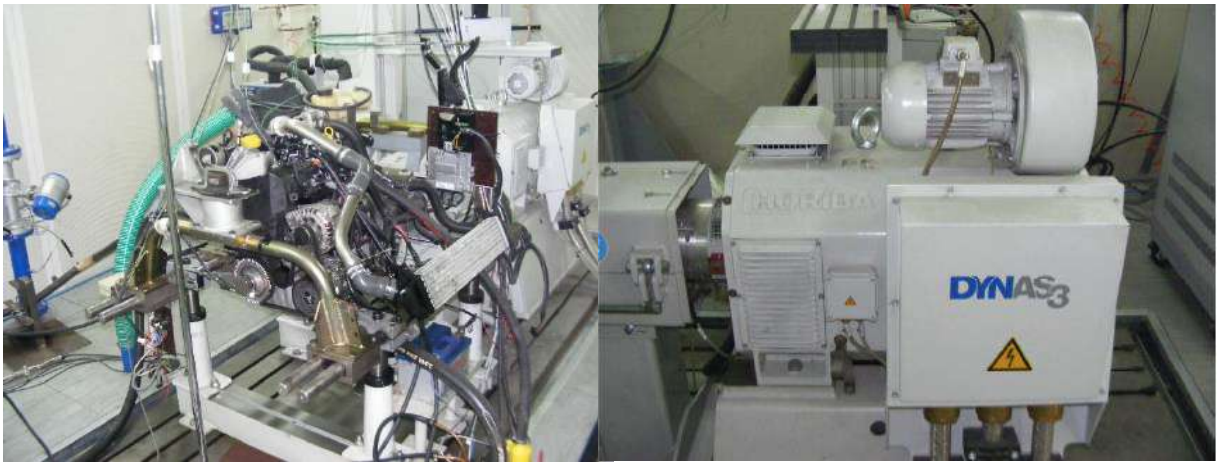

Fig.1.29 Horiba Titan T 250 stand, brake $DYNAS_3$

For soot emission measurement was used the AVL Smoke meter 415S which is an automatic measurement system; a controlled volume of exhaust gases is passed through a filter paper. The filtered soot causes blackening on the filter paper which is detected by a photoelectric measuring head and evaluated in the microprocessor to calculate the result in FSN or mg/m^3.
Exhaust emissions were determined by the Pierburg Hermann, tip HGA 400 analyzer.
Horiba Titan 250 stand is controlled and operated by the computer through the STARS automatic control system. Tests can be prepared independently of the test bed.

Fig.1.30 AVL 415S Smoke meter

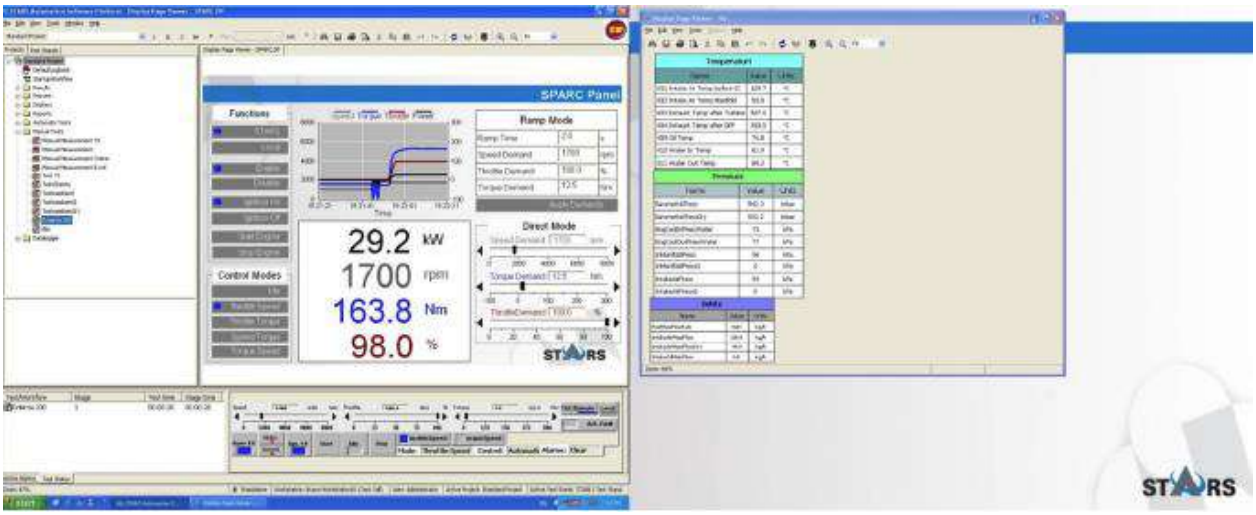

Fig.1.31 STARS software

The measured pollutant emissions are: carbon monoxide (CO), carbon dioxide (CO_2), nitrogen oxides (NO_x), unburnt hydrocarbons (HC) and smoke. The Pierburg Hermann HGA 400 analyzer was used to measure CO, CO_2, HC and NO_x.

Figure 1.32 The Pierburg HGA 400 analyzer

This analyzer works on the principle of chemiluminescence of the component elements. Infrared detection cells are used to measure the pollutant compounds in the exhaust gases.

Results and comments

In table 1.11, 1.12 and 1.13 are presented the results obtained with the engine running at full load. In this tables can be observed the values for torque, power and emissions that characterized the energetical and ecological potential of biodiesel blended with petroleum diesel fuel compared to pure petroleum diesel fuel.

Table 1.11 Pure diesel fuel

Speed	Power	Torque	Soot	CO	CO_2	O_2	HC	NO_x
[rpm]	[kW]	[Nm]	[mg/m^3]	[%]	[%]	[%]	[ppm]	[ppm]
1200	13.47649	107.2292	166.56	5.25	14.7	17.11	143	418
1700	29.37798	164.9864	89.59	1.25	15.6	16.87	141	883
2200	41.49626	180.1189	39.24	0.86	15.1	16.9	111	838
2700	63.83509	225.7622	30.25	0.8	14.5	16.23	89	1137
3200	69.4686	207.306	40.5	0.78	14	16.75	95	1168
3700	71.63496	184.8818	63.46	0.8	14.1	16.38	80	1248

Table 1.12 B10 - sunflower oil

Speed	Power	Torque	Soot	CO	CO_2	O_2	HC	NO_x
[rpm]	[kW]	[Nm]	[mg/m^3]	[%]	[%]	[%]	[ppm]	[ppm]
1200	12.7691	101.5908	144.32	2.35	12.7	20.52	39	978
1700	29.00575	162.8987	74.25	0.23	12.6	20.26	40	874
2200	42.14181	182.9082	32.46	0.06	12.1	19.97	35	898
2700	64.44046	227.9237	28.47	0.04	11.4	20.24	40	1173
3200	69.11801	206.2719	32.47	0.04	12	20.02	46	1165
3700	71.87303	185.4877	40.43	0.04	11.4	20.08	64	1198

Table 1.13 B10 - waste oil

Speed	Power	Torque	Soot	CO	CO_2	O_2	HC	NOx
[rpm]	[kW]	[Nm]	[mg/m^3]	[%]	[%]	[%]	[ppm]	[ppm]
1200	12.67961	100.8999	126.74	2.28	13.1	20.26	80	978
1700	29.21389	164.0858	67.14	0.23	13	19.93	79	910
2200	42.20342	183.1791	31.93	0.06	12.6	19.49	67	916
2700	64.22325	227.1576	27.41	0.04	11.5	19.21	62	1140
3200	69.39461	207.0703	29.94	0.04	11.6	19.02	42	1149
3700	71.62849	184.8628	44.41	0.04	11.2	19.09	41	1211

In figure 1.33 is shown the cylinder pressure variation for engine's full load at 3700 rpm for the tested blends. The highest pressure value was registered for pure diesel. The evolution of torque and power at full load relative to engine speed is illustrated in figure 1.34, for a B10 blends and pure petroleum diesel fuel.

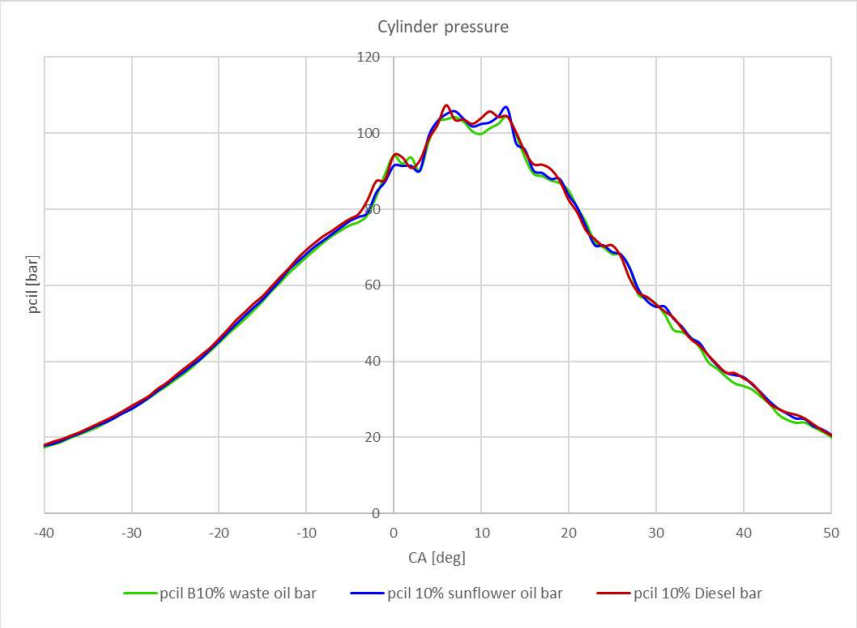

Fig. 1.33 Cylinder pressure evolution

The level of emissions for engine's full load is represented in figure 1.35 to figure 1.39. Figure 1.35, 1.36 and 1.37 indicate that CO, CO_2 and HC emissions decrease in case of biodiesel blends (10% in presented case). This effect is determined by the oxygen content in biodiesel, which generates a more complete oxidation in the combustion chamber.

NOx emissions are increased with biodiesel especially at low to medium speed, but at high speed (3200-3700 rpm) the difference is insignificant, obtaining even a higher value for pure petroleum diesel fuel. An increased level of NOx could be explained through high oxygen content of biodiesel. The soot level is decreased in case of B10 for all speeds (figure 1.39).

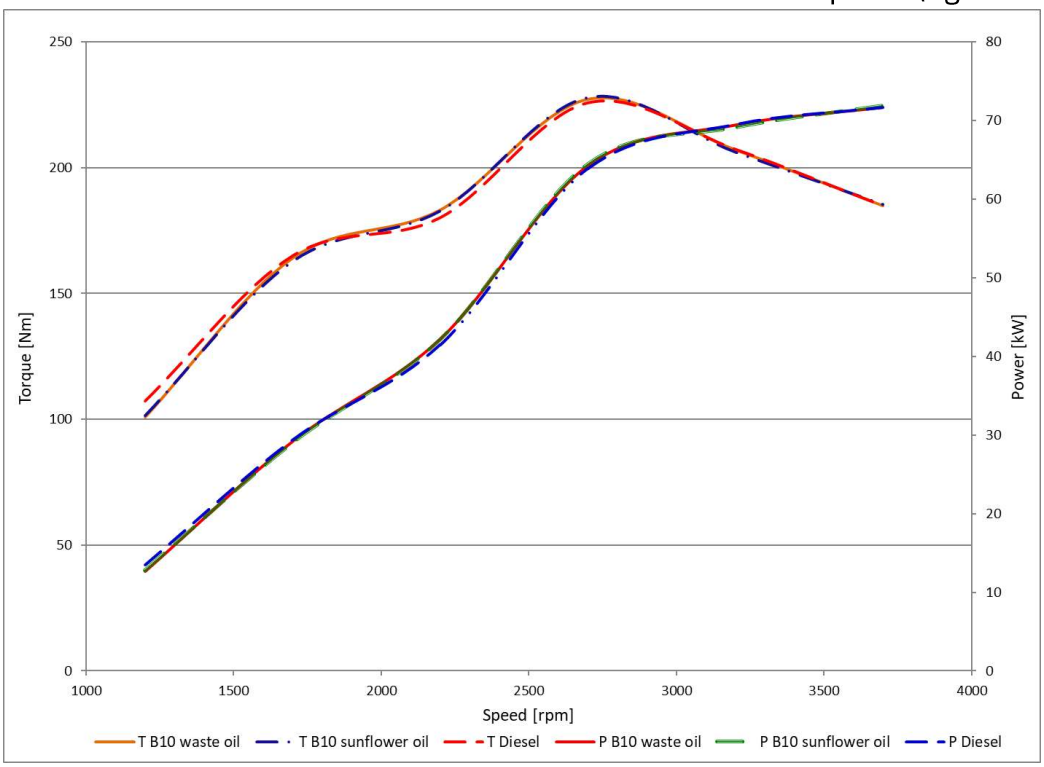

Fig. 1.34 Torque and power relative to engine's speed

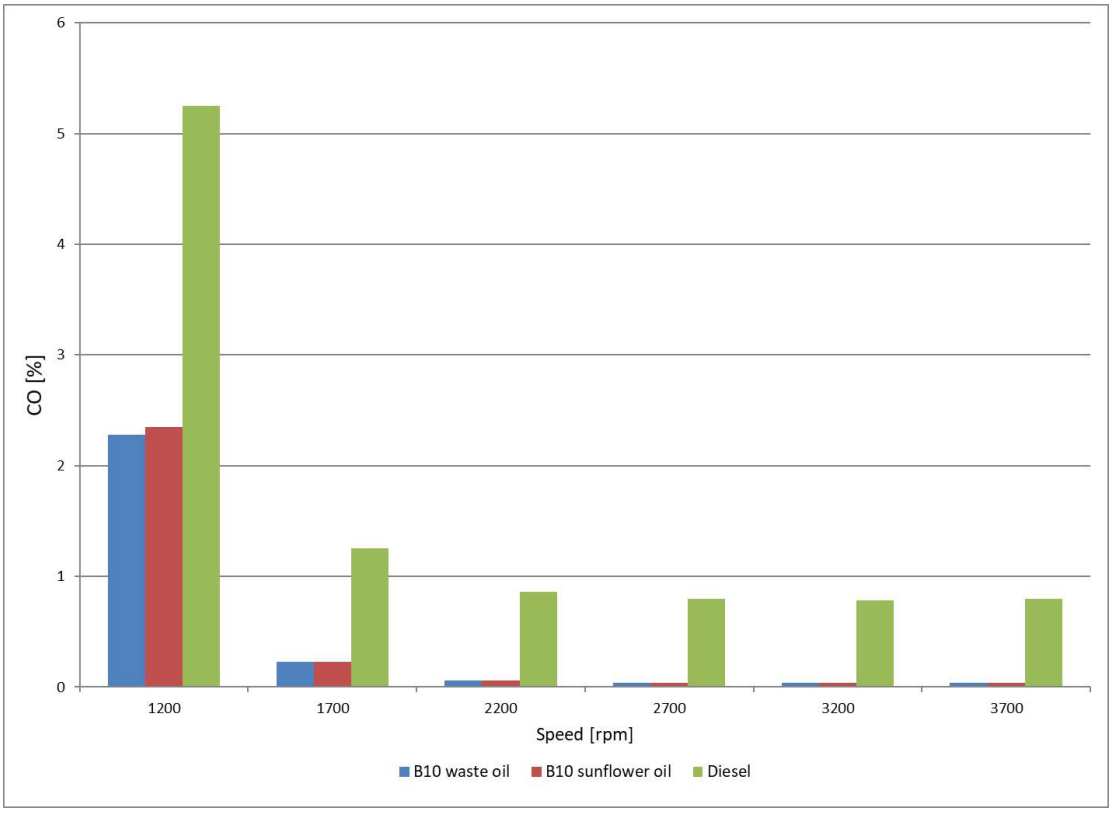

Fig. 1.35 CO emissions

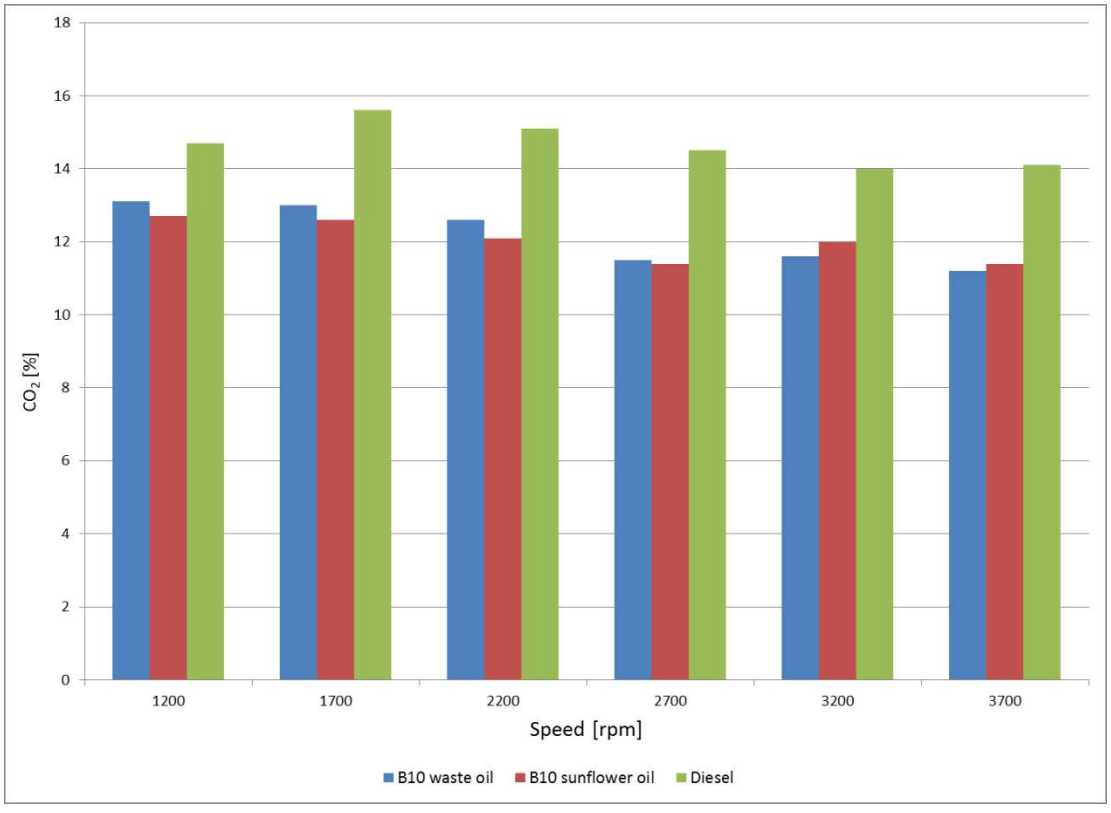

Fig. 1.36 CO_2 emissions

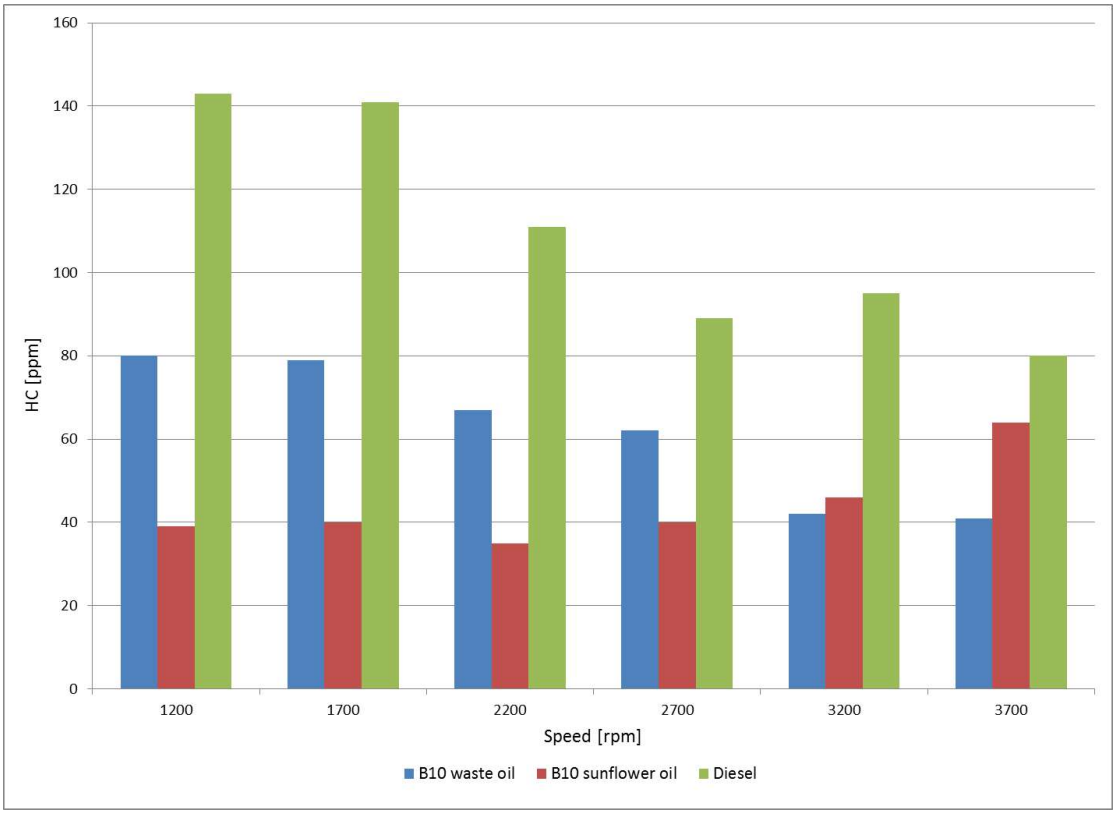

Fig. 1.37 HC emissions

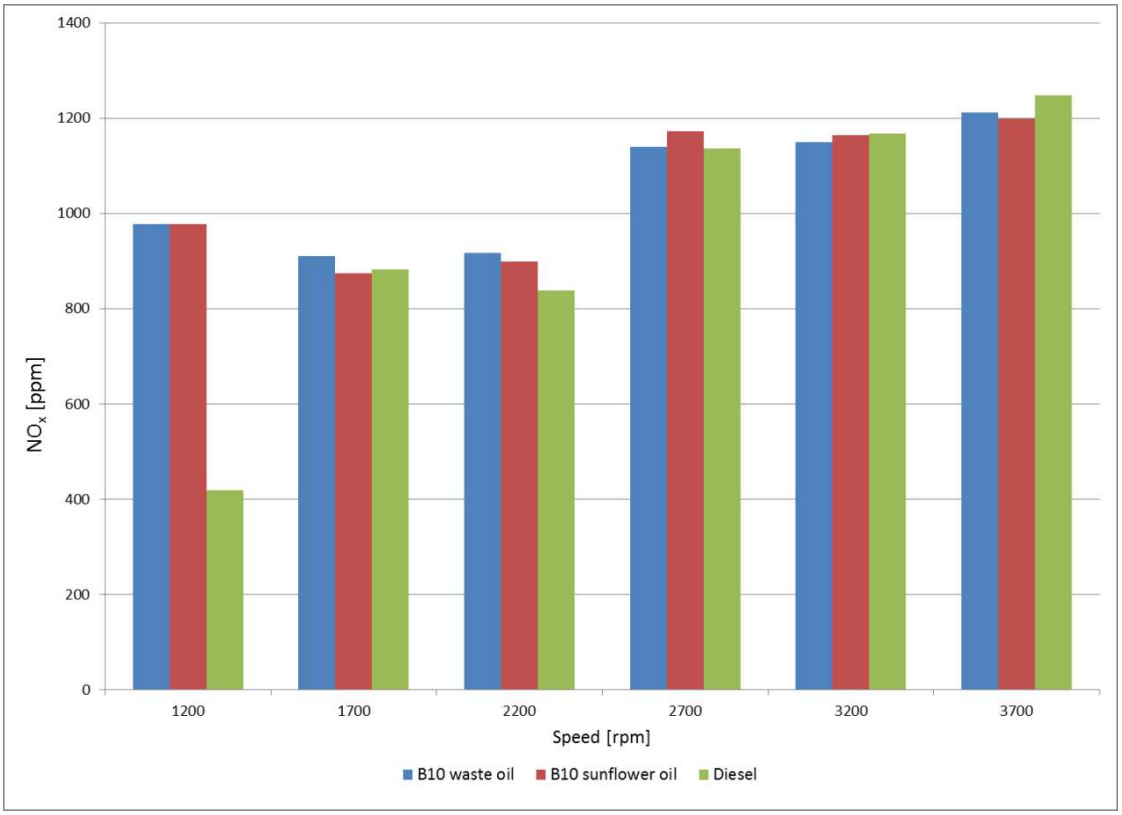

Fig. 1.38 NOx emissions

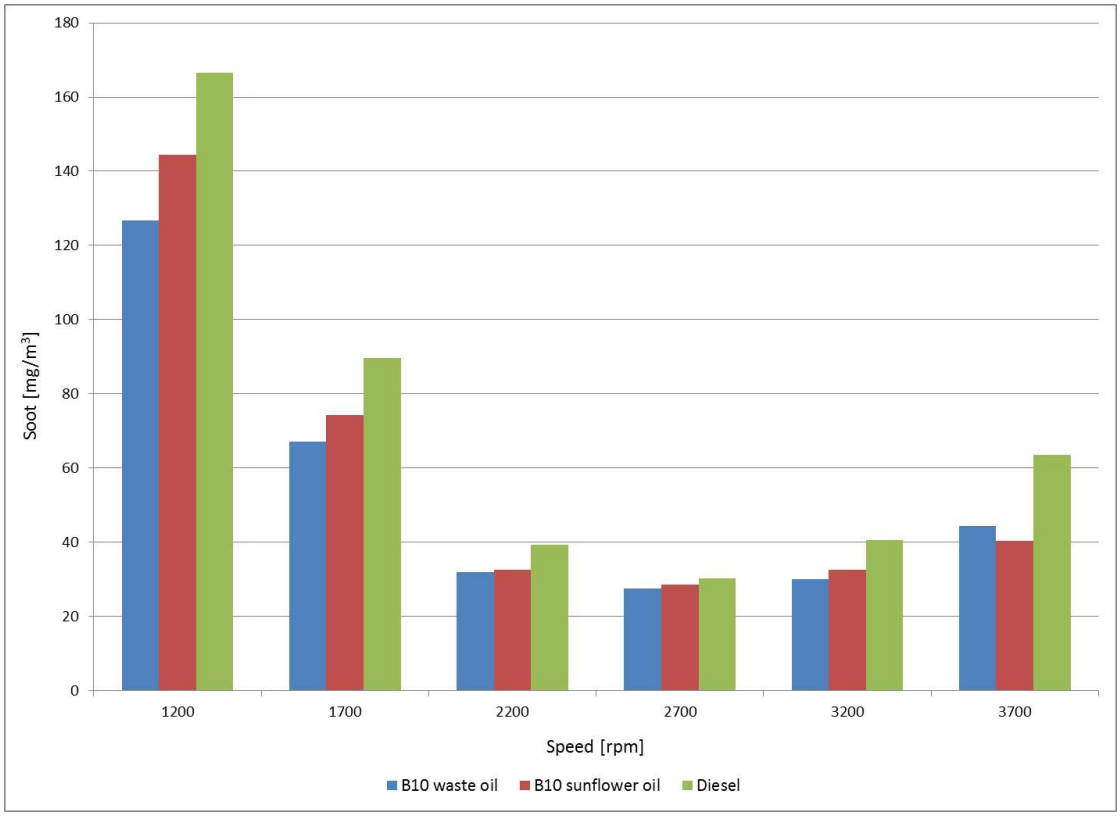

Fig. 1.39 Soot emissions

CO occurs due to incomplete combustion of the fuel, due to a lack of oxygen, the proportion of CO depending on the quality of the mixture. Other factors that influence CO emission are: mixture non-homogeneous, temperature gradient in the combustion chamber, insufficient time for the combustion reactions to complete. CO emissions decrease as engine speed increases, which indicates better mixture formation (ignition delay decreases).

By the point of view of CO_2 emissions, those in the case of biodiesel are lower on the entire tested speed range. By using biodiesel in mixture with diesel fuel a favorable CO_2 balance is obtained.

HC emissions occur due to fuel incomplete combustion. The HC emissions level varies over a very wide range, depending on the operating mode and operating conditions. At low loads and engine idling, HC emissions are higher than at full load. Wall temperature can also affect HC emissions by cooling the flame at the wall, causing either incomplete combustion or misfire.

The HC emissions decrease is caused by the presence of molecular oxygen in the biodiesel composition which contributes to an improved combustion process. The high cetane number leads to a lower autoignition delay and a longer combustion time. HC emissions are lower on the entire speed range in the case o B10 compared to diesel.

The tests carried out showed that, for the tested biofuels, CO and HC emissions are lower than those of a pure diesel fuel. HC and CO emissions decrease with increasing engine speed.

The amounts of NOx formed are influenced by the amount of oxygen and the temperature in the cylinder, the injection advance.

A superior cetane number reduces the autoignition delay and thus the NOx formation rate due to a lower pressure rise rate, which leads to a lower temperature of the combustion gases. Due to the lack of aromatic and polyaromatic hydrocarbons in biodiesel, the flame temperature is lower.
The particles generated from the combustion of the fuel are compounds of the carbon contained in the fuel. Their composition depends on the operating conditions of the engine and the exhaust temperature.
Soot emissions are lower for biodiesel.
It is found that soot emissions decrease when the engine is fueled with biodiesel due to the higher oxygen content that allows for complete combustion and oxidation of soot. Also, the absence of polyaromatics in the biodiesel structure leads to a reduction in the amount of soot.
The lowest amounts of soot are recorded in the area of maximum torque and minimum specific consumption. CO_2 emissions are lower on the entire speed range.

Conclusions

In terms of energetically performances, in case of B10 it can be observed that power and torque had an appropriate evolution, without notable differences compare to diesel fuel.
Regarding the ecological side, the usage of biodiesel blended with pure petroleum diesel fuel generally reduces most of emissions in compression ignition engines. The exception is represented by the NOx emission that is increased at some speed levels.
In conclusion it can be mentioned that B10 does not affect the energetically performance of the engine, while by the ecologically point of view, it generally represents an improvement.
Another aspect that must be considered is the material compatibility. The alternative fuel, as biodiesel, even blended can create unexpected problems in some fuel system parts such as: natural rubber hoses, gaskets, O-rings and metallic components.
Others elements that must be taken into account is the oil dilution in case of DPF regeneration, because of the lower energetic content of biodiesel, being more difficult to meet the regeneration temperature. Due to an extra-long post-injection the oil dilution can be increased. Also, the high evaporation temperature of the biodiesel, will determine at some engine working regimes, that the fuel from cylinder during the post-injection process, to not be able to evaporate and burn in order to ensure the DPF regeneration, but will remain in the cylinder and will be pumped by the piston rings into the oil pan, where will cause the oil dilution.
Biodiesel molecules are longer and heavier than diesel ones and tend to stick to the cylinder walls during prolonged post-injection. The possibility of evaporation of molecular fractions that dilute the oil is reduced compared to diesel molecules which are lighter. Biodiesel also contains oxygen and can accelerate oil oxidation.

Chapter 2. Influence of Road Infrastructure Design over the Traffic Accidents [DUM24b], [DUM19a], [DUM12], [TRU12]

Road accidents, their causes and effects represent a major problem for any country through medical, social and economic point of view. In this context, identification and understanding the complex factors that affect road accidents represent an essential research field for road safety.

Therefore, the need to improve road safety must be a mandatory objective for transport authorities that can be met through some strategies, such as: new or improved infrastructure, a tougher legislation, traffic participant's education, etc. The sooner it will intervene on the contributing factors of road accidents, the more visible the preventive effect will be.

All these aspects must be included in a safety system approach [CEO24] based on suitable procedures, methods and policies in order to develop, improve road safety. The interest for studying factors affecting road safety, the effects of road and traffic characteristics represent a dynamic field in continuous evolution.

The European Road Safety Observatory (ERSO) provides reliable and comparable data about road accidents, detailed information, analysis about road safety trends, procedures and policies in the European Union (EU). Considering ERSO annual report, the one for 2023 reveals a stalling progress in reducing road fatalities in too many countries [ERS23]. Despite this fact, reducing traffic accidents, their fatalities and improving road safety represents a continuous concern for EU.

In this regard the European Commission [EUR20] set a target for 2030 to halve the number of serious injuries in the EU, considering 2020 as landmark and in the long term for the year 2050, an ambitious objective of minimizing towards zero fatalities, "vision zero".

This goal aligns with United Nations resolution [RES20], which declared the period 2021 – 2030 as Decade of Action for Road Safety, having as target of preventing at least 50 % of all road traffic injuries and fatalities by 2030.

Going back to ERSO report, it also reveals that Romania is characterized by one of the highest road accidents incidence in EU. [POL24a] reveals that among the most common causes being excessive or inappropriate speed, especially in bad weather conditions. In Romania, most road accidents took place on national roads, but, important to mention, the most frequent fatal accidents take place on highways. Over 30% of the accidents that occurred, serious ones, were on national roads. It must be admitted that it is not only an infrastructure problem, but also have to think about the fact that accidents are caused by people.

The year 2022 represents the starting point of the National Road Safety Strategy implementation for the period 2022-2030. The main directions of action stipulated by it are: a high-performance management of road safety, safer conditions for the use of roads, increased security conditions for the infrastructure, prevention and monitoring, as well as optimal

interventions in case of emergency situations [POL24a].

In order to achieve similar goals [CEO24] foresees the implementation of a Safe Systems procedure to road safety, based on the following main elements:

- Human behavior, considering that no matter how well people are trained for a responsible road use, they can make mistakes and road infrastructure must be developed taking this aspect into account.
- Human frailty, consisting in limited resistance of the human body to various types of collisions and mechanical stress, the assessment of the injury risk and the severity of injuries. It represents another design criterion.
- Forgiving systems meaning that any human error must not be potentiated by the road, correlating with vehicle type, the interaction with other traffic participants.

An important aspect in the context of infrastructure sustainable development is to identify the risk factors related to it and their impact on road safety. It becomes obvious that such an in-depth analysis is specific to every EU country, for all road types considering aspects as road infrastructure design, environmental factors and traffic volume and control.

Contributing factors to road accidents can be grouped as follows [PAP19]: human factors (e.g. experience, fatigue, distracted driving, speeding, risky overtaking, the influence of alcohol and/or psychoactive substances), road infrastructure factors (e.g. road type, surface type, road segment configuration – alignment, curve, tunnels, junctions - road side configuration) traffic factors (e.g. vehicle mix, density - congestion), environment and weather (e.g. winding road, fog, rain, frost and snow), vehicle design and physical condition (e.g. safety systems, suspension condition, tires wear).

In the above road accidents favoring factors classification it is mandatory to include weather conditions too, because in many circumstances it represents an aggravating factor in accident occurrence frequency [BER13, MAL19] (accident risks are significantly higher during bad weather conditions). The meteorological phenomena type (e.g. rainfall intensity, fog, snow etc.) is another element that must be consider during the road infrastructure design process as well, by the perspective of forgiving roads [CEO24] The adverse weather conditions influence the driver's visibility (driver's standard reaction time is extended), reduce the friction coefficient between tires and carriageway, extend the stopping distance and in the worst-case scenario will determine vehicle skidding and aquaplaning.

From above analyses regarding the factors favorizing accident occurrence, having in mind [WEG95], it becomes obvious that in addition to the human factor, any road infrastructure improvement can either prevent or, in the most pessimistic scenario, reduce the effects of human error. So, a proper road system design can prevent the human errors and this will be materialized in less traffic accidents. It was considered three principles in order to prevent human errors during driving: keep away from an unintended road use, avoid considerable differences in direction, mass and speed, preventing unpredictability amongst road users.

Passing from human errors prevention to accident occurrence and injury severity in [WAN13]

those are explained through engineering system and human behavior as linked factors, that represents two major risks elements. An engineering solution can increase traffic safety, but in the same time it must not influence the driver's alertness. Road safety engineering and human behavioral adaptation represents key elements in reducing the number of accidents. In this context [ACE23] consider that road infrastructure design must be done in such a way as to ensure an optimal driver behavior in terms of speed, anticipation and attention. Situations as incorrect visibility of the carriageway, poor anticipation of road curves combined with inadequate speed, poor quality of tires or excessive wear of them doubled by unfavorable weather conditions (e.g. rainfall) can favor the occurrence of accidents.

The safe roads concept, in particular self-explaining roads [MAT05] involves an understandable one by the driver point of view, considering some important specific elements, such as: roadway quality in terms of adhesion and bumps free asphalt surface, day and night visibility, predictable road regardless of weather conditions, road markings and traffic signs, road sector optimal geometric configuration, etc. On the other hand, a high density of road signs or markings in complex traffic scenario according to [TOR13] may lead to an information overload and an increased risk of driving errors. An optimal practical combination of those elements is able to level up the driver confidence, anticipation and attention, influencing his reaction time both for a safe driving and to avoid certain dangerous situations within reasonable limits.

Considering all the above presented aspects, by evaluating the dependence between infrastructure features and drivers' behavior, including limit situations, it is possible to decrease or suppress traffic accidents, especially those generated by the road infrastructure faulty design.

In this context it is mandatory to analyze accidents causes and to develop efficient countermeasures to eliminate these causes, by carrying out professional road safety analyses with appropriate implemented measures.

One of these measures refers to the introduction of consistency rules [FIT00, WEG95] in road design. Design consistency refers to road geometry's conformity with driver expectancy, generating predictability. Theoretically, drivers make a fewer errors at geometric features that correspond with their expectations. An inconsistency in road design represents a geometric feature or a features mix with unusual characteristics that drivers may approaches in an unsafe manner. Such situations could lead to speed errors, inappropriate driving maneuvers and finally accidents. Their effects can be aggravated by inadequate roadside design, fact which will be detailed in the following.

2.1 The unforgiving – forgiving roadside concept

According to [TOR13] a significant percent of fatal road accidents in the EU are single-vehicle

type accidents, being classified as run-off-road accidents (vehicle leaves the carriageway and crashes to the roadside).

A roadside is called unforgiving [TOR13] if hazardous objects such as trees, poles are positioned too close to the road, increasing the chance of serious collisions. The purpose of the 'forgiving roadside' concept is to avoid crashes of drifting vehicles with potential hazards or to minimize accidents consequences.

The forgiving roads concept [WEG95] assumes driving errors consequences minimization, rather than preventing them and this mainly because of the human factor that only can be estimated.

Having this principle as a guideline, the entire road infrastructure must comply with the following:

Minimize the risk of vehicle leaving the carriageway by using vehicle active systems (e.g. line assist), correlated with appropriate road delineation;

Provide an adequate stopping distances or recovery area, when a car run-off the road;

If a collision still occurs with any roadside obstacles, it is mandatory that impact forces transmitted to the vehicle occupants to be at minor levels (no fatal or serious injury outcomes). According to [ALB13, PAP19], the main approaches for studying road safety are represented by infrastructure characteristics (e.g. road type and configuration, investment levels), environment (e.g. road geometrical design, weather conditions) and traffic conditions (e.g. vehicle types, traffic volume). Those elements are critically related, because a proper road infrastructure will have a beneficial impact on accidents number and gravity. Any other contradictory assumptions can be considered subjective, being dependent on drivers experience and education.

Two distinct road design concepts that aim to lower the overall number of accidents on the road network are self-explaining and forgiving roads. The concept behind self-explaining roads is that the design of the road itself can influence proper speed or driving behavior. As a result, there is less need for warning signs or speed limits.

A road-user-adapted design of various road features, including markings, signs, geometry, equipment, lighting, road surface, traffic and speed control, traffic rules, etc., is essential to a safe infrastructure. self-explaining roads are designed using the best possible combination of these road components.

Reducing the effects of an accident generated by driving errors, vehicles malfunctions, or bad road conditions is the top goal of forgiving roadsides. In order to prevent injuries or fatal run-off-road accidents, it must concentrate on treatments that force drifting cars back into the lane. Reducing the severity of the collision is the second priority if the car still collides with a road element. In other words, by lessening the severity of run-off-road accidents, the roadside should pardon the driver for its mistake.

2.2 Roadside hazards

The causes that determines the vehicle to leave the roadway are grouped in three categories:

- ✓ driver behavior and experience (e.g. excessive speed, dangerous maneuvers, fatigue, inattention, etc.)
- ✓ roadway conditions (e.g. asphalt adherence, lack of or poor road signs, markings, poor visibility, insufficient drainage, etc.)
- ✓ vehicle technical problems (e.g. tire excessive wear, steering, breaking systems malfunctions, etc.)

Roadside hazards can be grouped as follows [CEO24, TOR13]:

- ✓ single fixed obstacles (e.g. trees, vegetation, utility poles, road signs, safety barrier terminations, rocks, drainage features, etc.);
- ✓ continuous hazards (e.g. ditches, slopes, road restraint systems, kerbs, etc.);
- ✓ dynamic roadside hazards (e.g. pedestrian and bicycle facilities, parking).

Creating clear zones is a primary goal of forgiving roadsides design, however this isn't always feasible. Drivers may be at risk from certain roadside hazards. Frequently, it is impossible to avoid the location of some elements, like bridge barriers, traffic signs, and lighting poles. Roadside safety is impacted by additional features including ditches, slopes, and embankments, which need to be carefully managed. According to [USD86], a roadside object is considered dangerous if any or all of the following take place:

- ✓ the vehicle becomes unstable due to a roadside element;
- ✓ the vehicle is stopped abruptly, high deceleration;
- ✓ the vehicle passenger compartment is penetrated by an external object.

A. Single fixed obstacles

The most important single fixed objects are represented by: vegetation (e.g. trees), utility poles, traffic signs, lighting posts, tunnel entrances, abutments, safety barriers, boulder, rocks, drainage systems, etc.

In figure 2.1 are presented examples of hazardous tress located in proximity of carriageway. Due to their rigidity, trees are considered one of the most hazardous road side obstacles. Several studies considered that trees are dangerous when their diameter exceed 20 cm (10 cm in France [RIS06]) and the impact speed above 40 km/h.

In figure 2.2 are indicated examples of utility poles that located on the roadside and considered hazardous. Being made of concrete with different strength structures, during the impact their energy absorbance capacity is minimal to zero. The majority of accident are

produced in urban and rural zones, where these poles are in the proximity of the roadway.

Fig. 2.1 Examples of hazardous trees located on the roadside

Fig. 2.2 Examples of utility poles that located on the roadside

Traffic signs and lighting posts are generally placed near the roadway in order to be easy observed and to offer proper visibility of carriageway and surroundings. They cannot be relocated or removed, but in the case of an accident they must breakaway, otherwise are considered hazards.

Bridge piers, abutments, overpasses and underpasses walls generally are also made of concrete.

Fig. 2.3 Examples of hazardous bridge abutment and walls

Safety barriers known as forgiving roadside remedies are used to block dangerous objects

and/or stop cars from running off the road. On the other hand, the ends of rails or the junctions of two rail types may be dangerous roadside objects. When a safety barrier end does not flare away from the highway or is not adequately ramped down in the ground, it is deemed dangerous. When crashes with unforgiving safety barrier are produced, the passenger compartment frequently gets penetrated.

Fig. 2.4 Examples of hazardous safety barriers ends

In figure 2.4 are presented hazardous safety barriers ends. The transition between road safety barrier and bridge rail is missing. Also, the safety barrier end it's an unproper one and in a case of a crash, the car body will be penetrated by the barrier.
In figure 2.5 are two examples of hazards in a rocky environment and some boulders placed to close to the roadway. In the case of rocks, a clear zone near the carriageway is difficult to realize by technical point of view, and it's expensive.

Fig. 2.5 Examples of hazardous rocks and boulders

Another hazardous obstacle is represented by drainage systems that are often used on roads. In this case also the concrete is used for these systems, making them rigid without the ability to absorb impact energy.

Fig. 2.6 Examples of hazardous drainage systems

B. Continuous hazards

Continuous hazards are represented by considerable length objects that are frequently impractical to relocate or remove. In the following will be presented the main continuous hazards and their impact over the roadside safety.

A ridge of stone or dirt that supports a road or railroad is called an embankment. Roadside slopes of various types, including cut and fill slopes, are included in the term. The face of an excavated bank needed to lower the natural ground line to the desired road profile is known as a cut slope. On the other hand, the face of an embankment needed to elevate the intended road profile above the natural ground line is known as a fill slope. The height or depth, steepness, and distance from the road determine how dangerous a slope is.

When a car hits an embankment, there is a significant chance that it will roll over, particularly if the slope is steep. [RIS05] revealed that rollover is responsible for over one-third of all fatal embankment accidents. Out of all the objects in the analysis, this represents the largest percentage.

Fig. 2.7 Examples of hazardous cut and slopes

Generally running parallel to the road, ditches are drainage measures designed to channel water. They are designed to offer sufficient drainage and snow storage capacity and are formed by the side slope and backslope planes.

Fig. 2.8 Examples of hazardous roadside ditches

Road restraint systems (e.g. steel safety barriers, cable barriers, etc.) rank third in terms of roadside hazards after trees and utility poles. The rails themselves can also be regarded as roadside hazards, even though barrier terminations are struck the most often. A barrier's functions include keeping cars from running off the road and protecting vulnerable road users from vehicles. In order to keep vehicles moving in different directions, median barriers are frequently utilized.

Safety barriers should be built in such manner to smoothly reroute impacted cars at a low departure angle. But according to accident reports, redirected cars frequently collide with other cars, leading to serious accidents.

Fig. 2.9 Examples of collisions with safety barriers

Fig. 2.10 Unprotected terminals

Figure 2.10 presents an unprotected terminal (exposed terminal). A such barrier termination stops the vehicle abruptly and can penetrate the vehicle itself or cause the vehicle to roll over after impacting against the terminal (figure 2.9). This barrier end termination is aligned parallel (or nearly parallel) to the traveled lane that is within the roadside clear zone. In the event of a head-on impact, it can. Barrier end treatments known as crashworthy terminals aim to safely slow down a vehicle after a head-on collision with the terminal's nose or reroute it onto the carriageway. By its design cannot pass through the barrier.

Fig. 2.11 Crashworthy terminals [CEO24]

Dynamic roadside hazards

In the dynamic roadside features are included: bicycle facilities, pedestrian facilities and parking zones. Compared to previous analyzed, the dynamic hazards are not fixed, but moving and are more prevalent in urban environment than in rural ones. Especially in urban environments that are more dynamic all those features must be developed in order to ensure primarily optimal sight distance between traffic participants and a safe separation zone between travel lane and bicycle facilities and parking lots.
After identifying the potential hazards (described in detail above) that affect roadside safety, special procedures must be developed in order reduce or eliminate those risks. An example of such procedure is presented in the following:

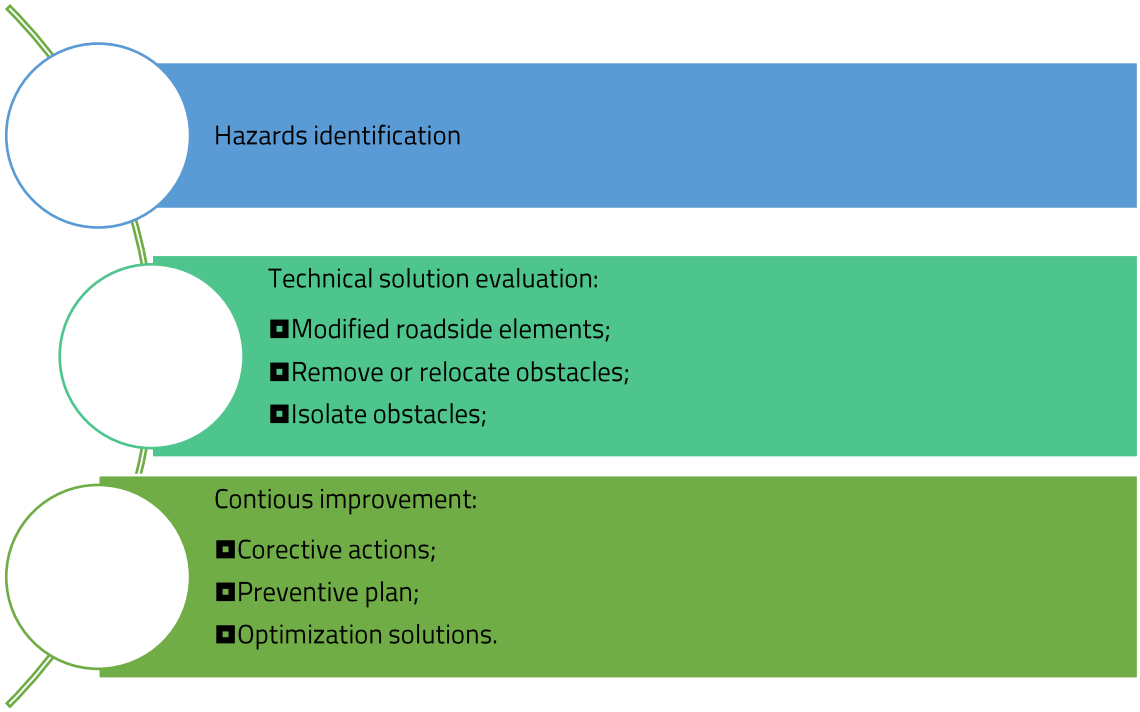

Fig. 2.12 Forgiving roadside solutions procedure

A first solution would be to provide a clear zone, a safety zone implemented on the roadsides. Hazards identification involves road sectors inspections and accidents type statistical analyses, with main causes. It must be included traffic volumes, speed, sectors geometry, surface conditions, crashes frequency and severity.

2.3 The study scope and background

The study's goal is to investigate the effect of the unforgiving roadsides on European route E68 (DN1) in Romania, over the degree of vehicle passenger's injury, respectively the level of car damage, having as a base point specific accidents produced on the road sector between the cities Brașov and Făgăraș, in Brașov county.

Also, the work aims to reconstruct through software simulation the probable mechanism of the production of such accidents.

The E68 (DN1) is one of the longest and most used roads in Romania, permanently recording high traffic values. The analyzed sector is a difficult one through its configuration. Supplementary the road sector is characterized by a high rate of accidents.

In the current study the continuous hazards are addressed, and ditches in particular, which generally are parallel to the roadway. The analyzed accidents are caused by vehicle's run-offs into ditches as can be seen in Figure 2.13. Here are illustrated some relevant crashes happened on E68 (DN1) in Romania on the specified road sector. As can be seen in the photos in most of the cases the impact between vehicle and ditch causes the car overturn or rollover.

In this scenario, besides the material damage it is very important to consider the accident effect over the vehicle occupants, too.

(a)

(b)

(c)

(d)

(e)

Fig. 2.13 Examples of accidents with hazardous roadside ditches [NEW04].

The photos reveal that, in most of the cases the vehicle – ditch accidents happened in adverse weather conditions (wet road surface), fact that indicates a prior vehicle skidding, most likely induced by speeding or by a sudden steering maneuver due to a poor understanding of that road section. Also, some photos show that the intervention of medical and extrication crews was necessary at the scene of the accidents, this fact representing an indicator of the crash severity.

In the presented context two factors cumulate: first a human error, then accentuated by an unforgiving roadside, a ditch. Thus, the study becomes relevant by establishing the probable collision dynamics, respectively through analyzing its effect over the vehicle occupants. More than this some forgiving measures are necessary to be implemented in order to compensate such human errors, by reducing or eliminate its effects.

Generally, as mentioned before there are a multitude of factors that can generate road accidents, being related to traffic volume, road configuration and type, weather conditions, environment and all road users. In this regard, traffic characteristics (such as speed, density), insufficient driving skills and road elements (such as geometry, quality and condition of the asphalt surface, roadsides design) can favor the occurrence of road accidents.

Due to multiple characteristics, national roads in Romania constantly represent the category where a large number of serious road accidents occur, characterized by high values of the injury and fatalities, speed being an important generating factor. Statistics show that 20% of serious traffic accidents in Romania are caused by speeding.

Several studies [AAR06, ELV04, NIL04, TAY00] analyses the dependence between speed and accidents frequency (accident rate), considering that an increased speed determines more accidents, many drivers go with high speed, but in limit situations they do not know how to manage them or the reaction time cumulated with an avoidance maneuver doesn't allow them

to avoid the accident In particular, a higher speed will also increase the total stopping distance of the vehicle and the probability of accident occurrence being higher, too especially in wet conditions (slippery road, poor visibility, different friction coefficient on tires, etc.). Thus, by reducing the speed, a decrease can be obtained in accident rate.

On the other hand, speed cannot be seen as a stand-alone factor of accident occurrence, in the speeding theory being necessary to include other mixed elements such its variations, road-tire interaction, driver experience, weather conditions, visibility, sudden trajectory change, erroneous estimation of a curve radius, etc.

Another major element in the safety field is the road itself, by its main design characteristics (geometry, alignment, curves, junctions and all other infrastructure elements, including roadsides) could play an important role in improving traffic safety. For example, an increased number of curves on a certain road sector can increase the possibility of accident occurrence. This fact can be accentuated by weather adverse conditions and drivers lack of experience in managing the relevant road section. Depending on the road sector particularities, the accident type, traffic conditions it can result only material damages, but occupants injuries can also occur. In this context the road infrastructure design affects in a negative manner the road safety.

In Romania, the special characteristics of the road (e.g. curve, tunnel, bridge, intersections, railway crossing) can be a generating factor in the road accidents occurrence. Similarly, for the analyzed years (2020, 2021 and 2022) in this study, the curve and the intersection represent the infrastructure elements with a high potential risk of accidents (Table 2.1, number of accidents per year). [POL24b] represents the source of statistical data that are analyzed in the present section of the study.

Table 2.1. The situation of road accidents according to the characteristics of the road.

Year	Road without specific elements	Road element	
		Curve	Intersection
2020	4092	1037	1061
2021	3332	744	790
2022	3138	739	795

The global analysis of the fatality index for the period 2020 – 2022 shows comparable values for accidents in the case of the curve as road main characteristic and the road without any specific characteristic (e.g. without curve or/and intersection - Figure 2.14). Although serious road accidents occur more frequently in intersections than in curves, the comparative statistical analysis indicates that the number of fatalities is lower in the intersection events (Table 2.2). It can also be mentioned that the highest rate was recorded for serious accidents in the case of the two analyzed characteristics (Figure 2.15).

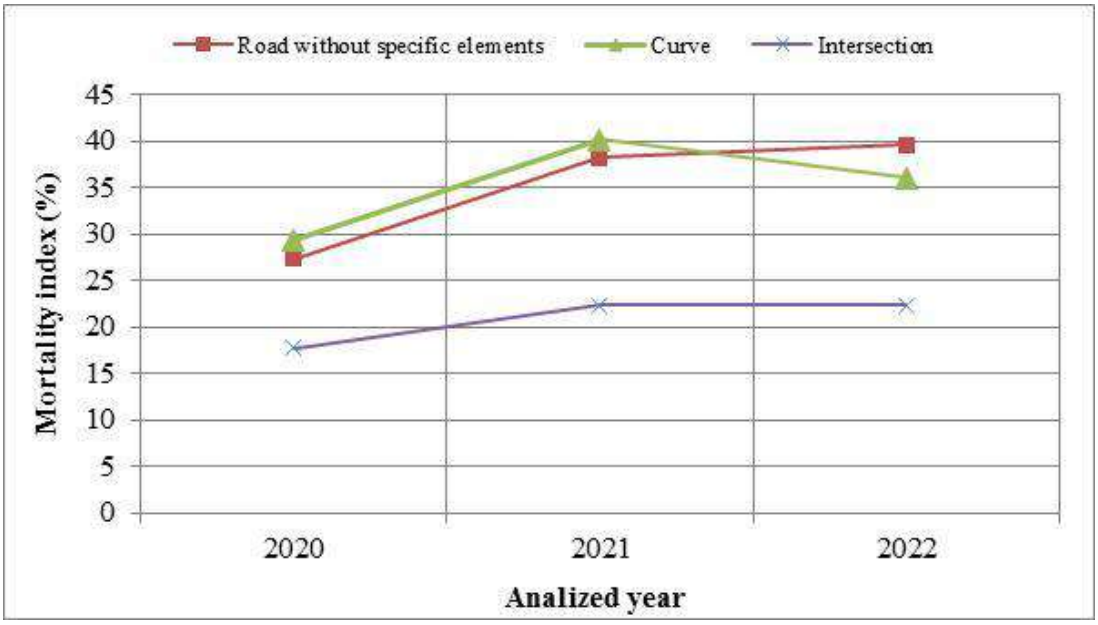

Fig. 2.14 Comparative analysis of fatality index.

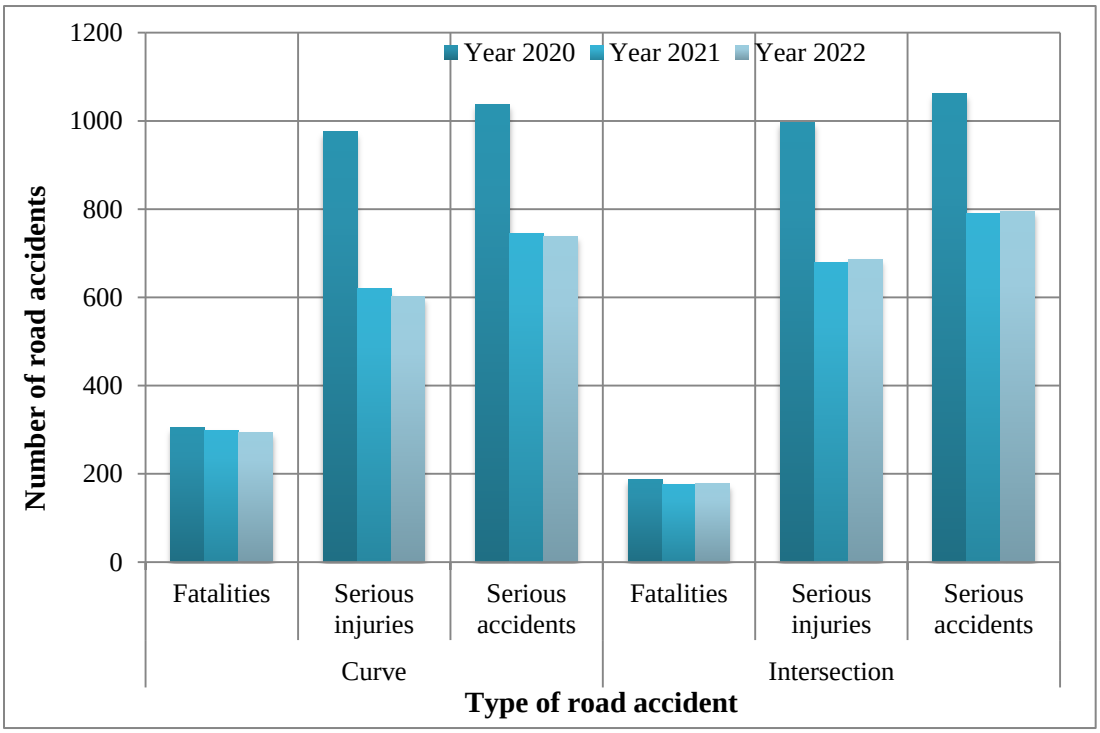

Fig. 2.15 Accidents analyses for the period 2020 – 2022.

Table 2.2. Serious road accidents depending on the road characteristics.

Year	Curve			Intersection		
	Fatalities	Serious injuries	Serious accidents	Fatalities	Serious injuries	Serious accidents
2020	304	975	1037	188	996	1061
2021	299	619	744	176	678	790
2022	293	601	739	177	686	795

Table 2.3 Fatality index.

Year	Road without specific elements	Road element	
		Curve	Intersection
2020	27.3	29.3	17.7
2021	38.2	40.2	22.3
2022	39.6	36	22.3

2.4 Methodology

The literature regarding the vehicle ditch accidents type is relatively limited [NIL04], an experimental study being complex, expensive and involving a considerable volume of work. A viable alternative solution is the software simulation of a such situation, considering as input data all the involved elements (e.g. vehicle rest position, deformations, road sector geometrical parameters, ditch main dimensions, weather condition, etc.). Trough simulation can be obtained realistic results and valuable information regarding the dynamics of this impact type (vehicle and occupants).

In the case of vehicle overturning or rollover, the car body strength is an essential fact by the point of view of deformations amplitude, their correspondence with the occupants' injury, being a major factor regarding the passive safety improvements.

Generally overturning accidents have as main cause cornering at high speeds, when the centrifugal force of the vehicle's mass is high enough to generate the overturning moment. A particular situation is represented by the impact of the wheels from one side of the vehicle with an obstacle in the roadside (ditch, curb), overturning being or not preceded by skidding.

During the vehicle movement, sudden variations in the transversal inclination of the vehicle body appear as a result of the car wheels from one lateral side passing over the ditch, then the imbalances of the vertical reactions on the wheels generate a moment that produces overturning and eventually subsequent rolling.

2.4.1 Preliminary data

As mentioned and illustrated previously the present paper was inspired by specific traffic accidents (vehicles that run-offs into ditches) produced on E68 (DN1) in Romania on Brașov – Făgăraș sector, one important aggravating factor being the unforgiving roadsides, bad weather conditions being another element to be considered, too.

To carry out the study a relevant curved road sector with an unforgiving continuous element was chosen (Figure 2.16), where were measured the main geometrical parameters of the ditch. Other relevant geometrical elements (e.g. curve radius) of the considered road sector were imported from Google Maps application in the simulation software, including the map zone.

The aspects from photos regarding the vehicles positions and materialized damages, road conditions and roadsides represented the starting point in the development of the simulation which allows the analysis of the dynamics of such an accident.

Fig. 2.16 E68 (DN1) – curved road sector used for the study.

2.4.2 Accident simulation scenario

For simulation of a such collision (vehicle – ditch) the specialized software PC-Crash was used, that enables the reconstruction and analysis of various traffic accidents. The simulation goal was to investigate the cumulated effect of the following factors – curved road, weather conditions, unforgiving roadsides – over the vehicle dynamics and occupant injury in the case of a vehicle that skids and run-offs into the ditch shown in Figure 2.16. The simulation scenario is a complex one and needs to consider and model a lot of parameters regarding road configuration, vehicle and occupants' dynamics, considering weather conditions, that favors the occurrence of such an event.

In order to generate the accident scene, the Google Maps specific zone was imported in the PC-Crash software, then a 3D road object tool was used to generate the specific road configuration, including the main ditch geometrical parameters (Figure 2.17).

The simulation was done for rainy weather conditions, a preponderant scenario for such accident occurrence, coefficient of friction between wheels and carriageway was adopted accordingly (wet conditions).

As a vehicle for simulation, a SUV type was used, this kind of vehicle being very popular in EU (in Romania, too). The vehicle dynamic parameters (e.g. speed, acceleration, braking, etc.) setup was made according to geometrical road configuration and in such a manner to accurately simulate a real-life vehicle skidding in the initial phase of the vehicle's movement into the curve, then resulted the vehicle runoffs into the ditch. In order to obtain a realistic accident mechanism and dynamics the simulation parameters were continuously modified and

optimized through iterations (e.g. speed, acceleration, braking, reaction time, etc.), until boundary conditions – vehicle rest position – was obtained.

For the calculation of movements and loads for vehicle occupants with PC-Crash, the multibody model was used (Figure 2.18). Interaction of the occupants with the vehicle interior is considered, too. Two restrained occupants were placed in the vehicle, on front seats in order to examine motion during the impact. The individual bodies of a multibody system are interconnected by joints and for restrained occupants, seat belts are modeled using spring damper elements. In the multibody model, for each body it can be specified different properties, like: geometry (a body being defined as an ellipsoid), mass, moments of inertia, contact stiffness and coefficients of friction [PCC20].

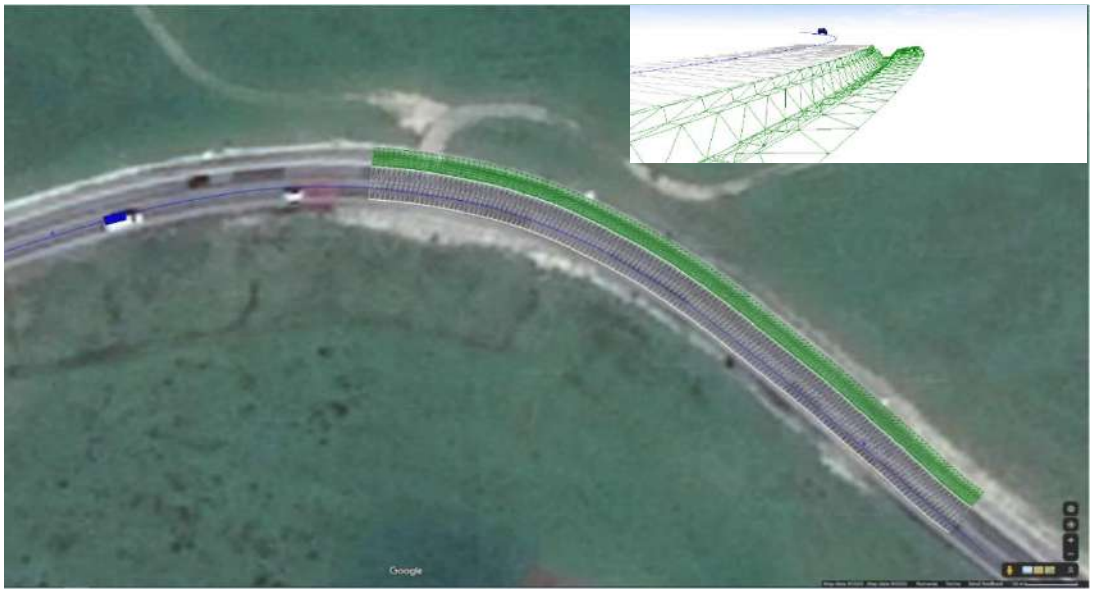

Fig. 2.17 Simulation scene, ditch profile – E68 (DN1).

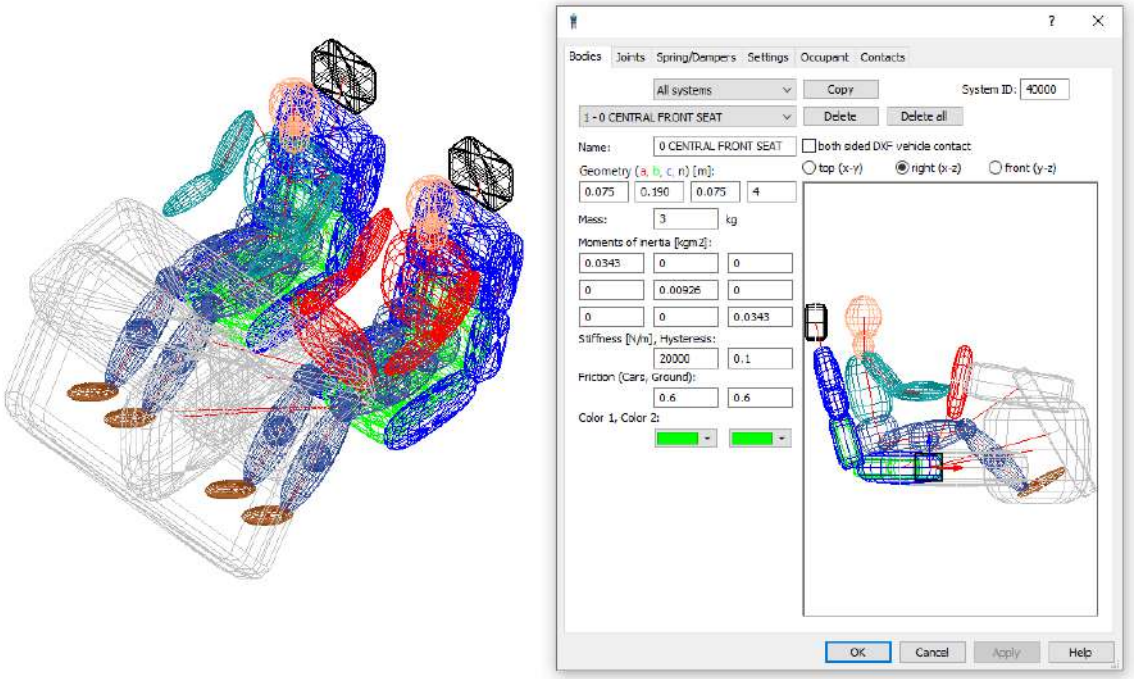

Fig. 2.18 Multibody model used in simulation.

In Romania the speed limit on European national roads is 100 km/h. On the considered road sector, the input data for the simulation are detailed in Table 4.

Table 2.4 Simulation input data.

Vehicle type	SUV, 4WD
Vehicle speed before entering the curve	90 km/h, case a) & b)
Friction coefficient, wet conditions	0.5
Maximum deceleration, wet conditions	4.91 m/s^2
Multibody model	2 front belted occupants: 80 kg, 1.8 m height each

2.5 Simulation results

The performed simulation considered two possible scenarios inspired by accidents presented in Figure 2.13 and the results are presented as follows:

a) The vehicle entering into the curve is skidding, leaves the road and enters into the ditch alongside with its direction of movement;

b) As entering on the curve, the vehicle skids, enters on the opposite direction and falls into the ditch on the left side of the travel direction. This scenario excluded the possibility of an impact with a vehicle coming from opposite direction, this aspect not being the object of the present study.

For the proposed scenarios, the performed simulation reveals that the accident production mechanism consists of two different phases: initially, the vehicle skidding appears due to the centrifugal force and then vehicle overturning and/or rollover is generated by the vehicle – ditch impact. In this case the vehicle overturning occurs independently of the road adhesion, being caused by the moment of the impact force.

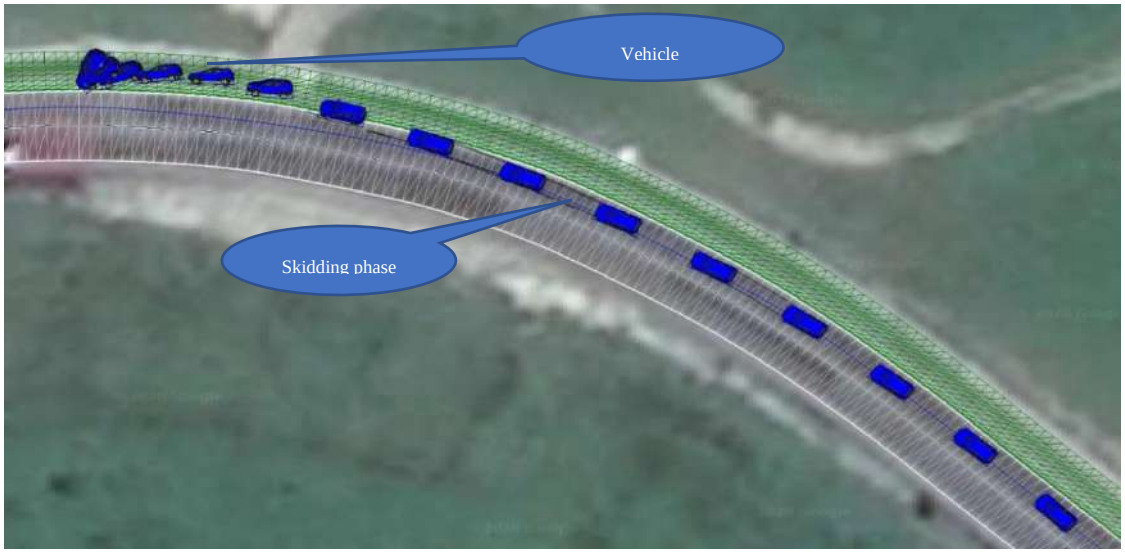

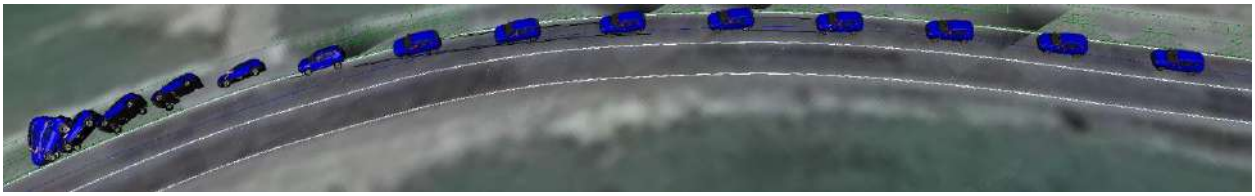

Fig. 2.19 Consecutive simulation sequences at time intervals of 0.4 s – case a)

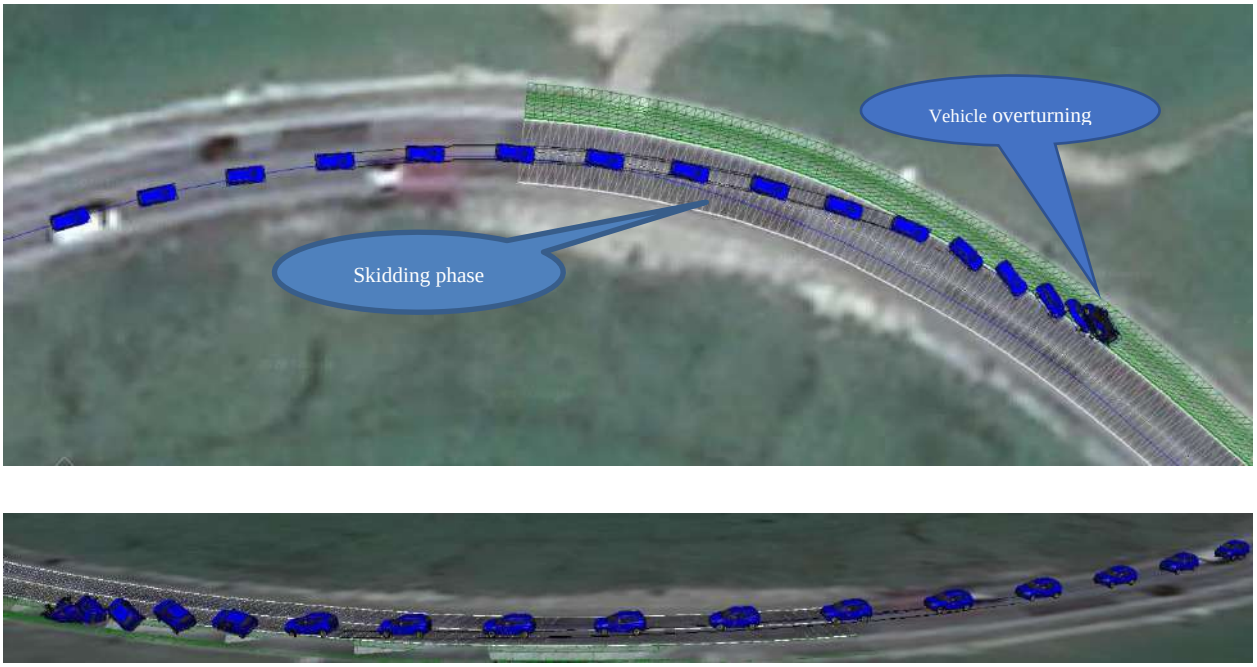

Fig. 2.20 Consecutive simulation sequences at time intervals of 0.4 s – case b).

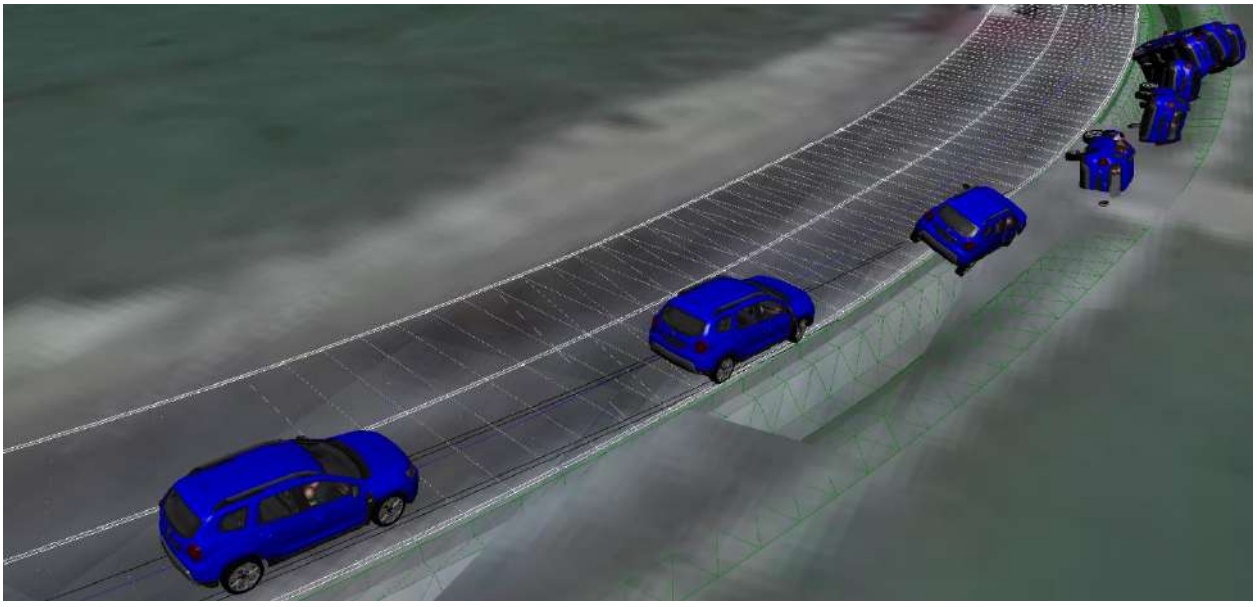

Fig. 2.21 Vehicle overturning phase – case a).

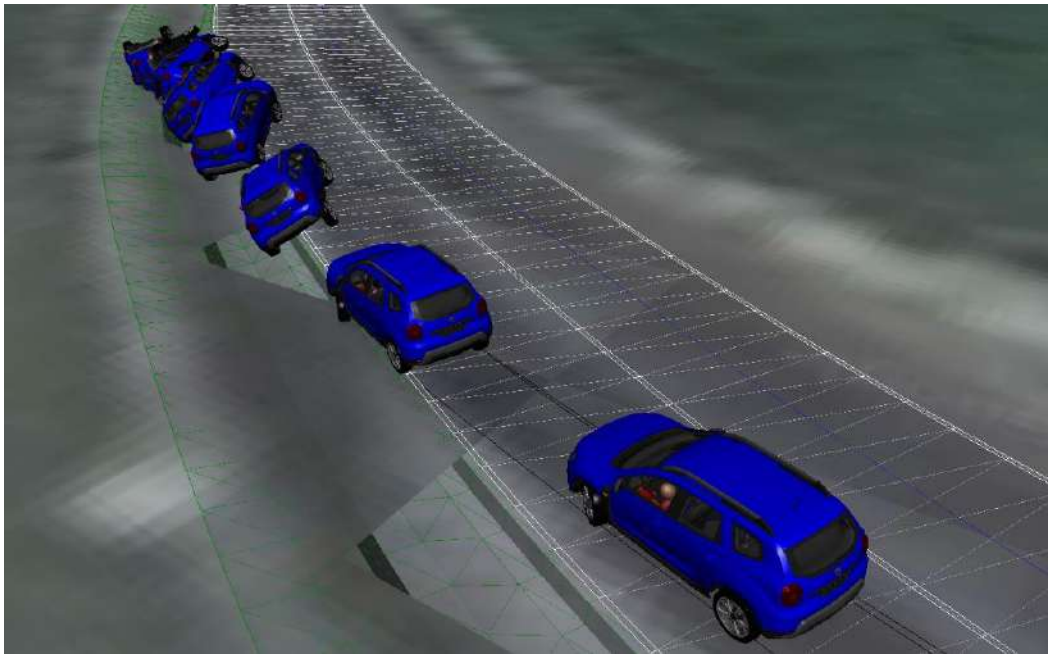

Fig. 2.22 Vehicle overturning phase – case b).

These two phases are illustrated in Figures 2.19 and 2.20, that consist of successive frames of the accident dynamics at time intervals of 0.4 s for both analyzed cases. In Figure 2.21 and 2.22 are detailed the vehicle overturning and rollover for the same time intervals and both cases, too.

In both cases, the skidding phase begins with instability of movement, due to the inappropriate behavior of the driver, who did not adapt the speed properly to the road conditions (one of the significant factors that generate accidents in Romania).

The skidding phase that appears is characterized by additional energy consumption due to vehicle lateral deviation and rotation tendency, friction with road surface being more intense. The energy consumption is equivalent to the increase in rolling resistance. This phase is considered ended when the vehicles leaves the carriageway and starts to fall into the ditch.

Figures 2.23 and 2.24 show the vehicle speed variation in time. In case b) compared to a), the vehicle speed at the time entering into the ditch is lower, 65 km/h versus 79 km/h, the initial speed being the same in both cases. In case b) the higher initial speed decrease is determined by cumulated factors, such as: driver reaction and braking attempt, vehicle skidding and entering on the opposite direction. These elements generated a supplementary time that permitted, through controlled and uncontrolled actions, that the impact speed with the ditch to be lower, theoretically with direct effect on occupants' level of injury (but depending on impact incidence angle, too).

The danger of injury of the occupants occurs mainly during the overturning phase, any intervention of the driver being excluded. The occupants' level of injury depends in this phase on the vehicle kinetic energy, and the obstacle (ditch) profile.

Practically, the overturning phase into the ditch is the one that generates the vehicle damage

and the injury level of the occupants, depending on the vehicle speed at the beginning of overturning or rollover and speed and acceleration variation during the phase.

From Figures 2.23 and 2.24 it can be seen that the speed drop (kinetic energy, too) during the vehicle – ditch impact is determined by following mechanism: vehicle body friction with the ditch surface and vehicle body deformation.

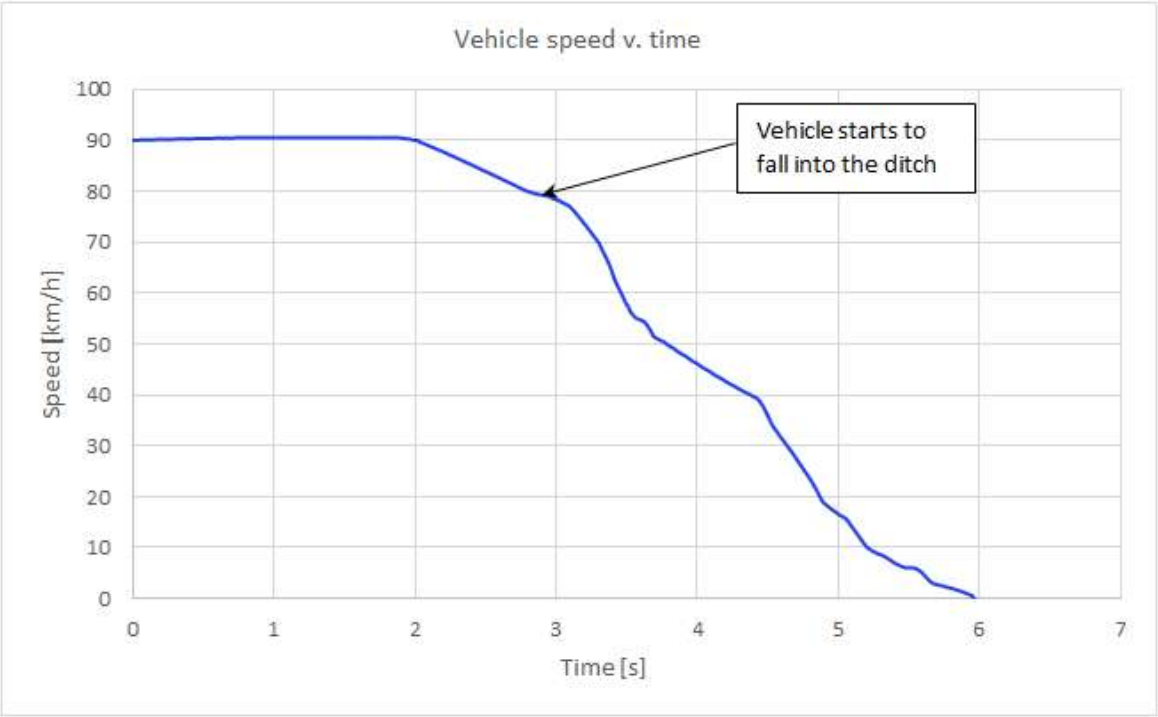

Fig. 2.23 Vehicle speed – case a).

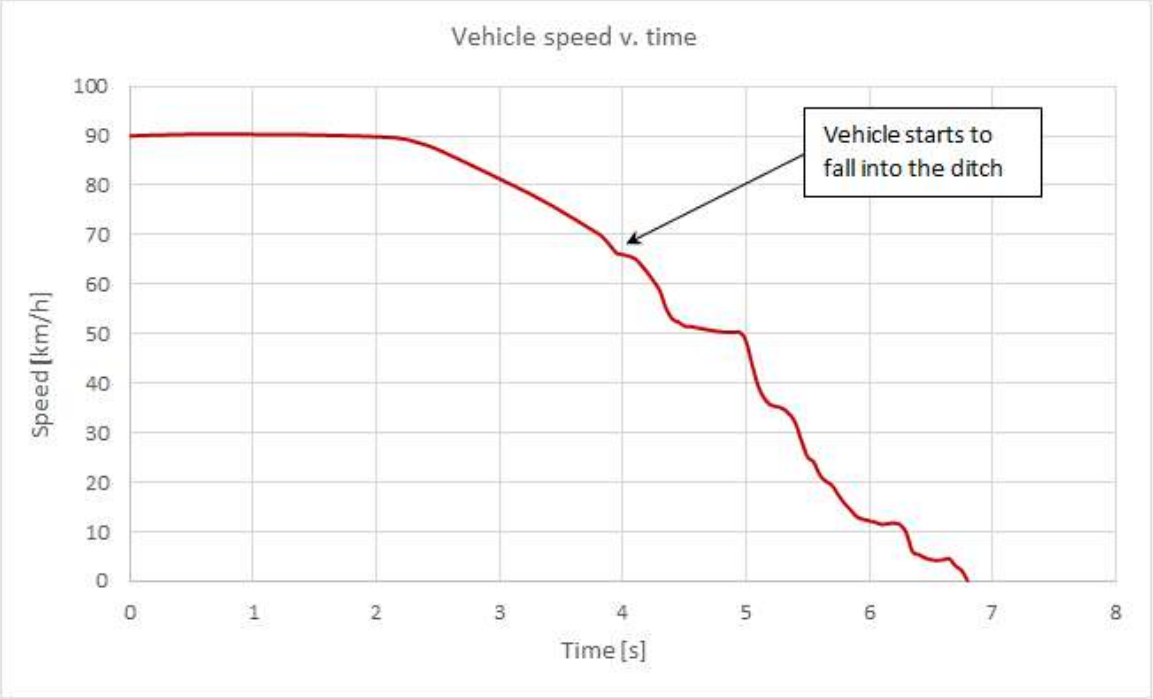

Fig. 2.24 Vehicle speed – case b).

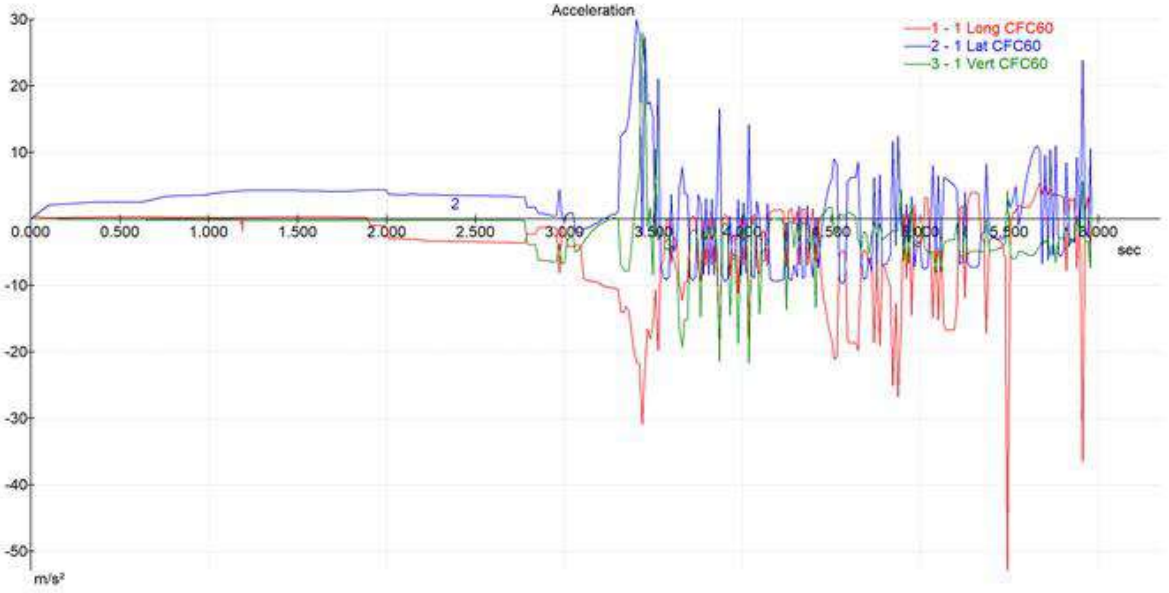

Fig. 2.25 Vehicle acceleration – case a).

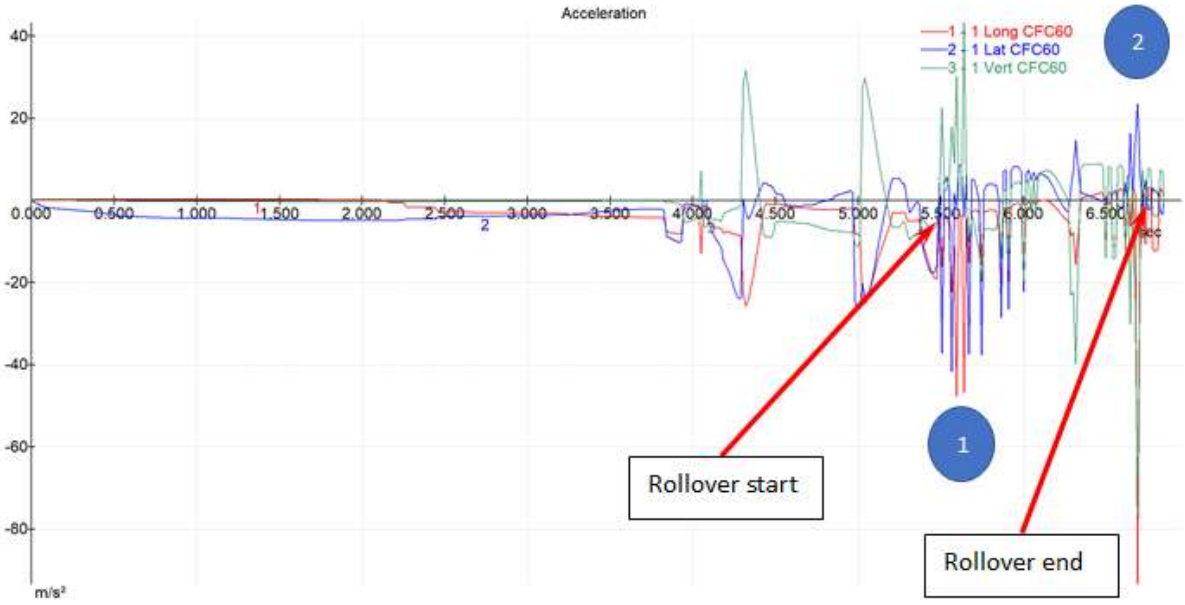

Fig. 2.26 Vehicle acceleration – case b).

The impact between vehicle body parts and ditch surface is highlighted by the acceleration graphs (longitudinal - long, lateral - lat and vertical - vert), Figures 2.25 and 2.26. A Channel Frequency Classes (CFC) 60 filter was used for processing the impact signals, to eliminate the high-frequency noise and reduce the signal peaks. By comparing the graphs for a) and b) cases, it can be seen that the vehicle acceleration dispersion, as impact effect, it is higher in case a), but as amplitude are comparable. Thus, in case a) predominant are longitudinal accelerations with a maximal magnitude about 50 m/s^2 and lateral accelerations is about 30 m/s^2, as a result of the vehicle sliding into the ditch. In b) case a high amplitude of accelerations is obtained during the rollover the car, but compared to a) time intervals were

these peaks are obtained is narrow about 0.5 s (interval 1, value 40 m/s^2) and 0.4 s (interval 2, value 85 m/s^2).

The simulation frames and accelerations magnitude indicate an increased level of vehicle body damages induced exclusively by the contact with the ditch surface. In case a) the front and right side of the car are damaged. In b) case, due to the vehicle overturn/partial rollover the entire vehicle body is affected (after a specialized damage evaluation it could be considered a total damage).

As mentioned before, for occupants' kinematics the multibody module was used. For them important speed differences occur in the case of collisions with other vehicles or obstacles. High accelerations appear when the vehicle, for example rotates around its longitudinal axis (overturning or rollover).

After the multibody simulation is performed, the most important data are those related to accelerations, because the severity of the occupants' injuries depends on them. In the case of the current research, the most susceptible human body parts that can be seriously injured are head and neck. This because of the possibility of hitting the head with the car roof or practically with any hard parts inside the passenger compartment. In this type of accidents other elements that can influence the injury severity are the vehicle size, vehicle body deformation level, rollover number, obstacle size, obstacle that penetrates passenger compartment, etc.

In order to avoid head injury, in theory the acceleration magnitude could not exceed a certain level, this being studied through head injury criterion (HIC), that considers the duration and severity of the impact. According to [VIR19] HIC is the most important parameter regarding human survival. It characterizes the brain injuries due to the impact of the head vehicle accidents. An alternative evaluation method refers to average acceleration that is greater than 80 g for no longer than 3 milliseconds (ms).

In [GAI09] is mentioned the human body supportability limit is about 10 – 35 g, at gradients of 500 – 1000 g/s with a maximum duration of 0.15 – 0.4 s. According to [BRI24] the human body exposure to acceleration higher than 30 g lasting longer than 0.2 seconds may cause fluid displacement or tissue deformation. The symptoms appear as a blood pressure drop, pulse rate rise, weakness and skin pallor. These aspects refer to a forward seated position. In the backward-seated position, acceleration up to 35 g can be tolerated without significant difficulties [BRI24].

In current study, in case a) (Figures 2.27 and 2.28) the maximum obtained value of head acceleration (right-side occupant) was about 240 m/s^2, 24 g, that correspond to HIC15 <130 (equivalent acceleration < 55, for 3ms) inducing to the occupant no concussion, eventually a headache or dizziness, with effects for less than an hour accordingly to [HIC24].

In case a) the vehicle entered tangentially into the ditch and an important amount of kinetic energy of the vehicle was dissipated through the friction between lateral side and the ditch wall, effect that contribute to non-injury of the occupants (but this a particular aspect induced

by a particular dynamics), only some temporary, minor effects. For the occupant the acceleration is higher due the fact that the vehicle hits first the ditch with its right lateral side.

In b) case (Figures 2.29 and 2.30) the maximum value obtained for the acceleration for the driver's head was about 210 m/s^2, that correspond to HIC15 <130 (equivalent acceleration < 55, for 3ms) inducing to the driver no concussion, eventually a headache or dizziness, with effects for less than an hour accordingly to [HIC24]. The maximum value for acceleration for the right-side occupant was about 412 m/s^2, 41 g, value that corresponding to HIC15 180, the occupant suffering mild concussion accordingly to [HIC24].

In the analyzed b) scenario the vehicle overturn (partial rollover) induced higher accelerations for both occupants, which indicate a different mechanism of kinetic energy dissipation for impact type.

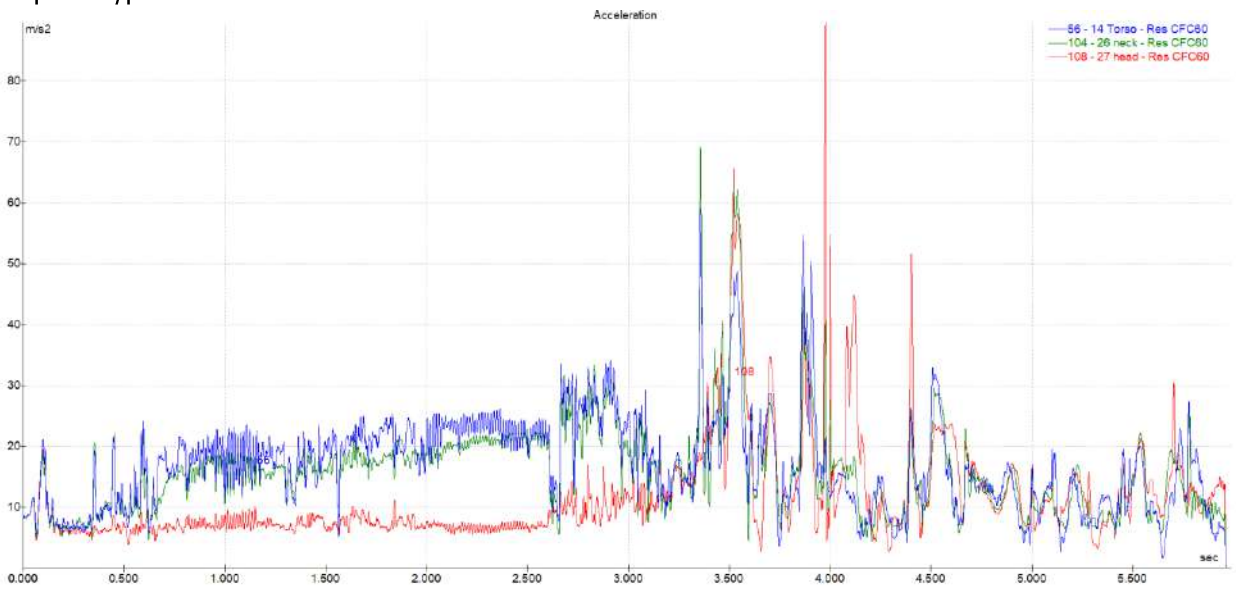

Fig. 2.27 Driver acceleration – case a).

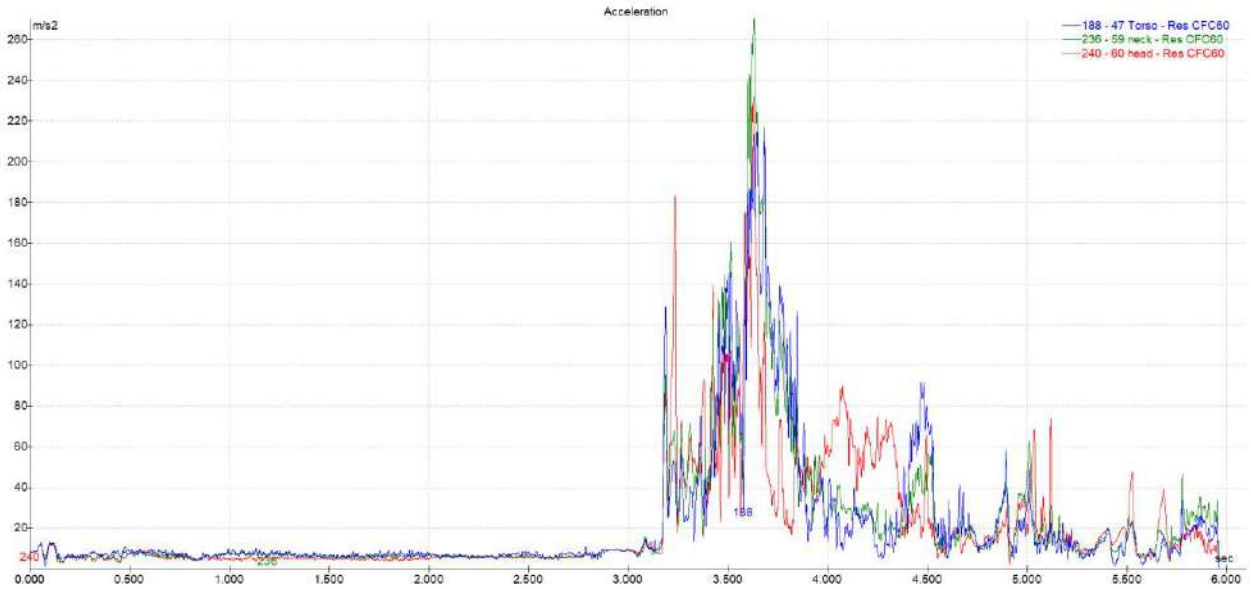

Fig. 2.28 Front right-side occupant acceleration – case a).

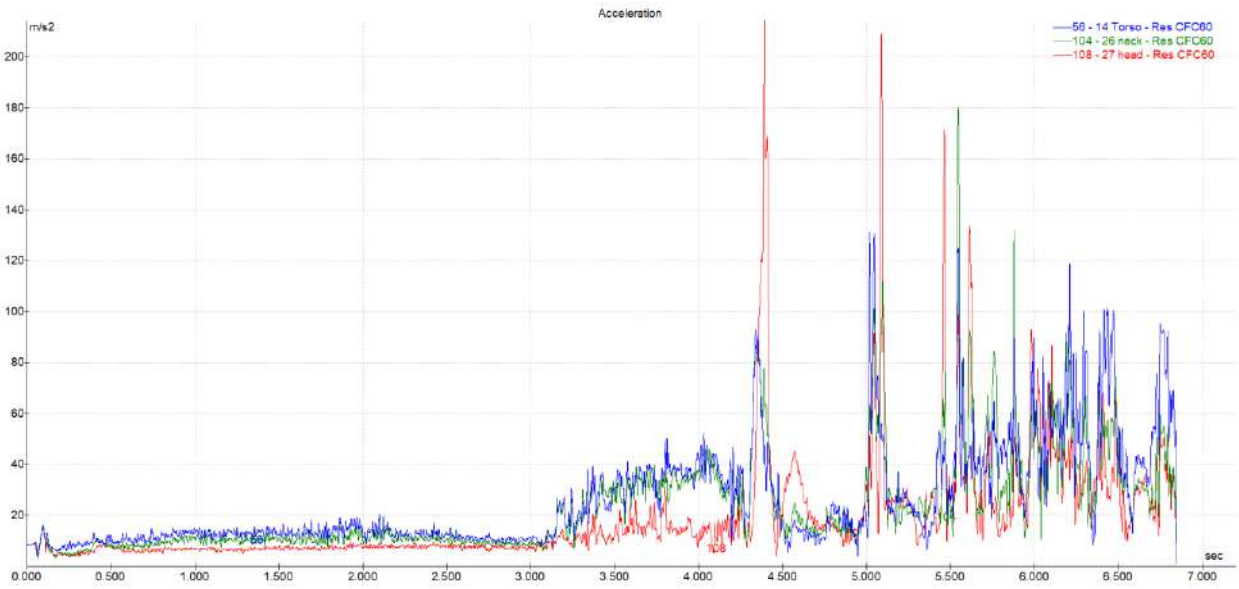

Fig. 2.29 Driver acceleration – case b).

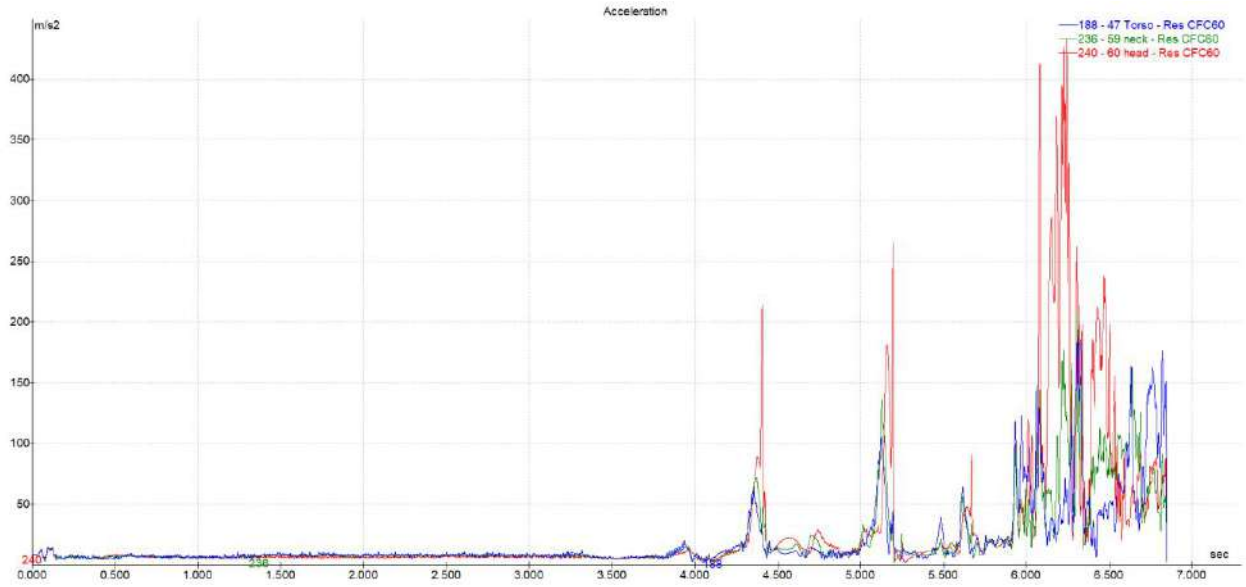

Fig. 2.30 Front right-side occupant acceleration – case b).

2.6 Discussions and recommendations

The majority of the accidents involving vehicle overturning or rollover occur outside the carriageway (vehicle leaves the road and enters to roadside), this type of accidents being considered as run-off-road accidents [TOR13]. Every such accident is unique due to its particularities: vehicle type and load, terrain characteristics, obstacles, road design, driver experience and perception, the incidence angle of the impact, obstacle dimensions, etc. If the vehicle during the rollover doesn't hit any obstacles this kind of accidents are less dangerous due the fact that vehicle kinetic energy is dissipated in a longer time compared with a crash between two vehicles.

The objective of the present study was to particularize and analyze the situation when the

vehicle overturn or rollover was induced by an unforgiving roadside, as effect of a run-off-road phenomenon. Simulation results show a major vehicle body damage induced exclusively by the impact with the ditch and obviously a considerable repair cost. In the situation of vehicle rollover, it may be considered the necessity to replace the car with a new one.

From the performed analysis results that the ditch represents an unforgiving roadside, because due to a human error, it caused the actual accident, being in contradiction with the concept of forgiving roadside [CEO24, TOR13]. Through this idea, in the case of a run-off vehicle the roadside must either avoid the accident or to minimize its consequences.

In this context the most important factor is the health and safety of the occupants and as it could be observed this type of accident could affect it in some manner. A more dangerous scenario, compared to the analyzed one could appear anytime in the case of some other types of vehicles, if the driver/occupants aren't belted, with different vehicle dynamic parameters, especially including different vehicle incidence angle with the obstacle (ditch). Different dynamic conditions then those analyzed in present paper could generate serious injury and vehicle damage.

For both studied cases, the vehicle damages took precedence compared to level of occupant injury, this being a positive aspect of the research. The injury level was a little bit serious in the b) case. Both scenarios had as starting point the unappropriated road configuration estimation by the driver, materialized in over speeding in wet conditions (a frequent real scenario). Even if the injury level obtained through PC-Crash simulation wasn't a significant one for the front occupants, it cannot be ignored the potential psychological trauma.

From the presented aspects, the study highlights the influence of an improper roadside design over the traffic safety in case of a human error occurrence. Another relevant element that results from the research is the importance of auditing problematic road sectors in order to implement on existing roads the forgiving roadside systems.

Following the elements detailed before in the paper, for analyzed problem (ditch – vehicle impact) as recommendation, the next solutions can be implemented in order to transform an unforgiving roadside into a forgiving one:

- Cover the ditch and creating a safety zone in proximity of carriageway, doubled by the measure of eliminating the extra potential obstacles in problematic areas with a high rate of roadsides accidents. In this manner the vehicle that is out of control will pass over the covered ditch and it will exist the possibility to regain its control or to stop on the field without major or zero damages. It is necessary that the adherence of the covering material to be close to asphalt one. This fact is illustrated in Figure 2.31, where by such a measure, the covered ditch with an appropriate carriageway shoulder represents a recovery area, which will allow the driver in limit situations to perform recovery maneuvers. The effect will be a non-injury occupant and a free of damages vehicle.

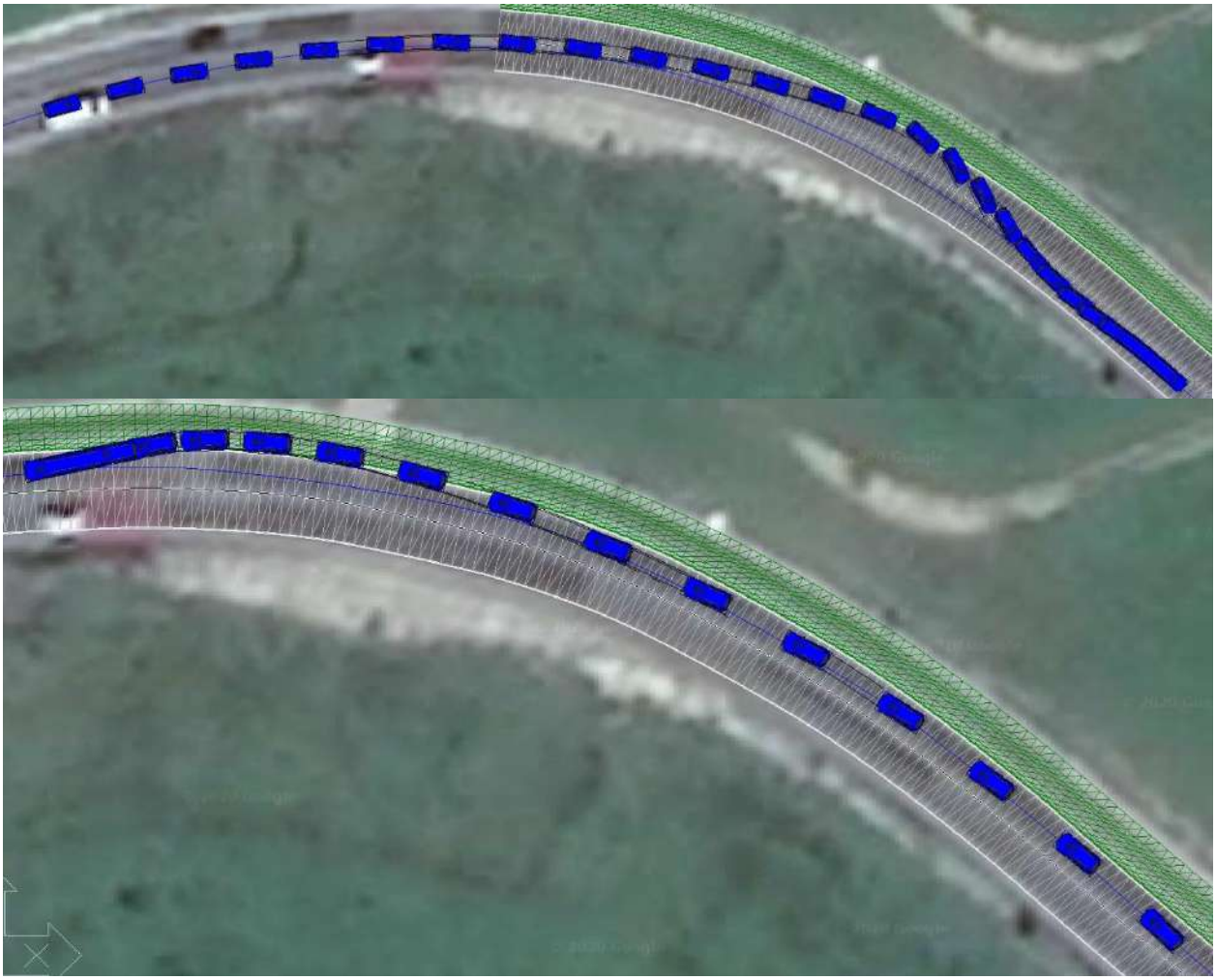

Fig. 2.31 The effect of covered ditch solution.

- Modify ditch slope ratio; the slopes should be kept as shallow as possible. A shallow slope will allow the driver to regain vehicle control over (Figure 2.32 [TOR13]).

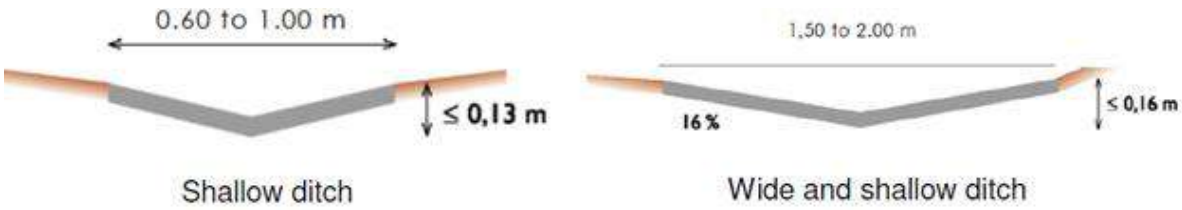

Fig. 2.32 Examples of safe ditch.

- Isolate the ditch by mounting appropriate roadside barriers (e.g. rolling barrier), that will minimize the effects of a vehicle out of control. It is recommended where a previous solution isn't possible trough environmental limitations.

Fig. 2.33 Rolling barrier.

- Enlarge and pave the road side shoulder (Figure 2.34), and by that measure is created, in reasonable limits a recovery zone for the drivers (where is possible on existing roads), in a similar way to the ditch covering solution presented previously. This is known as a safety zone, where a driver can regain control over the vehicle.

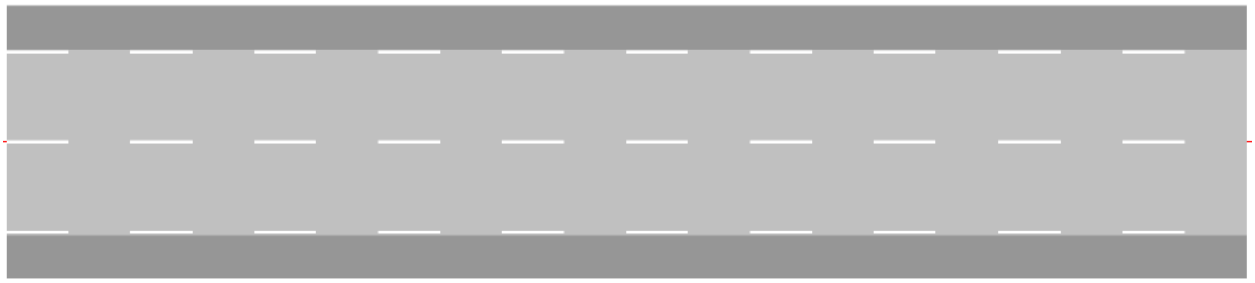

Fig. 2.34 Enlarge and pave the road side shoulder – safety zone.

Previous were indicated a few possible solutions, through which implementation are created real conditions in reduction frequent roadsides accidents and an increase of traffic safety in any conditions is obtained, both on the studied road sector and in general on Romanian national roads. The study had in mind to evaluate the vehicle damage and the occupants' injury severity for a simulated situation, inspired by real traffic accidents on the same European road sector. On the other hand, the approach can be seen as an input study for implementing the concept of forgiving roads in Romania, too with real life benefits in reduction of traffic accident and their injury severity.

The forgiving road concept, through its multiple possible technical solutions, will increase the road safety and through it, the confidence of all traffic participants during usage of the Romanian national road network.

The study also reveals the practical utility of developing a road safety system, including adequate technical solutions to make a road forgiving with direct effect on traffic safety. From this point of view the relevant technical solutions and good practices experience can be the starting point for standardization in the field of road safety.

Chapter 3. The Influence of Laser Micro-Perforation Parameters over the Airbag Processing and on the Efficiency and Passengers' Safety during an Impact [DUM24c], [DUM24d], [DUM24e], [DUM24f], [DUM24g], [RUS24a], [RUS24b], [DUM22], [DUM19b], [DUM18b], [DUM16], [DUM14]

In the automotive industry, passenger safety is a top priority. The airbag is one of the most critical components of passive safety systems, designed to protect passengers during a collision. A crucial aspect in the design and manufacturing of dashboards and other interior surfaces of vehicles is the compatibility of these components with the airbag system. In this context, laser perforation plays a vital role in ensuring the proper functioning of the airbag and its efficiency.

Synthetic leather and other finishing materials used on the dashboard and vehicle interiors are created not only for aesthetics but also to meet technical safety requirements. One such requirement is the perforation regime, which is essential to allow the airbag to deploy optimally in the event of an impact.

Airbag Function and the Importance of Proper Deployment

The airbag is an inflatable device that rapidly inflates during an impact to protect vehicle occupants. Its primary purpose is to prevent violent contact between passengers and hard components of the vehicle, such as the dashboard or windshield. The airbag's deployment must be swift and precise to offer the necessary protection within fractions of a second. Thus, the proper opening of the airbag depends on several factors, including the materials used in the dashboard's construction and the perforation regime applied to the areas where the airbag is concealed.

Laser Micro-Perforation Regime

Laser perforation is a process in which materials, including synthetic leather, are perforated with tiny holes using a high-precision laser. This technique is used to weaken the material in a controlled manner, allowing the airbag to penetrate the dashboard surface without compromising the aesthetic or structural integrity of the dashboard. In the area where the passenger airbag is mounted, a discreet weakening of the material is necessary to ensure the airbag can break through the surface without delays or blockages.

The laser perforation regime involves setting critical technical parameters, such as hole size and density, cut depth, and the distance between holes. These parameters must be carefully adjusted to balance aesthetics, material strength, and efficient airbag deployment.

The Role of Micro-Perforation of Airbag from the Passenger' Zone

Laser micro-perforation of airbags from the passenger' airbag zone has a significant impact on

how the airbag opens during an impact. Without proper micro-perforation, the dashboard's covering material, such as synthetic leather, can delay or impede the airbag's deployment, which could compromise passenger safety. If the dashboard is manufactured without this predefined weakening, the airbag may encounter more mechanical resistance, leading to a critical delay in full deployment.

A well-designed micro-perforation regime allows the airbag to break through the dashboard material almost instantaneously, ensuring effective passenger protection. Laser micro-perforation creates a controlled break point, making the material yield predictably and release the airbag without significant resistance. This is essential because a delayed or incomplete opening can severely affect safety during an accident.

Technical Parameters of the Laser Micro-Perforation Regime

To ensure optimal airbag performance, the micro-perforation regime parameters must be adjusted according to the thickness and type of material, the structure of the dashboard, and the location of the airbag. Key parameters include:

Hole size and density: The micro-perforations must be small enough not to compromise the dashboard's appearance or structural integrity, yet numerous and large enough to enable quick opening.

Perforation depth: The depth of the holes must be adjusted to optimally weaken the material's structure. Too shallow a depth can make the material too resistant during impact; while too deep can lead to premature cracks or visible defects in the dashboard.

Hole pattern: The holes must be evenly distributed in the airbag zone to ensure uniform opening. Asymmetrical patterns could affect how the airbag deploys and create weak points in the material.

Material type: More rigid or thicker materials generally require higher perforation density and deeper cuts to ensure efficient airbag deployment.

Influence of Micro-Perforation Parameters on Airbag Performance

The micro-perforation regime directly influences airbag performance and, consequently, the level of safety provided to passengers. When micro-perforations are properly made, the dashboard covering material yields quickly and efficiently, allowing the airbag to inflate fully in less than 30 milliseconds. This timeframe is critical for reducing the forces exerted on the passenger's body and preventing serious injuries.

If the micro-perforation parameters are not well-calibrated, the airbag deployment may be delayed, drastically reducing the protective effect. For instance, a material that is too resistant can delay the deployment by a few milliseconds, which may seem insignificant but could mean the difference between minor injuries and severe harm.

Optimal Airbag Deployment Time

The optimal airbag deployment time depends on several factors, including the speed and severity of the impact, but ideally, it should occur within 20 to 30 milliseconds from the moment of impact detection. Laser micro-perforation of the material in the airbag zone plays a critical role in achieving this optimal timeframe.

If the micro-perforation regime is not applied correctly, the airbag may encounter difficulties in breaking through the dashboard material, extending this critical time window. On the other hand, overly aggressive perforation could cause the material to tear too quickly, affecting the controlled inflation process and, consequently, the efficiency of the protection.

3.1. The analysis of laser micro-perforation process for automotive synthetic leather parts

Laser processing technology is seen as an efficient method due to its lack of tool wear, fast processing speed, ease of performance, possibilities for flexible automation, high-quality products and contactless nature; it can be employed in various industrial applications, such as drilling, cutting, milling, polishing, etc. [ANM20], [CAR04], [KAN23].

The production and testing of airbag parts involves the use of various specific equipment and technologies. In this context, the aim of this study is to analyze the laser micro-perforation process of airbag components considering the main influencing factors. The obtained results in the pull test are analyzed from the point of view of the influences of the laser power (P1 and P2) and the thickness of the material. The statistical analysis of the experimental data includes a goodness-of-fit test, regression analysis, analysis of variance (ANOVA) and multivariate and factorial analyses. All of these are applied to identify patterns, correlations and outliers within the dataset. Additionally, advanced visualization tools are utilized to emphasize the complex data relationships and trends, aiding in the interpretation of the results and the formulation of actionable insights.

The novelty in the laser micro-perforation process of textile materials refers to recent technological improvements that optimize both the process and the outcomes of this technique [DUM24b], [RUS24a], [RUS24b]. The updated laser technology allows for the creation of extremely precise and uniform perforations, which are essential for applications where the technical characteristics are crucial. Laser micro-perforation systems are much faster, enabling mass production without compromising product quality, thereby making the process more efficient and cost-effective for manufacturers. Additionally, modern technologies offer advanced control over the laser parameters, such as the power, frequency and pulse duration, allowing for fine adjustments based on the type of material and the desired outcome.

This exhaustive investigation represents a significant step towards enhancing the reliability

and consistency of airbag cutout laser processing methodologies. The comprehensive analyses and proposed remedial measures outlined herein underscore the collective commitment to quality assurance and process optimization within the auto-motive safety industry. It is imperative that stakeholders collaborate closely to ensure the seamless implementation of these measures, thereby fostering a culture of continuous improvement and excellence in manufacturing practices. By applying the specific methods, the following outcomes are expected.

- Uniform and precise perforations: The optimization of the laser parameters and rigorous control implementation should lead to uniform and precise perforations across the entire surfaces of synthetic leather parts.
- Reduction in defects and waste: Real-time process monitoring should enable the immediate detection and correction of any issues, thus reducing the quantity of damaged material and minimizing waste.
- Increase in efficiency and consistency: Through parameter optimization and con-tinuous process control, a significant increase in operational efficiency and improved consistency in the quality of end products is anticipated.

In order to monitoring, control and optimize the laser micro-perforation process technology for automotive synthetic leather parts, it was considered [DUM24b], [RUS24a]:

- Material preparation: The materials used for airbags include robust technical textiles such as nylon or polyester, which are treated for high tear and wear resistance. The airbag material must be securely fixed on a work platform to prevent movement during perforation, ensuring precision perforations.
- Laser configuration: The CO_2 laser used for the micro-perforation of airbag materials operates at a wavelength of 10.6 μm. This wavelength is effective for absorption by tech-nical textile materials. The laser power varies depending on the thickness of the material and the perforation specifications, with typical powers ranging from a few watts to hundreds of watts.
- Laser beam focusing: The optical system focuses the laser beam using lenses or mirrors to concentrate the beam into a small point. The size of the focused point deter-mines the diameter of the micro-perforation and the precise adjustment of the focus are essential to ensure high-quality perforations in airbag materials.
- Control and movement: A computer controls the movement of the laser and the perforation pattern, allowing the precise programming of the size, shape and distribution of the perforations. The movement system, which may include stepper motors or servomotors, ensures the precise movement of the laser or the platform holding the material, essential in achieving uniform perforations in the complex airbag materials.
- Micro-perforation process: The laser beam is emitted and absorbed by the material, causing the rapid evaporation of a small portion of the material and creating a perforation. In airbag materials, the perforations must be precise to ensure the proper and safe

deployment of the airbag during an impact. Lasers can operate continuously or in pulses, with short, high-intensity pulses often preferred to minimize the heat-affected zone (HAZ) and increase the perforation precision.

- Cooling and inspection: After perforation, the airbag material may need time to cool, especially if the process generates significant heat. Quality inspection is essential, with the perforated material being checked to ensure the size and uniformity of the perforations. Optical instruments or high-resolution cameras are often used for this inspection, thus guaranteeing compliance with the strict standards of the automotive industry.
- Important parameters in the micro-perforation process for airbags: The laser power is crucial to ensure precise and uniform perforations in the technical textile materials of airbags. The power must be sufficient to vaporize the material but not so high as to degrade the edges of the perforation or cause excessive material damage.

The pulse duration affects the precision of the perforations. Short pulses produce precise perforations and minimize the heat-affected zone (HAZ), essential to maintaining the structural integrity of the airbag material.

The movement speed of the laser affects the size and shape of the perforations. High speeds can produce smaller, shallower perforations, while slower speeds allow deeper penetration and larger perforations.

Beam focusing determines the size of the focused point, and precise focusing produces smaller, more precise perforations. The stability of the focus is crucial to ensuring uniform perforations across the entire airbag material.

The material type influences the absorption of the laser. The technical textile materials used in airbags have specific absorption rates for the CO_2 laser wavelength, and materials with high absorption require less power for perforation. The thermal properties of the material, such as the thermal conductivity and heat capacity, influence the heat dispersion and the size of the HAZ. The following materials and technology were utilized for the laser micro-perforation process.

- Synthetic leather: The synthetic leather parts used in this study were selected to represent common materials utilized in the automotive component manufacturing industry for airbag production. The sample size was 50 parts for each analyzed parameter: the laser power and material thickness. For the factorial analysis, 950 samples were considered. The material used consisted of synthetic leather produced from polyvinyl chloride (PVC) with a nominal thickness of 1.2 mm. This was laminated with a spacer fabric with a nominal thickness of 2.99 mm, with a specified tolerance of ±0.3 mm.
- Laser process: The micro-perforation process was conducted using a high-precision laser system, enabling precise control of the perforation parameters, such as the power and operating speed.

The main components of the machine setup for laser micro-perforation include a CO2 laser, mirrors, a laser beam and a gas nozzle. The most important parameters of the laser micro-

perforation process are the focus, laser power (P1, P2), impulses, robot speed (ms) and tolerance of material deviation.

The laser utilized in the conducted experiments operated in pulsed mode, exhibiting a pulse duration of 200 femtoseconds (fs) and a repetition frequency of 2 kilohertz (KHz). This configuration facilitated precise control over the laser's output, providing high-intensity pulses conducive to experimental investigations.

The analysis stages consisted of testing based on the following.

- Material characterization: Preliminary tests were conducted to characterize the material properties, including the thickness, texture and temperature resistance, before commencing the micro-perforation process.
- Laser parameter setting: Critical parameters of the laser process, including the power, frequency and beam traversal speed, were optimized to ensure efficient and uniform material perforation.
- Real-time monitoring and control: During the micro-perforation process, monitoring and control systems were implemented to detect and rectify any deviations in the operating parameters, thereby maintaining the quality and consistency of the perforations.

3.1.1 Methodology

The investigative approach adopted herein involved a meticulously planned and executed series of experiments, orchestrated with precision to closely examine the intricacies of airbag cutout laser processing. The methodology was designed to simulate re-al-world production scenarios, ensuring that the findings were applicable and relevant to industrial practices. Airbag cutouts, a critical component in automotive safety systems, underwent laser processing precisely 24 h after adhesive application, mimicking the timeline encountered in actual manufacturing settings. However, the key aspect of this investigation lies in the identification of a significant challenge: the inadvertent use of left-hand drive (LHD) parameters for right-hand drive (RHD) components during laser processing. This systemic inconsistency has far-reaching implications, potentially com-promising the quality and reliability of airbag cutouts, which are vital for passenger safety. The manifestation of nonconforming (NOK) outcomes during subsequent pull testing procedures underscored the urgency of addressing this issue, prompting a comprehensive examination of the underlying causal factors.

Laser Processing Investigation

The airbag cutout laser processing investigation detailed in this report represents a meticulous endeavor aimed at comprehensively understanding and rectifying the discrepancies encountered during the manufacturing process. With automotive safety as a paramount

concern, the study meticulously delves into the nuanced intricacies sur-rounding the application of LHD and RHD parameters in laser processing techniques. The optimization of production methodologies within the automotive safety industry is not merely a matter of efficiency but a critical aspect in ensuring passenger safety and regulatory compliance. This investigation, therefore, serves as a critical work in the quest for excellence in automotive safety standards. Through rigorous experimentation and analysis, the study aims not only to identify areas of improvement but also to pave the way for innovative solutions that elevate the standards of airbag cutout manufacturing processes.

Experimental Design and Setup

The experimental design was meticulously crafted to ensure robustness and reliability in data collection. Airbag cutouts, sourced from diverse production batches, were carefully selected to capture the variability inherent in real-world manufacturing processes. Prior to laser processing, the cutouts underwent stringent quality control checks to ensure uniformity and consistency across samples. Adhesive application was carried out using state-of-the-art equipment, adhering to industry best practices to minimize variability. The laser processing parameters, including the power, intensity and speed, were systematically varied to evaluate their impacts on the processing outcomes. Additionally, environmental conditions such as the temperature and humidity were closely monitored and controlled to minimize external influences on the experimental results.

Collection and Statistical Analysis

Data collection during the experimental phase was conducted with meticulous at-tention to detail, employing advanced instrumentation and data logging techniques to capture a comprehensive range of process parameters.

The inferential analyses of the recorded experimental data were performed using the Minitab v17 software. Considering a 95% confidence interval (CI) and a significance level of α = 0.05, the normal distribution of the experimental data was qualitatively and quantitatively validated by applying the Anderson–Darling (AD) goodness of fit [GIB73], [TAE14]. An analysis of means (ANOM) chat [NIS24] for a normal distribution was computed for different laser power levels (P1 and P2). We used an analysis of means for normal data and a two-way design to identify any significant interactions and main effects. The experiments were designed (DOE) [MAS03], [MON11] based on the process particularities by choosing the main control factors that affected the micro-perforation characteristics, applying a full factorial design.

3.1.2 Experimental data analysis

The pull test results and material thickness were statistically analyzed with a 95% confidence interval (CI) and a significance level of α = 0.05. The homogeneity of the experimental data was

tested by assessing the goodness of fit with a probability plot (Figures 3.1 and 3.2). Additionally, the quantitative assessment was performed with a hypothesis test, such as the Anderson–Darling normality test.

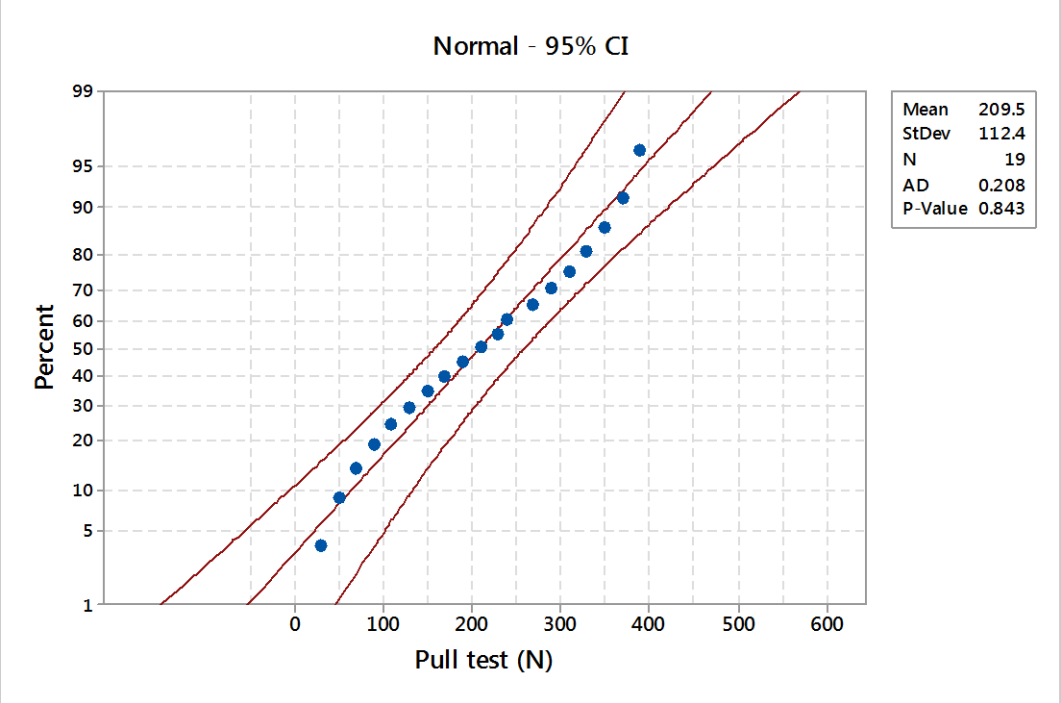

Fig. 3.1 Probability plot of pull test results.

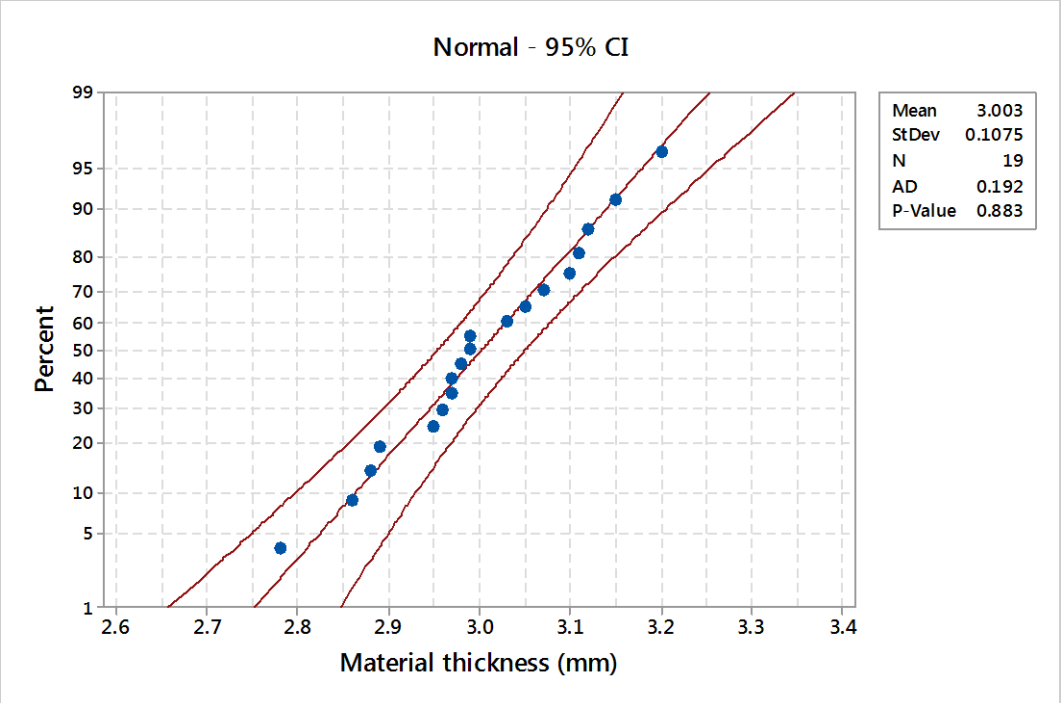

Fig. 3.2 Probability plot of material thickness.

The results of the goodness-of-fit normality test are synthetically presented in Table 3.1. A parametric distribution analysis was considered in order to estimate the statistical parameters of

the pull test and material thickness (Table 3.2).

Table 3.1 Anderson–Darling normality test.

Characteristic	AD	A-Squared	Correlation Coefficient	*p*-Value
Pull test (N)	0.208	0.21	0.990	0.843
Material thickness (mm)	0.192	0.19	0.992	0.883

Table 3.2 Descriptive statistics of analyzed characteristics.

Statistical Parameter	Pull Test (N)	Material Thickness (mm)
Mean	209.5	3.003
Standard Deviation	112.4	0.107
Minimum	30	2.78
1st Quartile	110	2.95
Median	210	2.99
3rd Quartile	310	3.10
Maximum	390	3.20
Skewness	0.014	–0.12
Kurtosis	–1.185	–0.27

Visually comparing the probability plots depicted in Figures 3.1 and 3.2, it can be concluded that the experimental data complied with a normal distribution. The points roughly follow the straight line, all of the points are within the lower and upper confidence boundaries, and the *p*-value is over 0.05.

The estimated mean of the pull test data is 209.5 (95% confidence intervals of 155.31 and 263.64), the standard deviation is 112.4 (95% confidence intervals of 84.91 and 166.18), and the median is 210 (95% confidence intervals of 127.28 and 292.72). Using a significance level of α = 0.05, the Anderson–Darling normality test indicates that the pull test data follow a normal distribution.

In the case of the material thickness, the mean is 3.003 (95% confidence intervals of 2.951 and 3.054), the standard deviation is 0.107 (95% confidence intervals of 0.081 and 0.159), and the median is 2.99 (95% confidence intervals of 2.958 and 3.074). Moreover, it can be underlined that the estimated value of the Anderson–Darling statistic is 0.192.

The overall inferential analysis concludes that the pull test results and material thickness are from a normally distributed population.

3.1.3 The analysis of the main factors for the laser micro-perforation process

The influence of laser power on the micro-perforation process of automotive parts

The approach of this analysis focuses on the influences of laser power as a critical parameter

in the micro-perforation process of automotive parts. The following steps outline the approach taken to investigate this relationship:

- Selection of Laser Power Levels: Various levels of laser power were selected for analysis, ranging from low to high intensities. This range was chosen based on preliminary studies and industry standards to ensure a comprehensive examination of the powers impact on micro-perforation quality.
- Sample Preparation: Automotive parts used in this study were prepared to identical specifications to maintain consistency. Each sample was subjected to micro-perforation using the selected laser power levels.
- Micro-Perforation Process: The laser micro-perforation was performed using a high-precision laser system. The parameters, except for laser power, were kept constant to isolate the effect of power variation. The lasers wavelength, pulse duration, and beam focus were maintained at optimal settings determined through preliminary testing.
- Data Collection: After the micro-perforation process, each sample was examined to measure the quality of the perforations. Parameters such as perforation diameter, edge sharpness, and overall consistency were recorded. Advanced imaging techniques and measurement tools were employed to ensure accurate data collection.
- Statistical Analysis: The collected data were subjected to statistical analysis to determine the effect of laser power on the quality of micro-perforations. The Anderson-Darling normality test was applied to validate the data distribution. This test is crucial for confirming that the data follow a normal distribution, enabling further analysis with parametric tests.
- Goodness-of-Fit Evaluation: The goodness-of-fit of the data was evaluated using Anderson-Darling statistics (A-Squared = 0.14, P-Value = 0.963). This step ensured that the data were homogeneous and suitable for detailed analysis.
- Analysis of Results: The relationship between laser power and the quality of micro-perforations was analyzed. The findings were interpreted to identify the optimal laser power level that ensures the highest quality of perforations, contributing to the reliability and performance of automotive components.

By focusing on laser power as the primary variable, this methodology provides a clear understanding of its impact on the micro-perforation process. The results of this study are expected to guide the optimization of laser settings in industrial applications, ultimately enhancing the quality of automotive parts.

Statistically analysis of laser power

The data analysis consists on influence of laser power parameter on manufacturing process. Using a significance level of 0.05, the Anderson-Darling normality test by computed statistics (A-Squared = 0.14, P-Value = 0.963) indicates that the laser power data follow very well a normal distribution (Figure 3.3). Additionally, based on summary report (Figure 3.4), it can be

underline that the mean of the laser power is 0.342 W (95% confidence intervals of 0.271 W and 0.413 W) and standard deviation is 0.116 W (95% confidence intervals of 0.083 W and 0.193 W). Also, it can be observed that the variance of analyzed date is low, skewness is 0.171 W and Kurtosis is - 0.566 W.

An overall graphically analyses show that the data are homogenous; the mean and median values are comparative.

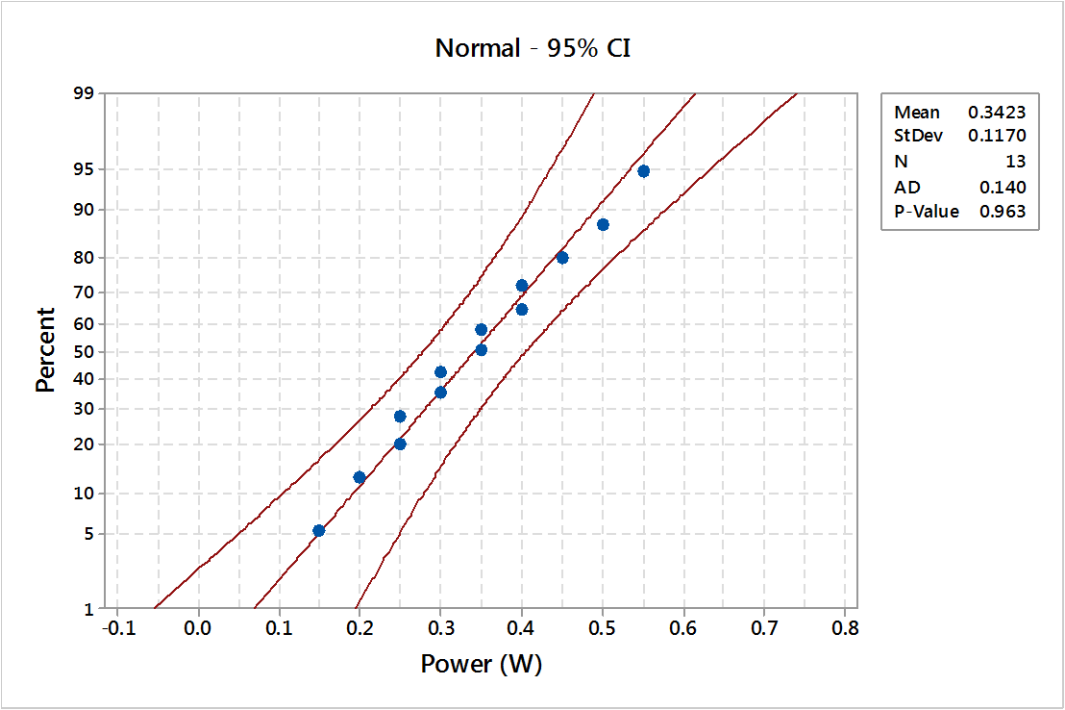

Fig. 3.3 Probability plot of laser power.

Considering the decision of goodness-of-fit, it was estimated the empirical cumulative density function (CDF) of laser power for normal distribution (Figure 3.5). For 87th percent, the estimated laser power is 0.4741 W. This result indicates the optimum set value in order to obtain the parts with high precision and quality.

Graphical analyses confirmed by homogeneity of the data, with mean and median values being comparable. The empirical cumulative distribution function for laser power, estimated for the 87th percentile, it indicates an optimal laser power setting. This result suggests that the quality and precision of the micro-perforated parts are significantly influenced by the level of laser power. Consequently, understanding and optimizing this parameter is crucial for enhancing the reliability and performance of automotive components.

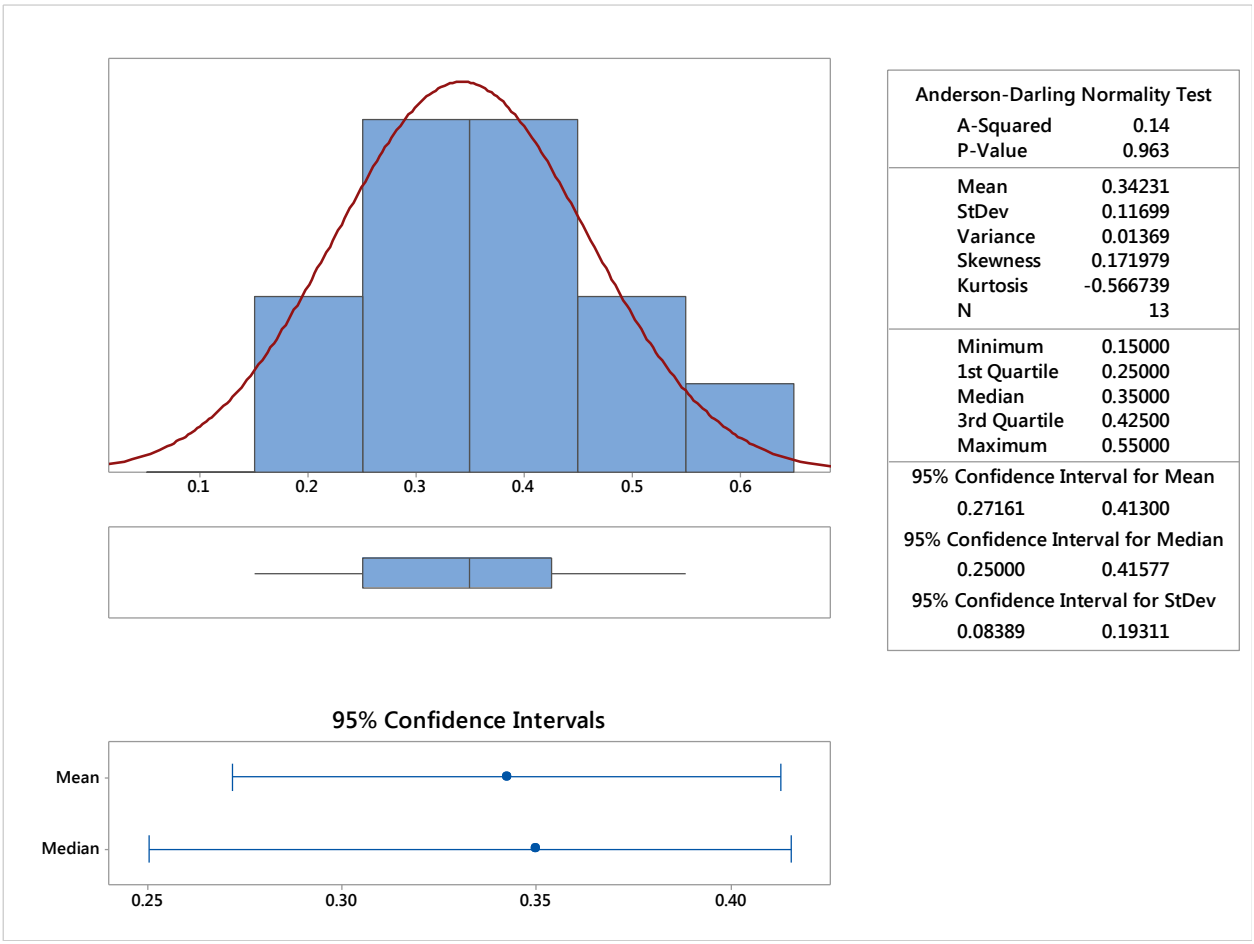

Fig. 3.4 Summary report for analyzed laser power.

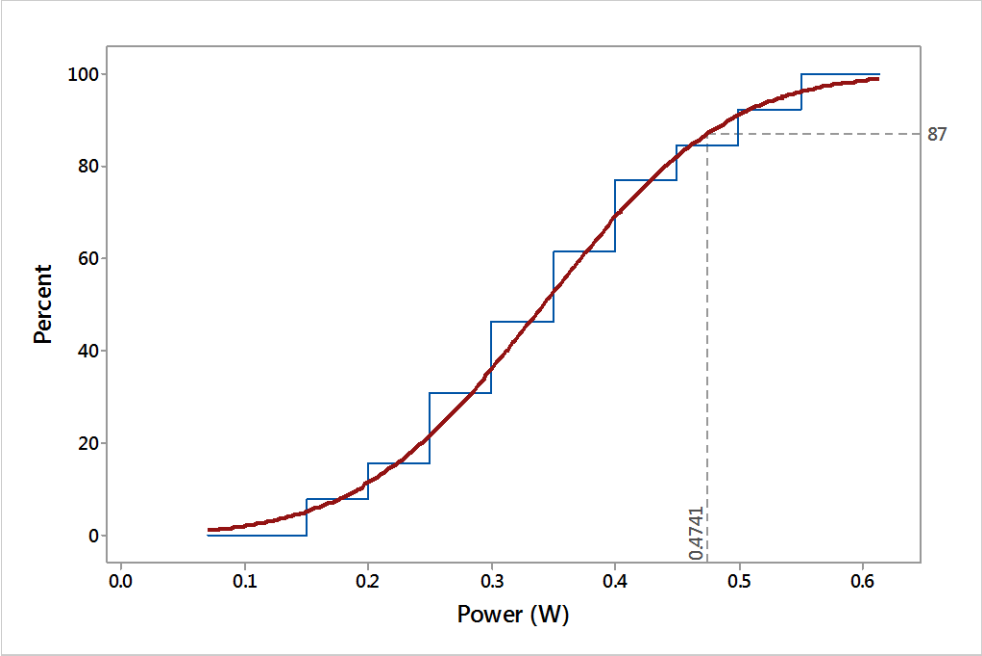

Fig. 3.5 Distribution plot for compression test.

Conclusions:

Through detailed data analysis, several crucial aspects for understanding and optimizing this process were highlighted. Firstly, laser power proved to be an essential factor in determining the quality of micro-perforations. The summary analysis indicated that the mean laser power is 0.342 W, with 95% confidence intervals between 0.271 W and 0.413 W. Additionally, the standard deviation is 0.116 W, with 95% confidence intervals between 0.083 W and 0.193 W. These results suggest a relatively low variation in laser power, which is favorable for the consistency of the micro-perforation process.

The Anderson-Darling normality test, applied at a significance level of 0.05, indicated that the laser power data follow a normal distribution (A-Squared = 0.14, P-Value = 0.963). However, the graphical analysis of the data showed that they are homogeneous, and the mean and median values are comparable.

The low variance of the analyzed data, along with a skewness of 0.171 W and a kurtosis of -0.566 W, indicates a slightly asymmetric and flat distribution of laser power. These statistical characteristics are important for understanding the behavior of the power parameter within the micro-perforation process.

The estimation of the empirical cumulative distribution function (CDF) for laser power considering normal distribution revealed that, for the 87th percentile, the estimated laser power is 0.4741 W. This result suggests that the optimal setting of laser power to achieve high-precision and high-quality parts is around this value.

The overall estimation highlights that the quality of the products depends significantly on the level of laser power. Therefore, understanding and optimizing this parameter is crucial for improving the micro-perforation process and, consequently, enhancing the reliability and performance of automotive components.

The theoretical and experimental analysis of the laser microfabrication applications emphasizes the influences of the power output of picosecond and femtosecond ultrafast lasers, underlining the advantages and the rapidity of the processing method using an ultrafast laser.

In conclusion, the study demonstrated that optimizing laser power is vital for improving the quality of micro-perforations in automotive components. The statistical and graphical analyses provided a clear understanding of the behavior of laser power, allowing for the identification of optimal values for practical application in the industry. This contributes to the enhancement of the reliability and performance of automotive parts, emphasizing the importance of precise control over process parameters.

3.1.4 The analysis of means chart (ANOM) of laser power on the micro-perforation process of automotive parts

The assessment of the main influencing factors on the micro-perforation laser process is based on the analysis of means chart (ANOM) for a normal distribution. An experiment was performed to assess the effects of the most important factors: the level I laser power (P1), the level II laser power (P2), the pull test results and the material thicknesses. The ANOM results are illustrated in Figures 3.6 and 3.7.

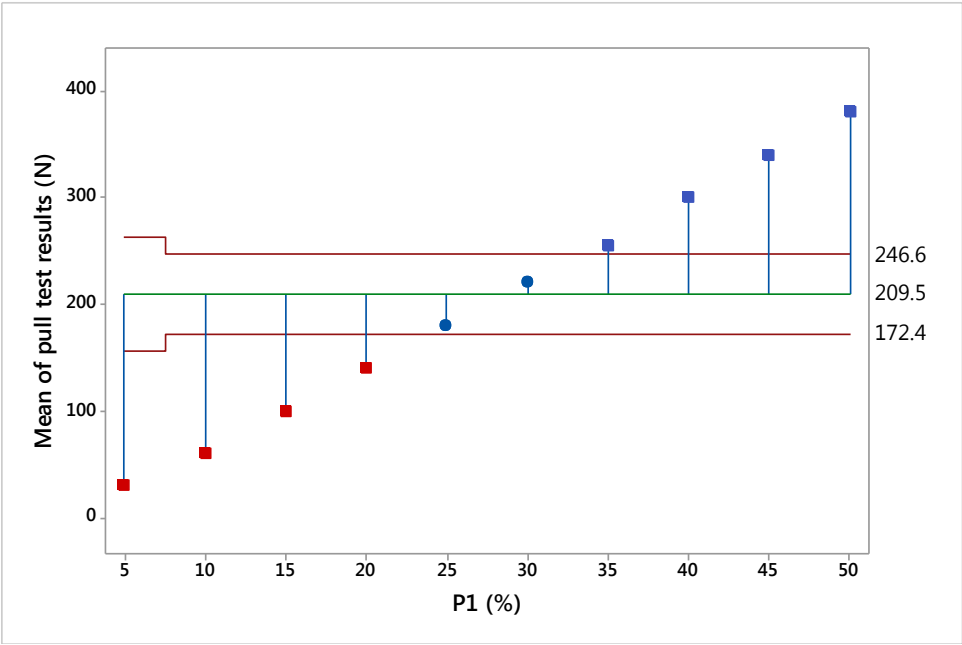

Fig. 3.6 Normal ANOM for pull test results vs. P1 laser power.

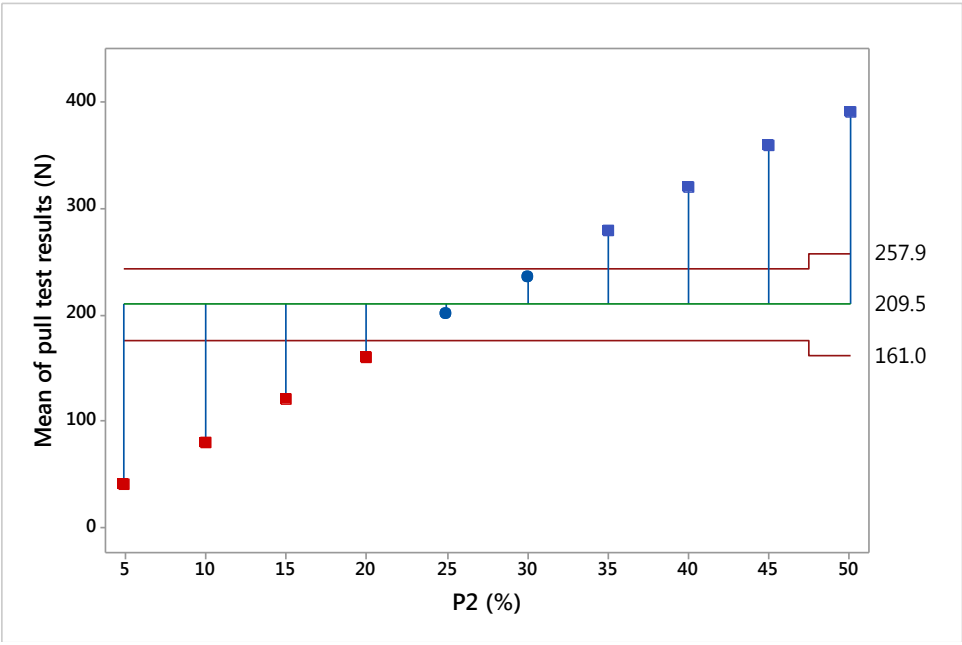

Fig. 3.7 Normal ANOM for pull test results vs. P2 laser power.

In the case of first level of the laser power (P1), the pull test results indicate that the lower delimitation limit is 172.4 N and the upper limit is 246.7 N, with a mean of 209.5 N (Figure 3.6) and standard deviation of 74.2 N. Tested parts that had recorded values below the lower limit value were declared scrap.

The normal analysis of means chart for the P2 laser power (Figure 3.7) showed a lower delimitation limit of 161 N, an upper delimitation limit of 257.9 N and a mean of 209.5 N with a standard deviation of 96.9 N.

The computed delimitation limits allow us to take appropriate measures to optimize the laser process. The indicated direction is to optimize the two laser powers, P1 and P2, to ensure the process stability.

The comparative analysis of the two laser powers emphasizes that the optimal level should be set around 0.25 W to ensure a material rupture force during testing. Additionally, quality limits can be easily determined from the comparative analysis: power of 0.20 W - beyond tolerance threshold; power of 0.21–0.24 W - within accepted limits; power > 0.25 W - higher precision, efficiency and stability (covers and removes material defects).

In order to highlight the interaction between the pull test results, laser power and material thickness and its effect on the micro-perforation process, a factorial analysis was designed. The magnitude and the importance of the effects were determined by applying the Pareto chart and Standardized effects chart (Figure 3.8 and Figure 3.9).

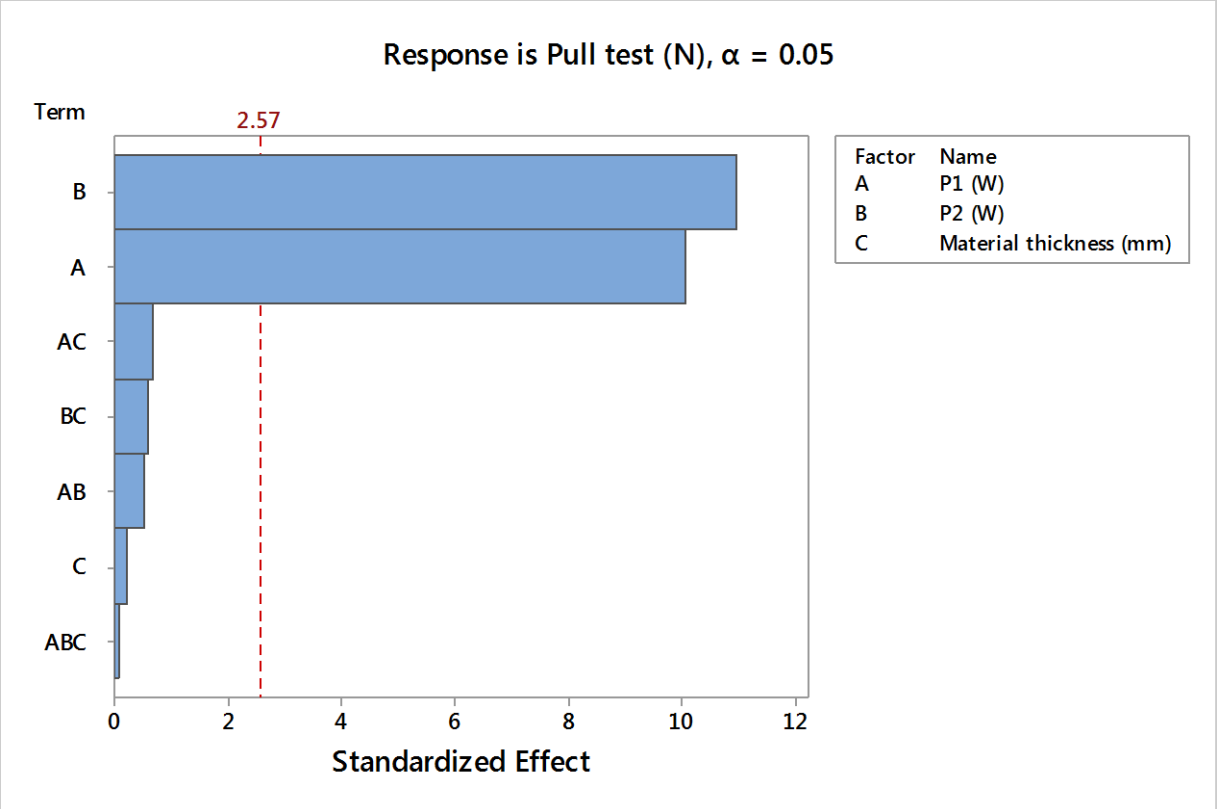

Fig. 3.8 Pareto Chart of the Standardized Effects

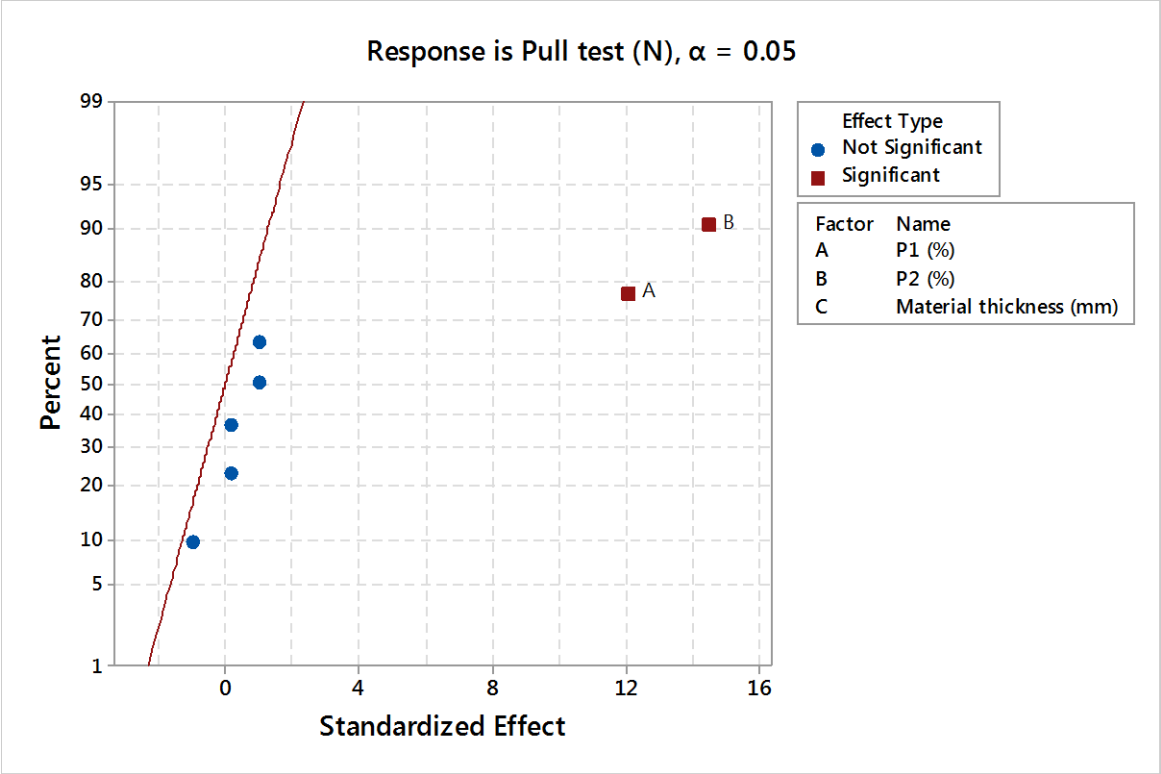

Fig. 3.9 Micro-perforation factor effects.

The interaction plot indicates that the material with the highest thickness depends on the P1 laser power, while the material with the lowest thickness depends on the P2 laser power. The difference between the P1 and P2 powers is given by the number of pulses. Specifically, a laser power fraction of 5–25% from the nominal laser power has a negative influence on the results of the pull test, while, for a laser power greater than 25%, the tested parts in the pull test are compliant.

In conjunction with an analysis of variance and design of experiments, we examined the differences among the level means for the three analyzed factors. The P1 and P2 laser powers appear to affect the pull test results compared to an overall mean of 209.5 N. A main effect is present because the different levels of the studied laser powers factors affect the response differently. Additionally, the graph for the material thickness shows that there is no main effect present.

The absolute effect values compared to the reference line show that the laser powers are statistically significant (Figure 3.9). Moreover, the standardized effects of the micro-perforation factors show a significant effect of the P2 (90%) and P1 (77%) laser powers.

3.1.5 Proposed measures

Laser processing with adhesive application on Bluemelt machine: Noteworthy consistency was observed within the specified tolerance limits, affirming the efficacy of this approach and

providing valuable insights for future process refinements.
Cross-testing RHD parts on LHD nest: The validation experiments yielded pull test results consistent with the acceptance criteria, highlighting the potential interchangeability of the manufacturing parameters and informing standardized practices.
New batch of material preparation: The rigorous assessment of the material batch's impact on the pull test tolerances can inform future manufacturing practices and enhance the process' predictability and repeatability.
Adhesive application and laser: The granular examination of the variances after adhesive application and laser processing can identify process optimization opportunities and minimize variability.

Detailed Analysis
Pull test influences: The in-depth analysis revealed the significant influences of the adhesive application techniques and spacer dimensions, necessitating meticulous control and calibration of the process parameters. The laser power needs to be set and optimized for both the P1 and P2 powers to ensure the coverage of defects from the previous process.
Parameter adjustments: The dynamic nature of the spacer thickness underscored the imperative for frequent iterations and standardization efforts to ensure consistent laser processing outcomes.
Continued research: The ongoing exploration of alternative laser processing scenarios, including variations in adhesive application techniques, is necessary to comprehensively delineate the process dynamics and inform iterative enhancements.
Glue application influence: The differential outcomes observed based on the adhesive application methodologies underscored the need for systematic evaluation and refinement to optimize the process parameters and ensure uniformity across adhesive types.

Proposed Enhancements
Spacer dimension standardization: The implementation of stringent protocols to standardize the spacer dimensions, minimizing the need for frequent parameter adjustments and enhancing the process stability and predictability.
Laser line optimization: The precision calibration of the laser line positioning to ensure seamless alignment with the spacer fabric, facilitating consistent pull test results and mitigating variability.
Refinement of glue application: The systematic evaluation of the adhesive application methodologies to ascertain the optimal parameters conducive to uniform outcomes across different adhesive types and enhance the process' repeatability.
Contingency planning: The development of robust contingency plans to preemptively address potential machine-related issues, safeguarding the production continuity and efficiency.
Noise parameter adjustment: The fine-tuning of the noise parameters to optimize the process'

stability and minimize adverse effects on the pull test outcomes, enhancing the overall process' reliability and repeatability.

Discussion

The investigation results indicate several significant findings and implications in the context of previous studies and working hypotheses. The detailed analysis of the airbag cutout laser process revealed substantial discrepancies in the application of LHD and RHD parameters, aligning with the initial working hypotheses. Additionally, other influences on the process, such as the adhesive application techniques and spacer dimensions, were identified.

Interpreting these results in the context of previous studies suggests that a more rigorous and systematic approach is needed to ensure consistency and reliability in the airbag cutout laser process. Compared to previous research, which has indicated similar challenges in laser processing for automotive applications, this investigation adds a new perspective by identifying and documenting detailed issues related to the incorrect use of the LHD and RHD parameters.

The implications of these findings are extensive and could significantly impact the production process across the automotive industry. Optimizing the airbag cutout laser process could lead to significant improvements in the quality and reliability of automotive safety components, thereby reducing the risk of failure and enhancing passenger safety.

Regarding future research directions, this investigation opens the door to several further studies. These include more detailed research into the influence of various process parameters on the final outcomes, exploring alternative adhesive application methods and assessing the impact of introducing new or improved technologies into airbag cutout laser processing.

These future research directions can contribute to the ongoing development of knowledge and practices in laser processing in the automotive industry and provide innovative solutions to improve the production processes and product quality.

Moreover, it is essential to consider the broader implications of autonomous vehicles beyond the manufacturing process. The widespread adoption of autonomous driving technologies has the potential to revolutionize urban mobility, reduce traffic congestion and minimize environmental impacts. By leveraging AI-driven autonomous vehicles, cities can reimagine transportation systems, optimize infrastructure utilization and enhance the overall quality of life for residents.

Furthermore, the ethical and societal implications of autonomous vehicles must be carefully examined. Issues such as liability, privacy and job displacement require thoughtful consideration and proactive measures to mitigate the potential risks and ensure equitable outcomes. Collaborative efforts between policymakers, industry stakeholders and the research community are essential to addressing these challenges and fostering public trust in autonomous driving technologies.

3.1.6 Conclusions

The overall conclusion of the presented study is that the level of the laser power has a significant influence on the micro-perforation process.
The analysis of the micro-perforation factors provides significant evidence for an interaction. The effect of one laser power factor depends upon the level of the other laser power. Moreover, the statistically significant difference is highlighted by the design of experiments analysis and main effects plots.
The laser micro-perforation process is optimal for a percentage of at least 25% of the laser power, with upper limits above 25% beneficial for both process stability and the material's resistance to the pull test. The analyzed parameters for the laser process, including the power (W) and material rupture resistance (N), are of paramount importance due to their critical characteristics (CC), significantly influencing the efficiency and quality of the process.
The analyses of the experimental results provide valuable insights into the factors influencing the airbag cutout laser processing outcomes. The inappropriate use of LHD parameters for RHD components significantly contributed to process variability, resulting in nonconforming outcomes during pull testing. The correlations between the processing parameters and product quality underscore the importance of parameter optimization for consistent outcomes. To address this, standardized parameter sets tailored to specific component configurations are recommended, alongside enhanced quality control protocols including real-time monitoring. Future research may explore advanced laser processing techniques, like adaptive process control and machine learning algorithms, to optimize the efficiency and quality.

3.2 The electromagnetic noise level influence during the laser micro-perforation process

This study aims to investigate the critical parameters and effects of generated noise (energy) during the laser micro-perforation process of synthetic leather airbag components. Noise in the context of laser processing refers to the unwanted energy variations that can affect the stability and precision of the laser beam. Such variations can lead to inconsistencies in perforation size, shape, and edge quality, all of which are critical parameters for maintaining the functionality and safety of airbags. By closely monitoring and controlling noise levels, the aim is to optimize the production process, ensuring that the resulting airbag components meet stringent quality and safety standards. This approach not only enhances the overall efficiency of the manufacturing process but also contributes to the development of high-quality products suitable for critical applications in the automotive industry.
Previous research has focused on optimizing laser parameters for various applications without deeply exploring the effects of electromagnetic noise on the quality and uniformity of laser-

perforated holes, especially in critical safety components like airbags. Noise in the context of laser processing refers to unwanted energy variations that can affect the stability and precision of the laser beam. Such variations can lead to inconsistencies in perforation size, shape, and edge quality, all of which are critical parameters for maintaining the functionality and safety of airbags.
In this context, in this study are detailed the experimental analysis, including the equipment and methodologies used, and present a comprehensive assessment of the results. To assess the effects of electromagnetic noise levels on pull test force results, a factorial analysis (DOE) was applied to underline the influences of the main effects and interactions of examined factors. The study findings will underscore the importance of control-ling laser noise to maintain the integrity and performance of airbag components, ultimately contributing to advancements in the field of laser material processing.
The researches from this study present a niche in the field of the impact of electromagnetic noise on the quality and consistency of laser micro-perforations in textile materials for airbags. Previous studies have largely concentrated on optimizing laser parameters without exploring deeply into how external factors like electromagnetic noise influence the process. By filling this gap, the research provides valuable insights into how controlling electromagnetic noise can improve the manufacturing process and enhance the safety and reliability of airbag components.

3.2.1 Quality assessment of laser micro-perforations in airbag zones components

The material subjected to testing is synthetic leather made from polyvinyl chloride (PVC) a nominal thickness of 0.8 mm. It is laminated with a spacer material having a nominal thickness of 2.99 mm and a specified tolerance of ±0.3 mm. The combined material must meet strict strength and flexibility criteria to ensure airbag functionality.
The synthetic leather parts used in this study were selected to represent common materials utilized in the automotive component manufacturing industry for airbag production. The sample size consisted of 400 parts for each analyzed parameter: the laser noise, material thickness and pull test results. For the factorial analysis, 1200 samples were considered.
The used equipment:

- ZwickRoell Z100 Testing Machine, featuring a maximum force capacity of 100 kN. It provides a testing speed range from 0.0005–1000 mm/min with an accuracy of ±0.1% of the set value. It ensures force measurement accuracy within ±0.5% of the measured value, up to 1/1000 of the maximum load cell capacity. The machine has a test stroke of 1100 mm without accessories and operates on a power supply of 230 V, 50/60 Hz.
- The INSTRON 5967 Testing Machine, with a maximum force capacity of 30 kN, offers a testing speed range from 0.001 to 3000 mm/min with an accuracy of ±0.1% of the set value. It ensures force measurement accuracy within ±0.5% of the measured value, up to 1/1000 of the maximum load cell capacity. The machine has a test stroke of 1130 mm without accessories,

operates on a power supply of 100-240 V, 50/60 Hz, and utilizes Bluehill Universal software.
The ZwickRoell Z100 testing machine is used for evaluating the mechanical properties of laser-processed materials. Its features, such as high force capacity and measurement precision make it ideal for testing textile materials, ensuring compliance with technical specifications.
The INSTRON 5967 testing machine is used for smaller scale testing and applications requiring lower forces. With similar accuracy and flexible power supply, it complements the capabilities provided by the ZwickRoell Z100.

The quality of laser micro-perforations process applied to materials used for airbags is evaluated based on several critical parameters.
The size and uniformity of the perforations must be consistent across the entire material surface, as variations can compromise the functionality of the airbag. The ideal shape of the perforations is circular, and any deformation may indicate issues with laser parameter settings or beam quality.
The quality of the perforation edges is also essential; they should be smooth and well-defined to prevent material degradation during airbag deployment. The depth of the perforations must be precisely controlled to ensure optimal performance, thereby avoiding any risk of structural failure.
The material surrounding the perforations must maintain its structural integrity without showing signs of thermal or mechanical degradation. It is important that the perforation process minimizes residue generation, as the presence of residues can affect both the aesthetics and functionality of the airbag.
The efficiency and speed of the micro-perforation process are important parameters for industrial production. An optimal balance between speed and quality is necessary to maintain efficient and economical production. To achieve high-quality perforations, it is crucial to optimize and precisely control laser parameters such as power, frequency, scanning speed, noise (energy in the electromagnetic field), and beam focus. The use of appropriate calibration equipment and regular maintenance significantly contributes to maintaining optimal performance.
For the analysis of the quality of laser micro-perforations in airbag zones, three test samples, each containing 400 pieces, were examined. These samples underwent a rigorous set of tests to evaluate the influence of the previously mentioned parameters: power and noise (energy in the electromagnetic field). The results of these tests provided essential data to ensure compliance with the safety and performance standards specific to the automotive industry.

Laser Processing
The laser used in this experiment has a total power of 2 kilowatts (kW), representing 100% of the device nominal power. The experimental settings include using 25% of the total power,

while the two laser powers are set at 50% used from this percent. Additionally, within this 0.5 kW setting, the powers P1 and P2 are adjusted to 50% of 0.5 kW, equating to 0.25 kW each. The measurement of the laser power is conducted in discrete increments of 100 watts, up to the full 2 kW capacity, to ensure a comprehensive evaluation of the laser efficiency across its operational range. These settings are crucial for evaluating the performance and efficiency of the material perforation process. The pulse duration is 200 fs (femtosecond). This is unusual for CO_2 lasers, which traditionally have much longer pulse durations (in the order of nanoseconds). However, there are advanced technologies where different types of lasers are combined to achieve very short pulse durations, such as the Ti series pulsed CO_2 lasers.

With a production cycle of 15 seconds per part, it is crucial that the quality of the part in the visible area is ensured throughout the vehicles lifespan. This means that micro-perforations resulting from the laser processing must not be visible and should not be influenced by factors that could compromise the integrity of the airbag or the aesthetic appearance of the components.

In conclusion, the Ti series pulsed CO_2 laser with pulse duration of 200 fs is a costly but efficient option for precision applications in airbag component production, ensuring high quality and long-term durability of the manufactured parts.

3.2.2 Electromagnetic noise level (EMI) analysis on laser processing

During the experiment, the electromagnetic noise levels (EMI) was monitored and controlled to understand its impact on the quality of laser perforations. Electromagnetic noise can be generated from various sources in the surrounding environment and can affect the stability and precision of the laser beam.

To evaluate the influence of EMI, pull tests were performed on the perforated materials under different electromagnetic noise conditions.

The experiments were conducted with meticulous attention, taking into account the imposed conditions and using advanced instrumentation and equipment.

The statistical analyses of the experimental data were performed using the Minitab v17 software (Minitab LLC, State College, PA, USA). Considering a 95% confidence interval (CI) and a significant level of $\alpha = 0.05$, the normal distribution of the experimental data was qualitatively and quantitatively validated by using the normal Anderson–Darling test (AD). A factorial design (DOE) was applied based on the process particularities by choosing the main control factors that affected the micro-perforation characteristics. To evaluate the influence of the electromagnetic noise levels, the interaction effects and main effects of factors was studied.

Statistical Analysis of Experimental Data

The electromagnetic noise levels and materials thicknesses were statistically analyzed considering 95% confidence interval (CI). In particular, the Anderson–Darling normality test

was applied to validate the data distribution [DUM18b]. Additionally, the homogeneity of the experimental data was tested by assessing the goodness of fit with probability plots (Figures 3.10 to Figure 3.13), indicating the nominal electromagnetic noise level.

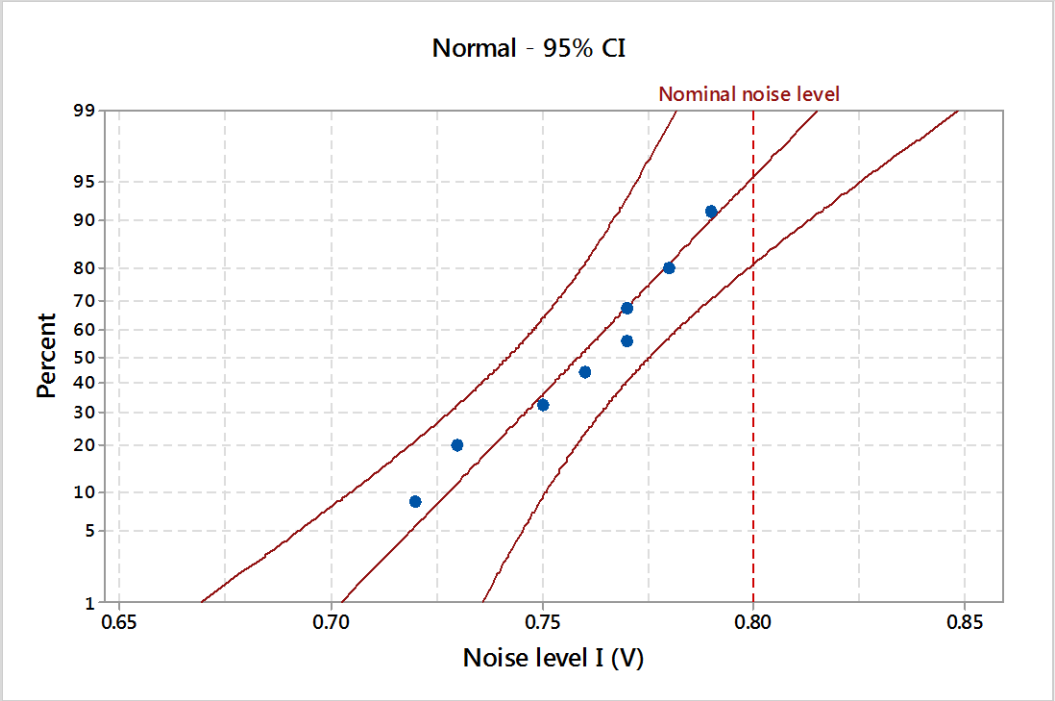

Fig. 3.10 Probability plot of noise level I for 0.8 V.

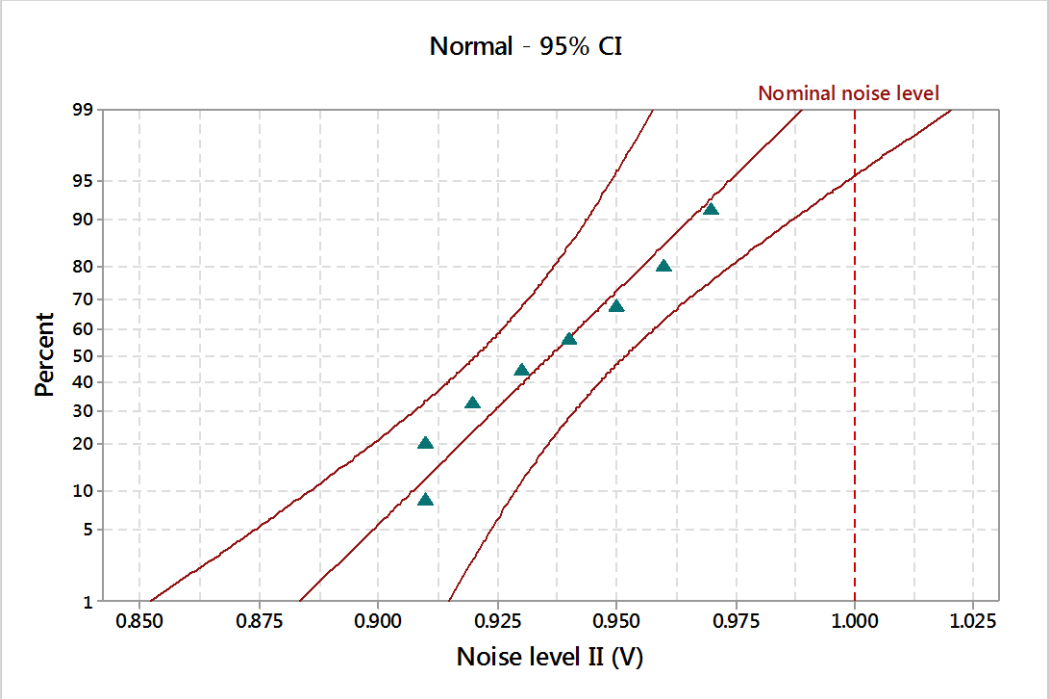

Fig. 3.11 Probability plot of noise level II for 1 V.

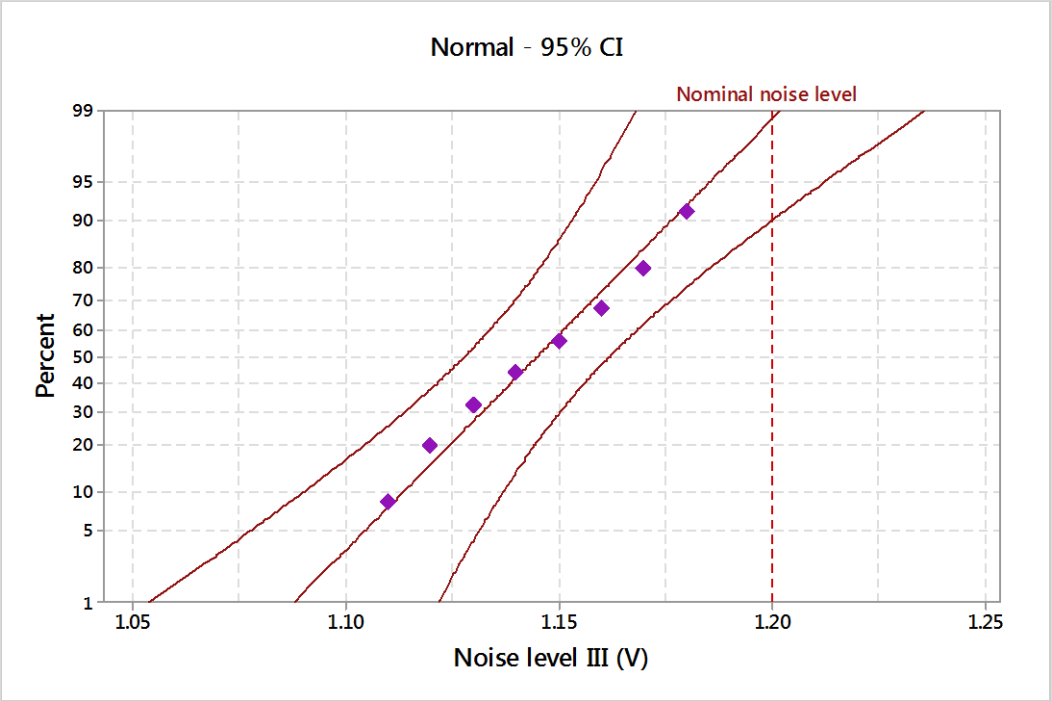

Fig. 3.12 Probability plot of noise level III for 1.2 V.

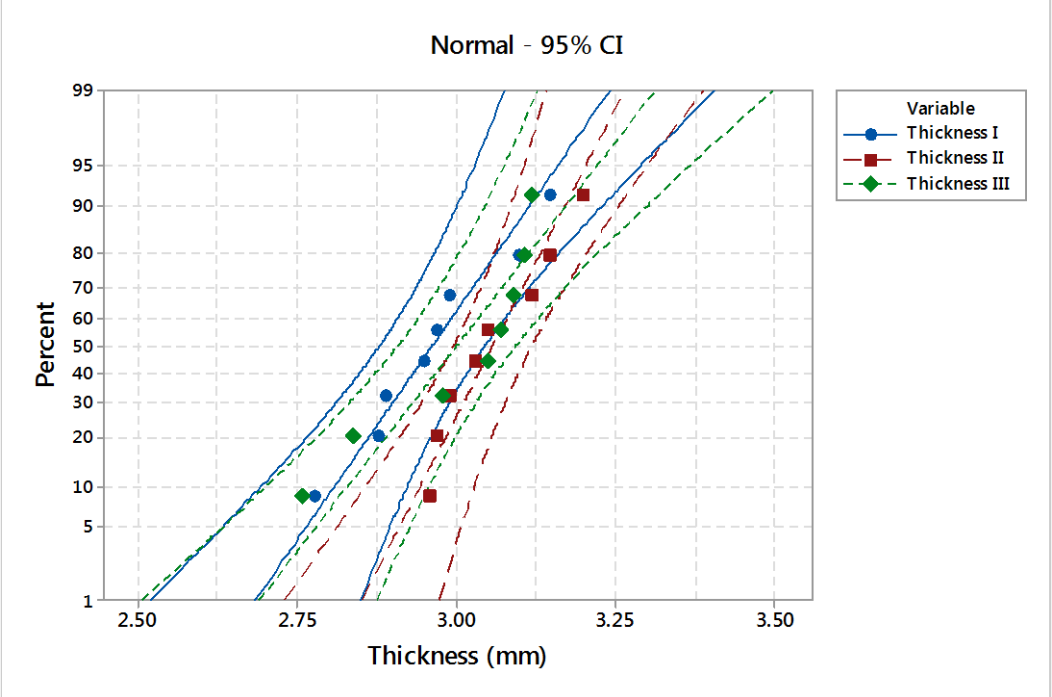

Fig. 3.13 Probability plot of analyzed material thicknesses.

The goodness-of-fit normality test results are presented in Table 3.3. The comparative analysis of the probability plots shows that all points are within the lower and upper confidence boundaries, respectively the p-value is over specify significance level of 0.05. Based on the estimated Anderson Darling statistics (AD) and correlation coefficient, it can be mentioned that the analyzed experimental data are homogeneous and it follows the normal distribution.

Table 3.3 Anderson–Darling normality test.

Characteristic	AD	Correlation Coefficient	*p*-Value
Noise level I (V)	0.247	0.979	0.649
Noise level II (V)	0.225	0.980	0.731
Noise level III (V)	0.134	0.996	0.961
Material thickness I (mm)	0.198	0.985	0.826
Material thickness II (mm)	0.287	0.972	0.524
Material thickness III (mm)	0.615	0.919	0.407

The descriptive statistics of analyzed electromagnetic noise levels and material thicknesses are synthetically presented in Table 3.4 and Table 3.5.

Table 3.4 Descriptive statistics of analyzed noise level.

Statistical Parameter	Noise level I (V)	Noise level II (V)	Noise level III (V)
Mean	0.759	0.936	1.145
Minimum	0.720	0.910	1.110
Maximum	0.790	0.970	1.180
Median	0.765	0.935	1.145
StDev	0.024	0.023	0.024
Q1	0.735	0.913	1.123
Q3	0.778	0.958	1.168
Skewness	-0.54	0.23	0.010
Kurtosis	-0.744	-1.412	-1.200

Table 3.5 Descriptive statistics of analyzed material thicknesses.

Statistical Parameter	Material thickness I (mm)	Material thickness II (mm)	Material thickness III (mm)
Mean	2.964	3.059	3.003
Minimum	2.780	2.960	2.760
Maximum	3.150	3.200	3.120
Median	2.960	3.040	3.060
StDev	0.120	0.089	0.134
Q1	2.883	2.975	2.875
Q3	3.073	3.143	3.105
Skewness	0.201	0.487	-1.159
Kurtosis	-0.287	-1.264	-0.035

The estimated mean of the electromagnetic noise level I is 0.759 V (95% confidence intervals of 0.738 V and 0.778 V), the standard deviation is 0.024 V (95% confidence intervals of 0.015 V and 0.049 V), and the median is 0.765 V (95% confidence intervals of 0.729 V and 0.780 V). With significance level of α = 0.05, the estimated parameters don't exceed the imposed nominal level of 0.8 V. Based on descriptive statistics results for electromagnetic noise levels II and III, it indicates falling within the specified limits for 1 V and 1.2 V.
In the case of the material thicknesses, the means are between 2.964 mm and 3.059 mm, and the standard deviations are between 0.089 mm and 0.134 mm with medians around to 3 mm. Although the differences between the main estimated statistical parameters are not significant, each piece is analyzed individually, and the material thickness influences the regime of the laser process.

3.2.3 Design of experiments of electromagnetic noise levels over pull test results

In order to highlight the interaction between the electromagnetic noise levels, material thicknesses, pull test results and its effect on the micro-perforation process, the effects charts was plotted (Figure 3.14 to Figure 3.16).

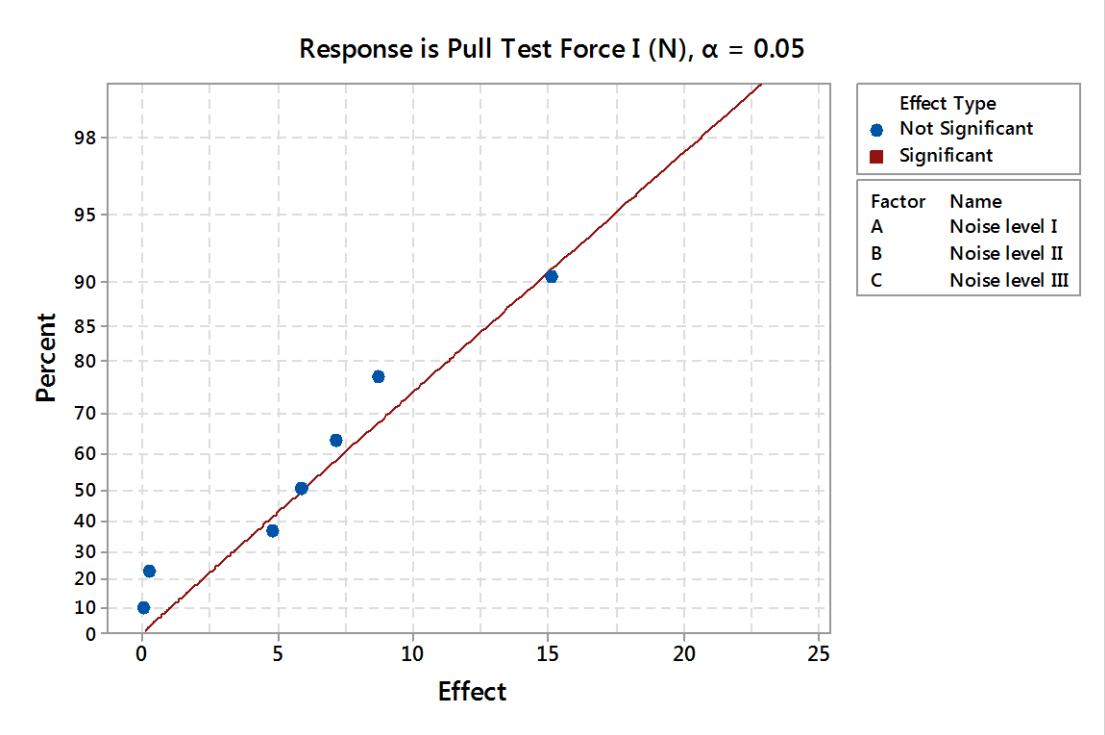

Fig. 3.14 Micro-perforation factors effects on pull test force I results.

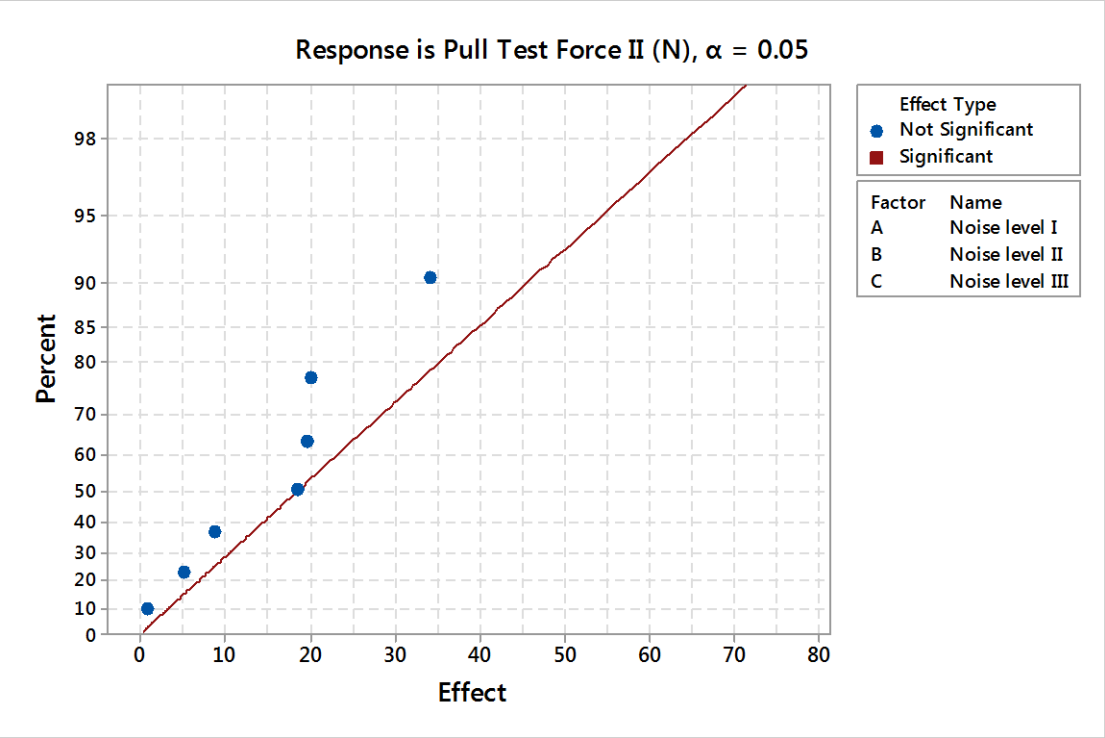

Fig. 3.15 Micro-perforation factors effects on pull test force II results.

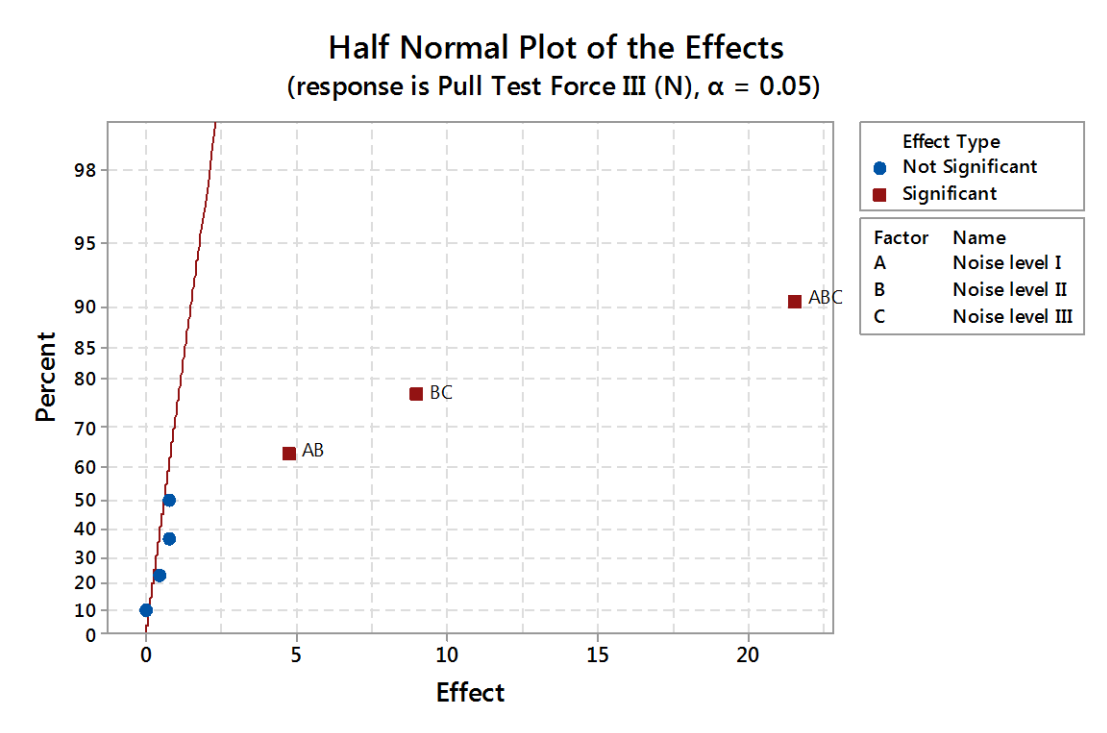

Fig. 3.16 Micro-perforation factors effects on pull test force III results.

The influence of electromagnetic noise levels and material thicknesses over pull test results is based on factorial design of experiments (DOE). The goal of the study is to examine these factors to determine which ones have the greatest influence. Because it was assumed that three-way and four-way interactions are negligible, a resolution IV factorial design was

adopted. We decide to generate a 16 run fractional factorial design. The interaction effects and main effects for factorial design results are presented in Figure 3.17 and Figure 3.18.

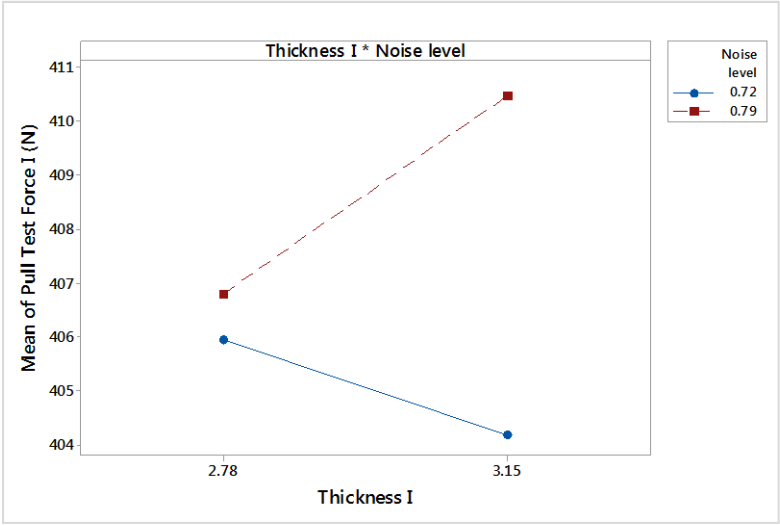

(a)

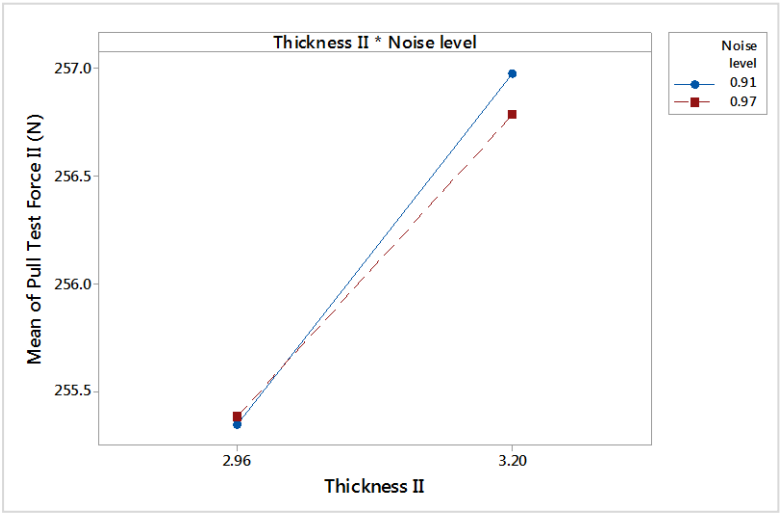

(b)

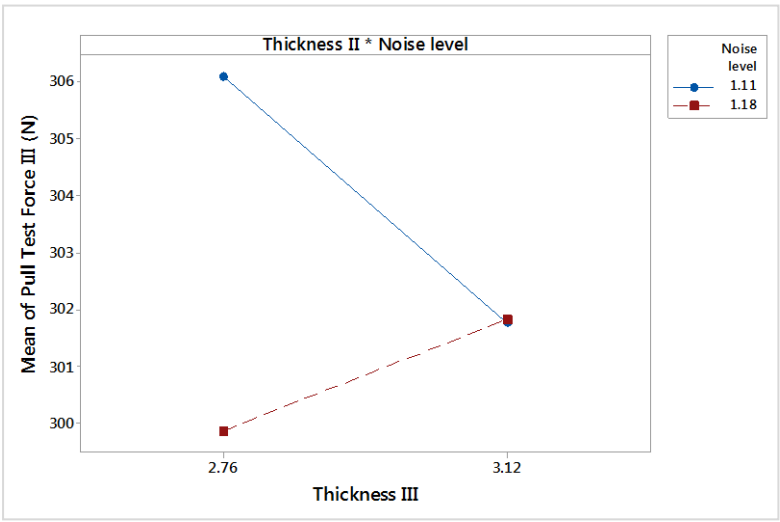

(c)

Fig. 3.17 Interaction plot of analyzed factors: (a) interaction effects of pull test force I; (b) interaction effects of pull test force II; (c) interaction effects of pull test force III.

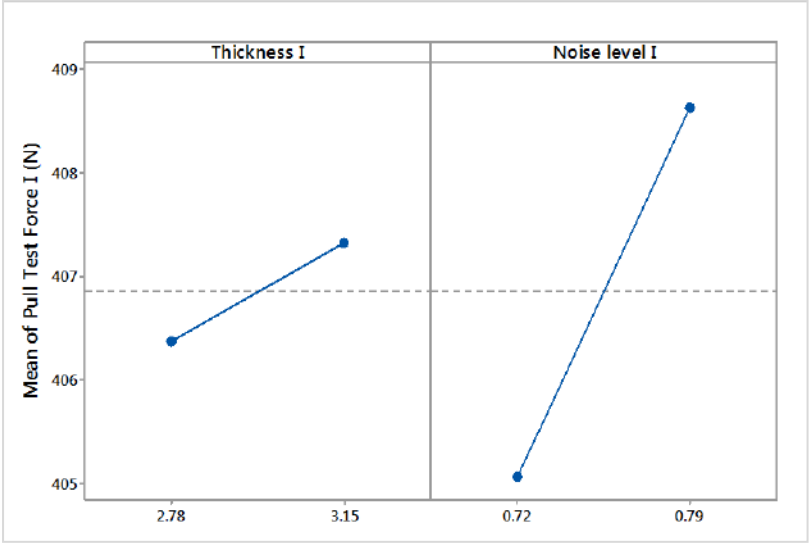

(a)

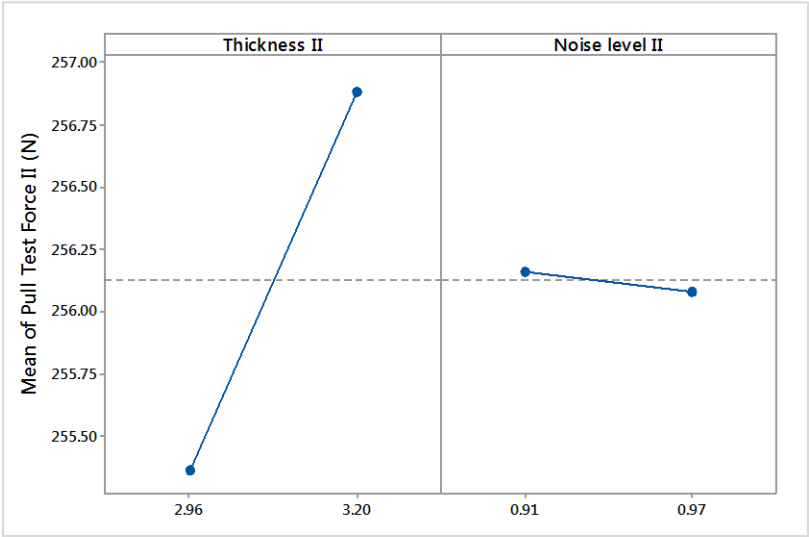

(b)

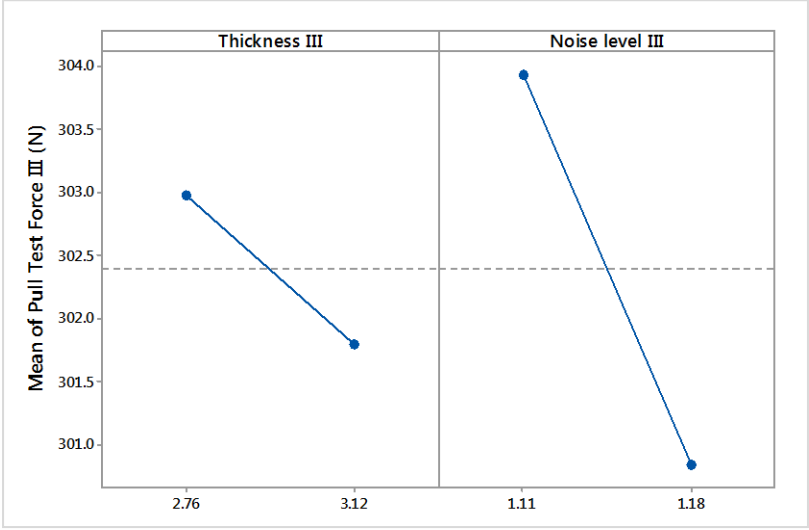

(c)

Fig. 3.18 Main effects plot of analyzed factors: (a) main effects for pull test force I; (b) main effects for pull test force II; (c) main effects for pull test force III.

The interaction plots show that there is a high degree of interaction for pull test force I and pull test force III. The electromagnetic noise level with the highest values has significant influence on pull test force results (Figure 3.17a and Figure 3.17c). Specific to pull test force II depicted in Figure 3.17b, the plot indicate no interaction.
The pull tests forces are adjusted according to the thickness of the material and its texture, the target value of the pull test being 303 N. From Figure 3.17a it follows that for a value of the noise level I of 0.79 V, the force for pull test is 410 N, this value not falling within the agreed tolerance. From Figure 3.17b it can be seen that for 0.97 V, the maximum value recorded in the pull test is 257 N. This result does not reflect the fulfillment of the imposed requirements. Analyzing Figure 3.17c, the pull test force value is 302 N at a noise level of 1.18 V, a result that indicates the supply of compliant products, but also the stability of the laser micro-perforation process.
The main effects plots indicate that the electromagnetic noise levels and material thicknesses influence the results of pull tests (Figure 3.18). Specifically, the noise levels compare to a nominal noise level of 0.8 V has a negative influence on the results of the pull test, while, for a nominal noise level of 1.2 V, it has a positive influence.

3.2.4 Evaluation of perforation quality in the presence of electromagnetic noise

The pull tests result conducted on the perforated materials were analyzed to determine the impact of electromagnetic noise on perforation quality. The tests revealed that, in the presence of electromagnetic noise there were significant variations in the size and shape of the holes, as well as the presence of irregular edges.
The structural examination of the perforated material using the Gemini 500 Zeiss electron microscope revealed the presence of defects such as excessive burns and deformations of holes edges in areas exposed to strong electromagnetic fields. These defects can compromise the integrity and functionality of the airbag, highlighting the necessity of EMI control in the laser process.

Analysis of Tensile Test Results
The results of the tensile tests reveal distinct performance characteristics between samples categorized as NOK (Not OK) and those categorized as OK. Specifically, samples classified as NOK exhibited an average tensile strength of 409 N at a noise level of 0.8 V, and an average of 255 N at a nominal electromagnetic noise level of 1 V. In contrast, samples categorized as OK demonstrated an average tensile strength of 303 N when exposed to a noise level of 1.2 V. These findings underscore the sensitivity of tensile strength to variations in applied noise levels, highlighting the need for precise control and optimization of experimental parameters in material testing protocols (Figure 3.19).

These results indicate that the tensile values are affected by the level of electromagnetic noise. At a noise level of 1.2 V, the tensile values are more consistent and closer to the optimal values, demonstrating that this level is favorable for achieving the desired quality of perforations.

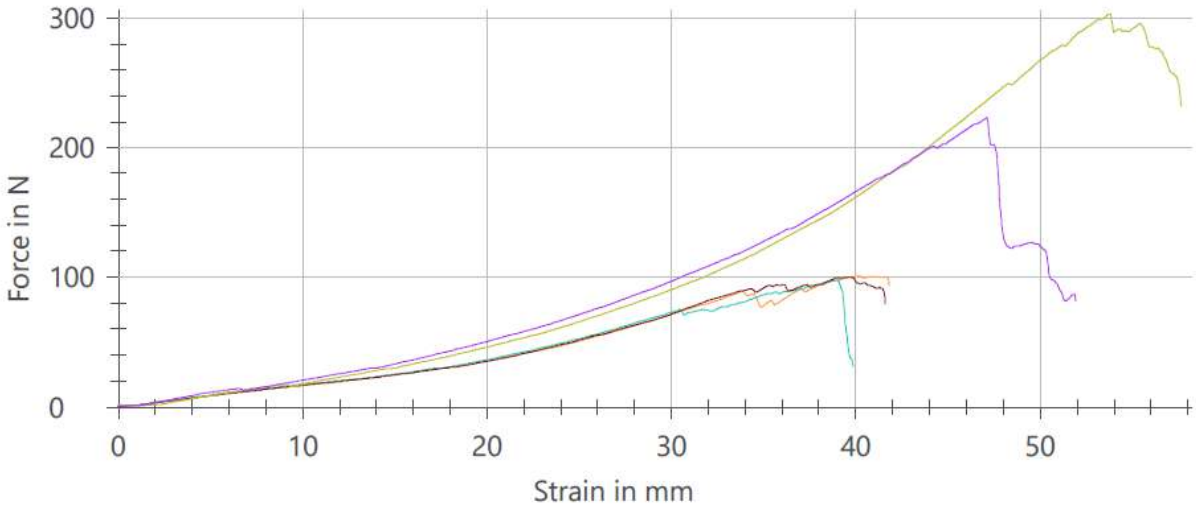

Fig. 3.19 Analysis results after pull test with OK values and noise set to 1.2 V.

Impact of Electromagnetic Noise on the Material

The 1.2 V noise level appears to favor greater consistency and stable quality of perforations compared to lower or higher noise levels (Figure 3.19). This noise level helps maintain a balanced mechanical performance and reduces variability in the size and shape of perforations.

Under 1.2 V noise conditions, defects and deformations are minimized, ensuring better structural integrity of the perforated material.

Electromagnetic Noise Level and Mechanical Performance Relationship

The results suggest that an electromagnetic noise level of 1.2 V offers an optimal balance between mechanical performance and consistency of results. While lower noise levels (0.8 V) provide higher tensile values, they are more variable and less predictable. At 1.2 V, the perforated material shows superior stability, which is crucial for critical applications such as airbags.

The perforated material was subjected to strength tests in the presence of electromagnetic noise, using the ZwickRoell Z100 and INSTRON 5967 testing machines. The results showed a decrease in mechanical strength in areas affected by EMI, emphasizing the importance of minimizing electromagnetic interference to maintain the final products quality.

Process Optimization

Laser processing of textile components for airbags has a significant impact on their quality and performance. Laser technology allows high precision and consistency in material perforation,

essential for ensuring the functionality and safety of airbags. However, the influence of electromagnetic noise can compromise these advantages, affecting the stability and accuracy of the laser process.

Using lasers in processing textile materials offers numerous advantages, such as the ability to achieve precise and uniform perforations and the efficiency of the process. However, the presence of EMI can introduce defects and variabilities that reduce the final products quality.

To improve the laser processing process and minimize the influence of electromagnetic noise, the following main recommendations can be mentioned:

- Electromagnetic Shielding: Continue using electromagnetic shielding equipment to maintain the optimal noise level at 1.2 V.
- Experimental Setup Isolation: Maintain adequate isolation of the experimental setup to prevent unexpected variations in electromagnetic noise.
- Power Supply Stabilization: Ensure a stable power supply to consistently maintain the optimal electromagnetic noise level at 1.2 V.

During the laser perforation of the airbags protective material, electrostatic energy is generated, which can impact the process. However, the primary objective of this procedure is to ensure precise and efficient perforation of the material without compromising the functionality or safety of the airbag.

To prevent any adverse effects and ensure the reliability of the airbags in the event of an impact, specific measures are implemented. The electrostatic energy produced by the laser device can potentially affect nearby materials or electronic components under certain conditions. Therefore, measures are taken to minimize electrostatic interference and to safeguard the integrity of both the airbag system and the associated electronic components.

To enhance the micro-perforation process and control the level of electrostatic noise, adjustable tolerances are utilized. These tolerances can be configured through the laser software, allowing parameters to be adjusted based on the material used for micro-perforation. This ensures that the perforation is carried out effectively without compromising the performance and safety of the airbag.

In this regard, the studies on influences of electromagnetic noise show that these factors must be detected, controlled and mitigated.

3.2.5 Results and discussions

Laser processing of textile components for airbags is a complex and crucial field for vehicle safety. By deeply understanding process parameters and the influence of external factors such as electromagnetic noise, superior results can be achieved that comply with the industry stringent specifications. Continuing research and continuous improvement of the technologies and methodologies used will ensure the development of high-quality products and maximum safety for end-users.

In conjunction with design of experiments analysis, it was examined the differences among the analyzed factors. The three noise levels appear to affect the pull test results compared to a target value of pull test force. The interaction effect is present because the different levels of the analyzed electromagnetic noise factors affect the response differently. Additionally, the plots of influence of electromagnetic noise levels compare to material thickness over pull tests forces results, its show that there is main effect present. Based on analysis of factors effects, it can be mentioned that the noise levels has significant influence over the micro-perforation laser process.

The unacceptable results demonstrate significant variation in tensile values under the influence of electromagnetic noise. At a noise level of 0.8 V, the average tensile value is 407 N, suggesting better mechanical performance but with reduced consistency. At a noise level of 1 V, the average tensile value drops to 256 N, indicating a significant deterioration in the quality of the perforated material.

The acceptable results show that at a noise level of 1.2 V, the average tensile value is 303 N. Although the absolute value is lower than that at 0.8 V, the consistency and stability of the results are superior.

A detailed analysis of the tensile test results under the influence of electromagnetic noise indicates that a noise level of 1.2 V is optimal for achieving the desired quality of perforations in textile materials for airbags. This noise level provides a balance between mechanical performance and consistency of results, minimizing defects and ensuring the necessary structural integrity for vehicle safety. Controlling and maintaining this optimal electromagnetic noise level will significantly contribute to improving the quality and re-liability of the final products.

3.3 Conclusions

In the automotive industry, the precision and quality of components are essential for the performance and safety of vehicles. One of the modern processes that significantly contribute to achieving these high standards is laser micro-perforation. This technology allows for the creation of fine and precise perforations, used in various applications ranging from ventilation to aesthetics. The main advantages refer to [KAN23], [PAR16]: precision, production and speed of processing, customizations and effects of processing, security performance, waste reduction, the decrease in non-quality costs, etc. In the domain of the manufacture of automotive parts, the laser technology is clean and precis. It often demands exact measurements and a high level of precision to ensure proper functionality, precision and safety. The laser process surpasses the capabilities of many traditional cutting methods, characterized by extreme accuracy and the capability to achieve high precision.

In order to meet the imposed regulation and to improve the quality of production, the

automotive sector is always at the forefront in the application of innovative technologies. The use of laser processing technology offers a number of advantages for car manufacturers, promoting efficiency, safety and quality.

The laser perforation regime in the passenger airbag zone is an essential technology for ensuring the proper and efficient functioning of the airbag during an impact. By precisely adjusting technical parameters such as hole size, depth, and distribution, it is possible to weaken the dashboard covering without compromising its aesthetic qualities, while also allowing for rapid and efficient airbag deployment. The influence of this process on airbag performance is significant, and the optimal deployment time can only be achieved if the perforation regime is properly implemented. Thus, this technology directly contributes to passenger safety and to saving lives in the event of an accident.

(B-ii) The evolution and development plans for career development

Professional activity summary

As I mentioned in (B-i) section, my academic activity has its debut in October 2001 as a full-time doctoral student at the Automotive and engines department, Faculty of Mechanics, Transilvania University of Brasov. Since 2002, I have been employed as a university assistant in the same department, then following all the stages of my university career until now when I hold the position of associate professor.

During this entire period my didactic activity consisted of:

- ✓ teaching at courses, seminars, laboratories and projects;
- ✓ author and coauthor of books and laboratory manuals;
- ✓ coordinator of the "Motor vehicles and Future Technologies" master degree program;
- ✓ coordinating students at diploma projects and dissertations, some of them with special practical achievements;
- ✓ coordinator of students technological practice;
- ✓ conducting technical visits to companies in the automotive industry filed with groups of students;
- ✓ member of admissions committees;
- ✓ introduction of new disciplines;
- ✓ permanent adaptation of teaching techniques to be useful and appropriate to students' requirements;
- ✓ coordinating students at an international competition.

The scientific activity had as guidelines the following aspects:

- ✓ coordinating two research projects as director;
- ✓ member of some research project teams with various research themes and competences in the field of automotive engineering;
- ✓ publishing scientific articles in prestigious international journals indexed by WOS with impact factor, classified in the Q1, Q2, ISI Thomson proceeding area, indexed in international databases, and at various national or international conferences;
- ✓ I proposed research projects and was part of teams that proposed such projects;
- ✓ participation in technical seminars for professional development;
- ✓ collaborations with research institutes;
- ✓ collaborations with companies from the automotive industry;
- ✓ member of international scientific committees.

My academic activity was complemented by that in the private environment, as a design engineer and project manager in companies with a field of activity in the automotive industry. Also, I am technical judicial expert in the specialty of Motor vehicles and road traffic.

Academic career development

A. In the targeted habilitation domain

In the field of *the evolution and development plans for career development*, through the specifics of my work environment I have in mind and propose two main directions of action regarding future professional evolution: the research activity and didactic activity.

In addition, considering personal perspectives generated by obtaining the habilitation certificate, an essential aspect of the further evolution of the academic career is related to doctoral supervisor in the field of Automotive engineering.

It is obvious that the evolution of academic career must be done in correlation with the socio-economic environment, with its specific requirements and future trends. This is motivated due the fact that I have as main objective to attract and coordinate PhD students from this environment, in order to identify and develop topics that meet current developments and future innovation requirements. I also intend to collaborate at internationally level in order to coordinate doctoral theses under co-supervisor.

More than this, currently the automotive industry is marked by uncertainty regarding the look of the future vehicle. In this context it is mandatory that the academic environment to adapt to future trends and to evolve synchronously with the industry. A proper way is ensured by the collaboration between the academic zone with industry field through doctoral students.

Through doctoral students and their thesis, it can be ensured the technology transfer between university and industry, and this represents the process by which knowledge and innovations developed in academia are applied and used in the industrial sector, with the aim of stimulating economic development and increasing competitiveness. This process involves close collaboration between researchers, academic institutions and companies.

In university we develop fundamental and applied research, and through collaboration with automotive industry and related ones, these early researches can be implemented to solve technical problems or to develop new innovative products and processes.

Many emerging ideas and technologies, which are just at the beginning in academia, can become successful technologies in the market through investment and practical application in industry, and this is an essential aspect regarding the link between a doctoral student, academia and industrial environment.

Thus, research and development partnerships can be established between university and automotive companies, where resources and expertise can be shared. Also, through the Research and Development Institute of Transilvania University of Brasov can be created links between academia and industry, dedicated to technology transfer.

The aspects detailed above, characterized by innovation, interdisciplinarity, partnership, technology transfer, training and continuing education represent my main strategy with clear objectives that I want to pursue after obtaining my habilitation certificate in order to coordinate doctoral students.

My previously exposed strategy regarding the activity as a doctoral supervisor, represents an approach that facilitates the collaboration between Transilvania University and industry, as well as the funding of joint research projects in various themes regarding de automotive domain. This process helps both, the academic sector to capitalize its research and the industrial sector to become more innovative and efficient, by gaining highly technically trained people with professional expertise.

Another major objective that I want to accomplish refers to the research activity with the PhD students that must contribute significantly to visibility increase of the research results, both by publishing articles in internationally recognized specialized journals, indexed by WOS with impact factor, but also by presenting at international scientific conferences with increased visibility in academic and research environments.

Also, in the category of important proposed objectives regarding the activity with the future PhD students, it must be mentioned the realization of new scientific research projects, followed by the valorization of the results that contribute to the development of knowledge in the specific field.

B. Scientific and research field

Scientific activity contains two directions that complement each other, namely: the research activity itself and the dissemination - publication, patenting of the results of the research carried out.

The scientific and research activity development primarily will follow the main directions summarized in the present habilitation thesis, which represents the premises for future identification and evolution of new research directions.

Pursuing the expansion of the field of competences into an interdisciplinary one is welcome, and can be achieved by establishing collaborations with other universities and research institutes, through the involvement of PhD students and students, especially those from master's programs.

By involving master's students, the premises are created for their familiarization with the research area and implicitly the desire to continue their professional development in the doctoral study cycle may arise.

First of all, I want to attract funds through grant proposals / scientific research projects with national and international funding.

Experimental and innovative research involves maintaining and expanding collaboration with the industrial economic environment, the need to increase the competitiveness of products made by SMEs representing a national priority, Partnership-type projects necessarily involving the participation of the economic environment in the financing scheme.

International visibility will be supported by the annual publication of scientific articles in WOS indexed journals with impact factor, as well as articles indexed in WOS proceeding, international databases or at prestigious national and international conferences. The results of future scientific research will also be found in specialized books.

To increase the visibility of my research results at national and international level, will also be achieved through participation in prestigious international scientific congresses and conferences whose papers are indexed by WOS or SCOPUS.

C. Didactic activity

The main directions in the development of the university teaching career will aim the following:

- ✓ promoting a teacher-student partnership so that students' needs are correctly identified;
- ✓ didactic activity focused on interactive courses in which students actively participate, as well as their involvement in solving case studies, projects and practical applications in the field of automotive engineering;
- ✓ implementing modern teaching-learning techniques and methods, in order to ensure professional training in line with practical realities from the industrial field;
- ✓ continuous adaptation of master degree program "Motor vehicles and Future Technologies" that I am coordinating to the dynamics of the automotive industry and implicitly to its requirements;
- ✓ permanent updating of the teaching materials content of the subjects taught, in order to ensure the consistency between their content and the objectives of the specializations, as well as adaptation to the real needs of the labor market;
- ✓ involvement in the modernization and laboratories endowment, in order to ensure optimal practical support for the taught disciplines;
- ✓ introducing new disciplines in accordance with the requirements of the educational market and students;

- ✓ permanent development and expansion of partnerships with the socio-economic environment in order to facilitate interaction between potential employers and students;
- ✓ Continuing the activity of publishing specialized books in international and national publishing houses in accordance with the disciplines in which I teach, and in the future, I will be constantly responsible for updating course notes.

(B-iii) Bibliography

[AAR06] Aarts, L.; van Schagen, I. Driving speed and the risk of road crashes: a review. *Accident Analysis and Prevention* 2006, *38 (2)*, 215–224.

[ACE23] Acerraa, E. M.; Lantieria, C.; Vignalia, V.; Pazzinia, M.; Andreaa, S. Safety roads: the analysis of driving behavior and the effects on the infrastructural design, *Transportation Research Procedia* 2023, *69*, 336–343.

[ALB13] Albalate, D.; Fernández, L.; Yarygina, A. The road against fatalities: Infrastructure spending vs. regulation? *Accident Analysis & Prevention* 2013, *59*, 227–239, https://doi.org/10.1016/j.aap.2013.06.008

[ANM20] Anming, H. Laser Micro-Nano-Manufacturing and 3D Microprinting; Springer Series in Materials Science; Springer Nature Switzerland AG: Cham, Switzerland, 2020; Volume 309.

[BAS19] Basile A., et al. Ethanol Science and Engineering, Elsevier 2019, ISBN: 978-0-12-811458-2

[BER13] Bergel-Hayat, R.; Debbarh, M.; Antoniou, C.; Yannis, G. Explaining the road accident risk: Weather effects. *Accident Analysis & Prevention* 2013, *60*, 456–465, http://dx.doi.org/10.1016/j.aap.2013.03.006

[BRI24] Available online: https://www.britannica.com/science/deceleration-injury

[CAR04] Caristan, C.L. Laser Cutting Guide for Manufacturing; Society of Manufacturing Engineering: Dearborn, MI, USA, 2004.

[CEO24] A Guidance Document for the Implementation of CEDR Forgiving Roadsides report. National Roads Authority (NRA). Available online: https://www.tii.ie/media/3idngybj/forgiving-roadsides.pdf

[CHE09] Cheung C.S., Zhang Z.H., Chan T.L., et al. Investigation on the effect of port-injected methanol on the performance and emissions of a diesel engine at different engine speeds. Energy Fuels 2009; 23 (11):5684–94.

[CRI24]Carbon Dioxide Emissions to Renewable Methanol Value, https://carbonrecycling.com/technology

[DUM12] **Dumitrașcu D.-I.**, Truşcă D.D., Vehicle-Pedestrian Accident Reconstruction, COMAT 2012, 18- 20 October 2012, Brasov, Romania, http://scholar.google.ro/scholar?q=Vehicle-Pedestrian+Accident+Reconstruction%2C+Dumitrascu&btnG=&hl=ro&as_sdt=0%2C5

[DUM13] **Dumitrascu D.-I.**, Benea B., The Energetical and Ecological Performances of D.I. Diesel Engine Fueled with Biodiesel, ADVANCES in PRODUCTION,AUTOMATION and TRANSPORTATION SYSTEMS, pp. 389-394, ISSN: 2227-4588, ISBN: 978-1-61804-193-7, June 1-3, 2013, Brasov, Romania, http://www.wseas.org/main/books/2013/Brasov/ICAPS.pdf

[DUM14] **Dumitrascu D.-I.**, A Case Study Regarding Risk Management Implementation, The 3rd International Conference Research & Innovation in Engineering, COMAT 2014, 16-17 October 2014, Brasov, Romania, http://scholar.google.ro/scholar?hl=ro&q=A+Case+Study+Regarding+Risk+Management+Implementation&btnG , http://aspeckt.unitbv.ro/jspui/handle/123456789/653

[DUM16] **Dumitrascu D.-I.**, Dumitrascu A.-E., Chiru A., A Case Study Regarding the Implementation of Six Sigma in an Assembly Process for the Automotive Parts. 12th International Congress of Automotive and Transport Engineering (CONAT 2016), p. 643-650, October 26-29, 2016, WOS: 000390821400071, https://doi.org/10.1007/978-3-319-45447-4_71

[DUM18a] **Dumitrașcu D.-I.**, Combustibili și lubrifianți. Îndrumar de laborator. Universitatea „Transilvania" din Brașov, 2018.

[DUM18b] **Dumitrascu D.-I.**, Morariu C.O., Dumitrascu A.-E., Ciobanu D.V., Reliability estimation of towed grader attachment using finite element analysis and point estimation. Transactions of FAMENA, 42(1), 2018, p. 85-98, ISSN: 1333-1124, Impact Factor: 0.797, SRI: 0.187, revistă în zona Q4, WOS:000432786300008, https://doi.org/10.21278/TOF.42108

[DUM19a] **Dumitrașcu D.-I**, Assessment of potential risks that influence the traffic accidents, COMEC 2019, 21-22 Noiembrie, Brasov, https://intranet.unitbv.ro/Portals/0/UserFiles/User591/_Comec2019_Dumitrascu.pdf

[DUM19b] **Dumitrascu D.–I.**, Dumitraşcu A.–E., Design Failure Mode and Effects Analysis (DFMEA) for automotive safety systems, RECENT, ISSN 1582-0246, Vol. 20 (2019), no. 3 (59), 2019, p. 119-122, https://doi.org/10.31926/RECENT.2019.59.119 , http://www.recentonline.ro/2019/059/Dumitrascu-R59.pdf https://journals.indexcopernicus.com/search/details?jmlId=4064&org=RECENT,p4064,3.html

[DUM21] **Dumitraşcu D.–I.**, The influence of the gasoline octane number on a turbocharged engine performance. International Journal of Computational and Applied Mathematics & Computer Science, ISSN 2769-2477 , p, 30-33, Volume 1, 2021, https://www.wseas.com/journals/camcs/2021/icamcs(2021)-005.pdf https://journals.indexcopernicus.com/search/details?id=69674

[DUM22] **Dumitrascu D.–I.**, Quality Management for Industrial Projects, RECENT J. (2022), 68:118-122, ISBN: 1582-0246, https://www.recentonline.ro/2022/068/Dumitrascu-R68.pdf, https://doi.org/10.31926/RECENT.2022.68.118 https://journals.indexcopernicus.com/search/details?jmlId=4064&org=RECENT,p4064,3.html

[DUM24a] **Dumitrașcu D.-I.**, Procese si caracteristici ale motoarelor cu ardere interna. Suport de curs. Universitatea „Transilvania" din Brașov, 2024.

[DUM24b] **Dumitrascu D.-I.**, Influence of Road Infrastructure Design over the Traffic Accidents: A Simulated Case Study. Infrastructures, 9(9), 2024, ISSN 2412-3811, Impact Factor: 2.7, SRI: 1.232, revistă în zona Q2, https://doi.org/10.3390/infrastructures9090154

[DUM24c] **Dumitrascu D.-I.**, Rusu A.-N., Dumitrascu A.-E., The Influence of the Laser Power on the Manufacturing Quality Specific to Automotive Parts. The 3rd International Conference on Energy and Green Computing - ICEGC'2024, November 21-22, 2024, Higher School of Technology – Meknes, Morocco, https://www.iraset.org/icegc2024/

[DUM24d] **Dumitrascu D.-I.**, Rusu A.-N., Dumitrascu A.-E., Efficiency and Precision of Welding Process for the Automotive Parts. The 3rd International Conference on Energy and Green Computing - ICEGC'2024, November 21-22, 2024, Higher School of Technology – Meknes, Morocco, https://www.iraset.org/icegc2024/

[DUM24e] **Dumitrascu D.-I.**, Dumitrascu A.-E., Failure Modes and Effects Analysis for Automotive Trim Parts Processing. Engineering Proceedings - 1st International Conference on Industrial, Manufacturing and Process Engineering (ICIMP – 2024), 76(1), 22, ISSN: 2673-4591, 27-29 iunie, 2024, Regina, SK, Canada, https://doi.org/10.3390/engproc2024076022

[DUM24f] **Dumitrascu D.-I.**, Rusu A.-N., Dumitrascu A.-E., Quality Defects Analysis for Manufacturing Processes of Automotive Trim Parts. Engineering Proceedings - 1st International Conference on Industrial, Manufacturing and Process Engineering (ICIMP – 2024), 76(1), 32, ISSN: 2673-4591, 27-29 iunie, 2024, Regina, SK, Canada, https://doi.org/10.3390/engproc2024076032

[DUM24g] **Dumitrascu D.-I.**, Rusu A.-N., Dumitrascu A.-E., The Improvement of Industrial Products Quality through Six Sigma Method Implementation. 12th International Conference on Machine and Industrial Design in Mechanical Engineering (KOD 2024), Springer Series - Mechanisms and Machine Science, ISSN 2211-0984, 23-26 May 2024, Balatonfüred, Hungary, http://www.kod.ftn.uns.ac.rs/ , http://www.kod.ftn.uns.ac.rs/ConferenceProgramKOD2024.pdf

[ELV04] Elvik, R.; Christensen, P.; Amundsen, A. Speed and Road Accidents: An Evaluation of the Power Model. TOI report 740. Oslo: The Institute of Transport Economics, 2004.

[ELV22] Elvers B., et al. Handbook of Fuels, Energy Sources of Transportation Second, Completely Revised, and Updated Edition, WILEY-VCH, 2022, 78-3-527-81348-3

[ERS23] European Road Safety Observatory (ERSO), European Commission, 2023. Available online: https://road-safety.transport.ec.europa.eu/european-road-safety-observatory_en

[ETH23] Annual World Fuel Ethanol Production, https://ethanolrfa.org/markets-and-statistics/annual-ethanol-production

[EUR20] European Commission, 2020. Next Steps towards 'Vision Zero': EU Road Safety Policy Framework 2021-2030. Directorate-General for Mobility and Transport, Publications Office, 2020. Available online: https://data.europa.eu/doi/10.2832/39127

[FIT00] Fitzpatrick, K.; Anderson, I.; Bauer, K.; Collins, J.; Elefteriadou, L.; Harwood, D.; Irizarry, N.; Krammes, R.; McFadden, J.; Parma, K.; Passetti, K. Evaluation of Design Consistency Methods for Two-Lane Rural Highways, Executive Summary. Report No. FHWA-RD-99-173, US Development of Transportation, Office of Safety Research and Development, August 2000, Available online: https://highways.dot.gov/sites/fhwa.dot.gov/files/FHWA-RD-99-173.pdf

[FOL22] Folkson R., Sapsford S., Alternative Fuels and Advanced Vehicle Technologies for Improved Environmental Performance, Towards Zero Carbon Transportation, Second Edition, 2022, Woodhead Publishing, ISBN: 978-0-323-90028-7

[GAI09] Gaiginschi R., Road Accident Reconstruction and Expertise (In Romanian: Reconstrucția și expertiza accidentelor rutiere), ISBN 978-973-31-2345-3, Publishing House Tehnica, 2009.

[GIB73] Gibra Isaac, N. Probability and Statistical Inference for Scientists and Engineers, 1st ed.; Prentice-Hall: Hoboken, NJ, USA, 1973.

[HEY18] Heywood J.B., Internal Combustion Engine Fundamentals, Second Edition, McGraw-Hill Education, 2018, ISBN: 978-1-26-011610-6

[HIC24] Head Injury Criteria Tolerance Levels, Available online: http://www.eurailsafe.net/subsites/operas/HTML/Section3/Page3.3.1.htm

[HUA10] Hua Z., Advanced direct injection combustion engine technologies and development, Volume 1: Gasoline and gas engines, Woodhead Publishing Limited, 2010, ISBN 978-1-84569-389-3

[KAN23] Kannatey-Asibu, E. Principles and Laser Materials Processing. Developments and Applications, 2nd ed.; John Wiley & Sons, Inc.: Hoboken, NJ, USA, 2023.

[LAC10] Lackne M., et al. Handbook of Combustion, Volume 3, Gaseous and Liquid Fuels, Wiley-VCH, 2010, ISBN: 978-3-527-32449-1

[LAH14] Lahane S., Subramanian K.A., Impact of nozzle holes configuration on fuel spray, wall impingement and NOx emission of a diesel engine for biodiesel-diesel blend (B20), Applied Thermal Engineering 64, p.307-314, 2014

[MAL19] Malin, F.; Norros, I.; Innamaa, S. Accident risk of road and weather conditions on different road types. *Accident Analysis & Prevention* 2019, *122*, 181–188, https://doi.org/10.1016/j.aap.2018.10.014

[MAS03] Mason, R.L.; Gunst, R.F.; Balding, D.J. Statistical Design and Analysis of Experiments with Applications to Engineering Science; John Wiley & Sons: Hoboken, NJ, USA, 2003.

[MAT05] Matena S. et al. Road Design and Environment – Best practice on Self-explaining and Forgiving Roads. RIPCORD-ISEREST deliverable D3, 2005.

[MON11] Montgomery, D.C.; Runger, G.C. Applied Statistics Probability Engineers, 5th ed.; John Wiley & Sons: Hoboken, NJ, USA, 2011.

[NEW04] Accidents photos sources, Available online: https://newsbv.ro, https://mytex.ro, https://brasovmetropolitan.ro, https://www.isujbv.ro.

[NIL04] Nilsson, G., 2004. *Traffic Safety Dimensions and the Power Model to Describe the Effect of Speed on Safety*, Bulletin, 221. Lund Institute of Technology, Department of Technology and Society, Traffic Engineering, Lund.

[NIS24] NIST/SEMATECH. e-Handbook of Statistical Methods. Available online: https://www.itl.nist.gov/div898/handbook/

[PAP19] Papadimitriou, E.; Filtness, A.; Theofilatos, A.; Ziakopoulos, A.; Quigley, C.; Yannis, G. Review and ranking of crash risk factors related to the road infrastructure, *Accident Analysis & Prevention* 2019, *125*, 85–97. https://doi.org/10.1016/j.aap.2019.01.002

[PAR16] Parry, L., Ashcroft, I. A. and Wildman, R. D., Understanding the Effect of Laser Scan Strategy on Residual Stress in Selective Laser Melting Through Thermo-Mechanical Simulation. Addit. Manuf. 12 (2016).

[PCC20] PC-CRASH. A Simulation Program for Vehicle Accidents, Operating and Technical Manual; Version 12.1; Dr. Steffan Datentechnik: Linz, Austria, April 2020.

[POL24a] Available online: https://www.politiaromana.ro/ro/prevenire/buletinul-siguranteirutiere

[POL24b] Available online: https://www.politiaromana.ro/ro/structura-politiei-romane/unitati-centrale/directia-rutiera/statistici

[RES20] Improving global road safety. Resolution A/RES/74/299, United Nations, 2020. Available online: https://www.who.int/teams/social-determinants-of-health/safety-and-mobility/decade-of-action-for-road-safety-2021-2030

[RIS05] RISER consortium. D05: Summary of European Design Guidelines for roadside infrastructure. RISER deliverable, February 2005

[RIS06] RISER consortium. D06: European Best Practice for Roadside Design: Guidelines for Roadside Infrastructure on New and Existing Roads. RISER deliverable, February 2006

[RUS24a] Rusu A.-N., **Dumitrascu D.-I.***, Dumitrascu A.-E., Monitoring, Control and Optimization in Laser Micro-Perforation Process for Automotive Synthetic Leather Parts. Processes, 12(6), 2024, ISSN 2227-9717, Impact Factor: 2.8, SRI: 1.029, revistă în zona Q2, WOS: 001256521600001, https://doi.org/10.3390/pr12061275

[RUS24b] Rusu A.-N., **Dumitrascu D.-I.***, Dumitrascu A.-E., The Electromagnetic Noise Level Influence on the Laser Micro-Perforation Process specific to Automotive Components. Materials, 17(16), 2024, ISSN 1996-1944, Impact Factor: 3.1, SRI: 1.792, revistă în zona Q1, WOS:001304651200001, https://doi.org/10.3390/ma17164131

[SIL15] Sileghem L., A study of the combustion of alcohol-gasoline blends in internal combustion engines. Ghent University; 2015.

[STA23] Biofuel industry worldwide - Ethanol production for fuel use worldwide from 2016 to 2023, https://www.statista.com/statistics/274142/global-ethanol-production-since-2000/

[TAE14] Taeger, D.; Kuhnt, S. Statistical Hypothesis Testing with SAS and R; John Wiley & Sons: Hoboken, NJ, USA, 2014. https://doi.org/10.1002/9781118762585.ch11

[TAY00] Taylor, M.C.; Lynam, D.A.; Baruya, A. The Effects of Drivers' Speed on the Frequency of Road Accidents. TRL Report 421. Crowthorne, Berkshire: Transport Research Laboratory, 2000.

[TAY02] Taylor, M.C.; Baruya, A.; Kennedy, J.V. The Relationship Between Speed and Accidents on Rural Single-carriageway Roads. TRL Report 511. Crowthorne, Berkshire: Transport Research Laboratory, 2002

[TOR13] F. La Torre, Forgiving roadsides design guide, Conference Europeenne des Directeurs des Routes, ISBN: 979-10-93321-02-8, 2013, https://www.cedr.eu/download/Publications/2013/T10_Forgiving_roadsides.pdf

[TRU12]Truşcă D.D., **Dumitraşcu D.-I.**, Experimental Research Regarding Night Visibility In Road Traffic, COMAT 2012, 18- 20 October 2012, Brasov, Romania, http://scholar.google.ro/scholar?q=Experimental+research+regarding+night+visibility+in+road+traffic%2C+Dumitrascu&btnG=&hl=ro&as_sdt=0%2C5

[USD86] U.S. Department of Transportation. Roadside improvements for local roads and streets. Federal highway administration, USA, October 1986

[VER19] Verhelst S., Turner J., et al. Methanol as a fuel for internal combustion engines, Progress in Energy and Combustion Science 70, 2019, 43–88.

[VIR19] Virzi Mariotti, G.; Golfo, S.; Nigrelli, V.; Carollo, F. Head Injury Criterion: Mini Review. Am J Biomed Sci & Res. 2019, *5*, 406–407. https://doi.org/10.34297/AJBSR.2019.05.000957

[WAN13] Wang, C.; Quddus, M.; Ison, S. The effect of traffic and road characteristics on road safety: A review and future research direction, *Safety Science* 2013, *57*, 264–275.

[WEG95] Wegman, F. Influence of Infrastructure Design on Road Safety. SWOV Institute for Road Safety Research, The Netherlands, 1995.

[YAO08] Yao C., Cheung C.S., Cheng C., et al. Effect of diesel/methanol compound combustion on diesel engine combustion and emissions. Energy Conver Manage 2008; 49 (6):1696–704.